UNDERSTANDING THE ROLE OF THE RECEPTOR FOR ADVANCED GLYCATION

END-PRODUCTS (RAGE) IN PANCREATIC CANCER

A Dissertation
Submitted to the Graduate Faculty
of the
North Dakota State University
of Agriculture and Applied Science

By

Priyanka Swami

In Partial Fulfillment of the Requirements
for the Degree of
DOCTOR OF PHILOSOPHY

Major Department:
Pharmaceutical Sciences

May 2019

Fargo, North Dakota

North Dakota State University
Graduate School

Title

UNDERSTANDING THE ROLE OF THE RECEPTOR FOR
ADVANCED GLYCATION END-PRODUCTS (RAGE) IN
PANCREATIC CANCER

By

Priyanka Swami

The Supervisory Committee certifies that this ***disquisition*** complies with North Dakota

State University's regulations and meets the accepted standards for the degree of

DOCTOR OF PHILOSOPHY

SUPERVISORY COMMITTEE:

Dr. Estelle Leclerc

Chair

Dr. Jagdish Singh

Dr. Sanku Mallik

Dr. Steven Qian

Dr. John Wilkinson

Approved:

July 01, 2019	Dr. Jagdish Singh
Date	Department Chair

ABSTRACT

Expression of the Receptor for Advanced Glycation End Products (RAGE) and is

upregulated in a several cancers. Based on published studies, we hypothesized that RAGE, when

overexpressed in pancreatic cancer cells, will promote cell proliferation and migration. To study

the role of RAGE in pancreatic cancer, we selected the human pancreatic cancer cell-line PANC-

1, and stably transfected the cells with full length RAGE to generate model cell-lines that

overexpress RAGE. We obtained two cell-lines PANC-1 FLR2 and PANC-1 FLR3 and

examined the influence of RAGE on cellular properties. A significant increase in proliferation

but a reduction in migratory abilities of PANC-1 FLR2 and PANC-1 FLR3 cells was observed.

The increase in proliferation and reduction in migration was reverted upon knockdown of RAGE

in PANC-1 FLR2 cells with siRNA specific for RAGE. The reduction in migration was

supported by the reduced levels of vimentin and several integrins in RAGE transfected cells.

Furthermore, we observed a downregulation in FAK, AKT, ERK1/2 and NF-κB activity.

Growing evidence supports that RAGE is essential for pancreatic cancer progression. It

has also been shown that RAGE facilitates pancreatic tumor cell survival by enhancing

autophagy and inhibiting apoptosis. The goal of our study was to determine the effect of RAGE

inhibition during gemcitabine chemotherapy on the growth of pancreatic tumor. Hence, we

investigated the effect of RAGE inhibitors and their combination with gemcitabine in an

orthotopic mouse model of pancreatic cancer using mouse pancreatic cancer cell-line KPC 5508.

We used two RAGE inhibitors, an anti-RAGE monoclonal antibody (IgG2A11) and a small

molecule RAGE inhibitor (FPS-ZM1). We observed a significant reduction in tumor weights of

the mice treated with the combination of IgG2A11 and gemcitabine as compared to gemcitabine

alone treated mice. The reduction in tumor growth was accompanied with increase in p62 levels

(marker of autophagy) and increase in levels of cleaved PARP (marker of apoptosis). We also observed reduction in HMGB1 and phosphorylation levels of ERK1/2 in tumors from the group treated with the combination as compared to the gemcitabine alone treated group.

ACKNOWLEDGEMENTS

During the past five years, I have learnt several things outside the lab too. I want to thank Dana, Lori and Jean for all those corridor conversations about life and things besides the lab. I have immensely grown as a person because of them. I would also like to thank Janet and Diana for always being ready to help with anything and everything. They make our (graduate students) lives so much easier. I would also like to thank my lab mates for being very cooperative and helpful.

DEDICATION

Dedicated to the Almighty,

my parents, Rekha Swami and Anil Swami

and my husband, Shravan.

TABLE OF CONTENTS

LIST OF TABLES

LIST OF FIGURES

LIST OF ABBREVIATIONS

AB……………………………………………………………………………..AlamarBlue

AGE…………………………………………………………..Advanced glycation end products

Akt…………………………………………………………………………….Protein kinase B

BCA…………………………………….. ……………………………….Bicinchoninic acid assay

BSA……………………………………………………………………...Bovine serum albumin

Cdc-42……………………………………………….Cell division control protein 42 homolog

cDNA……………………………………………………………………...complementary DNA

CTLA-4…………………………………………………...Cytotoxic T-lymphocyte antigen 4

DNA…………………………………………………………………. Deoxyribonucleic acid

ECL………………………………………………………………Enhanced chemiluminescence

EDTA……………………………………………………. Ethylenediaminetetraacetic acid

ELISA……………………………………………………………Enzyme linked immunosorbent assay

EMT……………………………………………………………Epithelial to mesenchymal transition

ERK…………………………………………………..……….Extracellular signal-regulated kinases

FAK…………………………………………………………………Focal Adhesion Kinase

FBS……………………………………………………………….……Fetal bovine serum

FDA…………………………………………………………………Food and drug administration

FITC………………………………………………………………... Fluorescein isothiocyanate

FL_RAGE…………………………………..Full length receptor for advanced glycation end products

HMGB-1……………………………………………………High-mobility group protein B1

HRP………………………………………………………….……….Horseradish peroxidase

IACUC……………………………………………...Institutional animal care and use committees

IgG……………………………………………………………….………Immunoglobulin

JNK…………………………………………………………………....c-Jun N-terminal kinases

GENERAL INTRODUCTION

Pancreatic Cancer

Pancreatic cancer is one of the most fatal types of cancers and the overall incidence of the disease is on a rise in the US as well as across the globe. Pancreatic cancer accounts for about 3% of all cancers and about 7% of all the cancer deaths in the US, and is presently the fourth leading cause of cancer-related deaths in the United States [1,2]. About 56,770 new cases of pancreatic cancer and 45,750 deaths are projected in 2019 [3]. According to the United States Surveillance, Epidemiology, and End Results Program (SEER) 2018 data for 2008-2014, the five-year survival rate for pancreatic cancer is 8.5% [4]. The SEER data show that, between 1973 and 2014 there was 1.03% increase in the age-standardized incidence rates of pancreatic cancer each year [4]. Therefore, by 2030 pancreatic cancer is predicted to become the second leading cause of cancer related deaths in the United States [4,5].

Types of pancreatic cancer

The pancreas is a secretory gland with exocrine and endocrine functions [6]. Pancreatic cancer can be of two types based on whether it originated from exocrine cells or endocrine cells (Figure 1). The more common type of pancreatic cancer arises from exocrine cells and can be divided into two histological subtypes. About 90% of the exocrine tumors start in the ducts of pancreas and are known as ductal adenocarcinoma. Tumors that arise in the acini, which are less common, are called acinar adenocarcinoma [7]. Exocrine cancers are very aggressive and often metastasize to other organs [8].

Less common tumors are the endocrine tumors which arise in the islet cells [7]. They usually grow slower than exocrine tumors and comprise about 7% of all pancreatic cancers.

Based on the cells of their origin and the hormones that they secrete, they can be divided into insulinomas, glucagonomas, and gastrinomas [9].
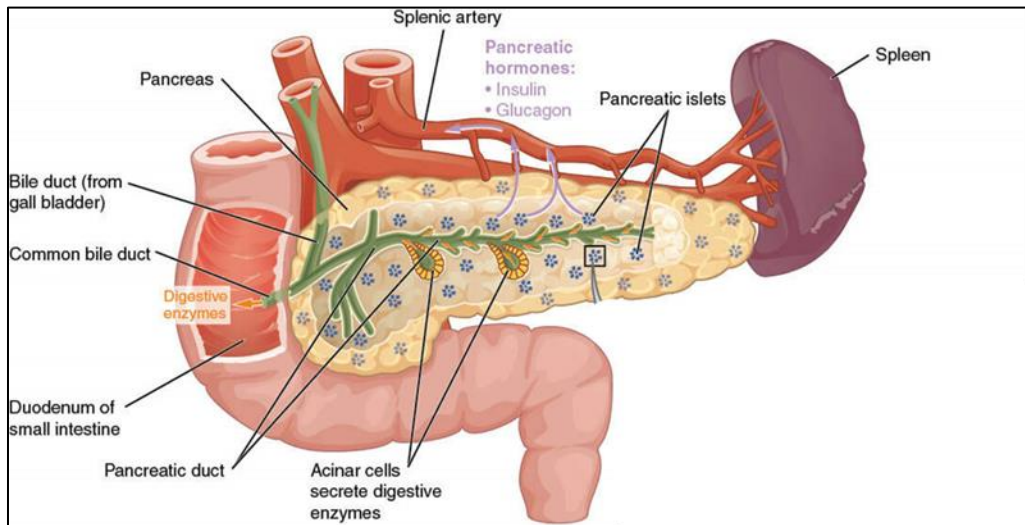
Figure 1: Diagrammatic representation of the pancreas.
Figure taken from https://www.olivelab.org/the-pancreas-overview.html

Risk factors

Numerous risk factors that contribute to the development of pancreatic cancer have been identified [10]. Pancreatic cancer is largely known to be diagnosed in older people. In the US, the majority of the patients diagnosed with pancreatic cancer fall between the ages of 40 and 80 years, 71 years of age being the median age at diagnosis [11]. Cigarette smoking is the most common and important risk factor for pancreatic cancer [12]. Occurrence of pancreatic cancer is found to be 30% more commonly in men than women [13]. Another important risk factor is family history. Patients with history of pancreatic cancer in their family have significantly higher risks of developing the disease [14]. A number of syndromes have been identified as risk factors for pancreatic cancer. Individuals who carry a germline mutation in BRCA2 are at a 10-fold higher risk of developing pancreatic cancer [15]. Other syndromes include: mismatch repair nonpolyposis colorectal cancer—the Lynch II variant (hMSH2, hMLH1) [16], hereditary

carcinoma FAMMM syndrome (p16) [17] and Peutz-Jeghers syndrome with germ-line mutations in *STK11/LKB1* gene [18]. Diabetes is another common risk factor for pancreatic cancer. It can be a risk factor as well as a manifestation of pancreatic cancer. Studies have shown that if the duration of diabetes is more than or equal to 10 years, the patient will be at a higher risk of pancreatic cancer [19,20].

Genetic alterations in pancreatic cancer

Whole exome-sequencing studies have revealed that PDAC is a molecularly heterogeneous disease characterized by four commonly mutated genes: oncogenic KRAS mutation and inactivation of the tumor suppressors CDKN2A, TP53 and SMAD4 [21]. The most prevalent amongst these genetic alterations is the mutation in *KRAS* oncogene and is present in around 95% of the cases [22,23]. *KRAS* codes for a small GTPase that mediates several cellular functions such as proliferation, cell motility, cell survival and cytoskeletal remodeling [24,25]. The outcome of *KRAS* mutation is inhibition of GTP hydrolysis which ultimately results into longer activated states of KRAS [26]. This leads to activation of key mitogenic downstream signaling pathways such as RAF/MEK/ERK pathway as well as activation of phosphatidylinositol 3 kinase (PI3K), resulting in uncontrolled cell proliferation facilitating cancer growth and spreading [27,28]. TP53 (also known as p53) is a tumor suppressor and is inactivated in nearly 50–75% of pancreatic cancers [29]. The p53 protein controls several essential cellular functions such as regulation of the G1-S cell cycle checkpoint, the repair of damaged DNA and the induction of apoptosis [30]. p53 is also known to facilitate the expression of the cyclin-dependent kinase inhibitor CDKN1A which in turn functions to stop cell cycle progression [31]. Therefore, the loss of p53 function results in the accumulation of other genetic abnormalities, the loss of DNA binding ability and uncontrolled cell proliferation [32]. Loss of

p53 function is also associated with aneuploidy (presence of abnormal number of chromosomes in a cell) which is an important characteristic of pancreatic cancer, implying that p53 function is critical in maintaining genomic stability [33]. Another commonly mutated gene in pancreatic cancer is *p16/CDKN2A* (*INK4A)* which is a tumor suppressor [34,35]. *p16/CDKN2A* encodes for a protein which belongs to the cyclin dependent kinase (CDK) inhibitor family and inhibits cyclinD-CDK4 and cyclinD-CDK6 complexes, both complexes being responsible for cell cycle progression through the G1-S cell cycle checkpoint [36]. Loss of *p16/CDKN2A* expression leads to increased cyclin dependent kinase 4 activity resulting in uncontrolled cell proliferation, poorly differentiated tumors as well as the presence of metastatic disease [37,38].

Moreover, many other gene alterations have been associated with pancreatic cancer and the mutated genes may vary widely in individual tumors [22]. Mutation in the gene encoding for C-Myc was identified in about 30% of pancreatic cancer cases [39]. Whole-exome sequencing analysis performed for 99 pancreatic cancers patients also revealed mutation in genes related to chromatin remodeling. Chromatin remodeling is defined as a stable alteration in the structure of nucleosomes and the distribution on DNA [40]. Alterations in genes related to chromatin remodeling like *EPC1*, *ARID2, MLL3* and DNA damage repair (*ATM*) have been identified [22,41]. Additionally, significant alterations in *ROBO1/2* and *SLIT2*, which are genes related to the axon guidance pathway, were identified [41]. Some other genes altered in pancreatic cancer include *MKK4*, *TGF-beta receptor, BRCA2*, and LKB1/STK11 [42,43].

Pathophysiology

This paragraph describes the most common type of the pancreatic cancer, pancreatic ductal adenocarcinoma (PDAC) which is commonly referred to as pancreatic cancer. About 65% of pancreatic cancers are localized at the head of the pancreas, but may also be located in the

body (20%), and the tail (10%) of the pancreas [44]. Several studies have described histologically distinct precursor lesions in the pancreas [45]. Based on the extent of cytologic and architectural atypia, these precursor lesions are described as pancreatic intraepithelial neoplasia (PanIN), intraductal papillary mucinous neoplasm (IPMN) and mucinous cystic neoplasm (MCN) [46]. PanINs are microscopic lesions that are less than 0.5 cm, appear in smaller pancreatic ducts and are classified morphologically into three grades (Figure 2) [45]. PanIN-1 lesions comprise of columnar epithelial cells with round nuclei and flat cells in PanIN-1A and papillary cells inPanIN-1B lesions [45,47]. PanIN-2 lesions display complex nuclear abnormalities, such as loss of nuclear polarity, nuclear crowding, variation in nuclear size (pleomorphism) and pseudostratification [45,47]. PanIN-3 lesions exhibit the highest extent of dysplasia with papillary, cribriform structures and the nuclei become enlarged, pleomorphic and poorly oriented. "Budding off" of small clusters of epithelial cells into the lumen is also observed [45,47,48]. KRAS gene mutations appear in early low-grade PanIN lesions (PanIN-1), while mutations in p16/CDKN2A gene are observed in intermediate PanIN-2 lesions, and SMAD4, TP53, and BRCA2 mutations appear in late PanIN-3 lesions [46]. Telomere shortening is also observed in PanIN-1 lesions which may lead to accumulation of chromosomal abnormalities in PanINs [49].

IPMNs are larger lesions which occur on the main pancreatic duct and/or its branches, with varying extent of papillary epithelial component, mucin secretion, cystic dilatation and invasiveness [50]. MCNs arise in the body and tail of the pancreas and do not communicate with pancreatic duct system [51].
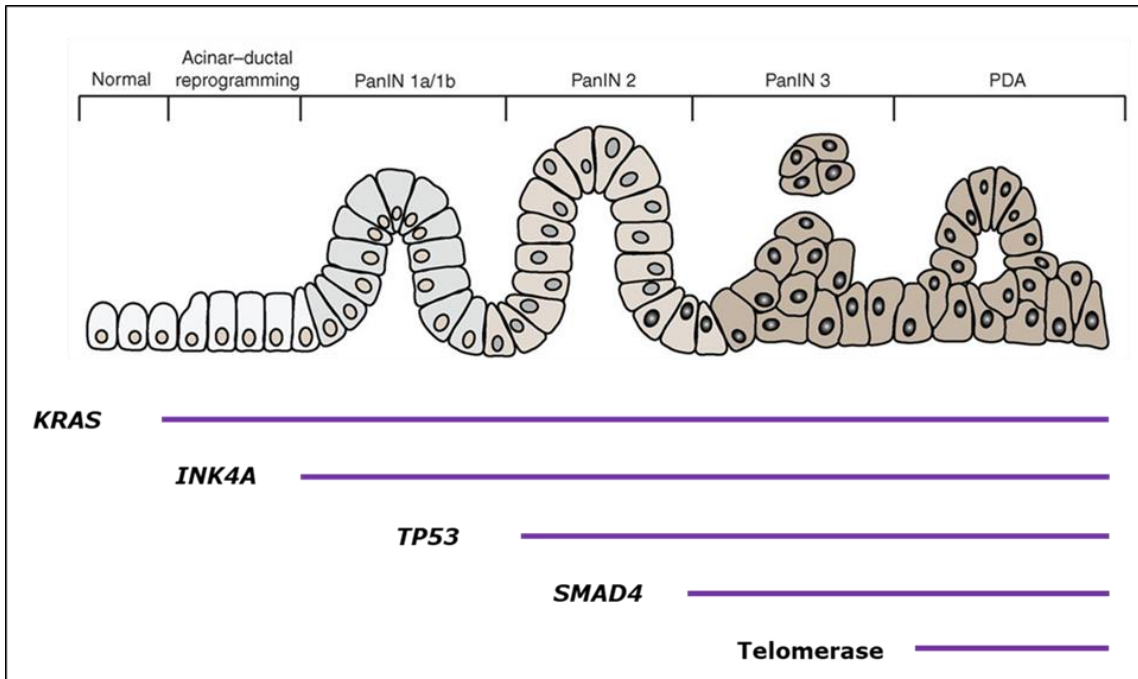
Figure 2: Schematic representation of the multistage progression of pancreatic ductal adenocarcinoma (PDA).
PDA arises from the multistage progression of precursor lesions known as pancreatic intraepithelial neoplasia (PanIN). As shown, molecular changes occur through progressive stages of pathogenesis, with increasing nuclear and cytoskeletal abnormalities. Genetic alterations commonly observed in these lesions are indicated with respect to the stages in which they most often occur. Adapted from [52] and [53]

Biomarkers

Pancreatic cancer is one of the deadliest malignancies with continuously growing rates of incidence. The poor prognosis can be attributed to the aggressive nature of the tumor, detection at a very late stage and resistance to chemotherapy [54]. Therefore, it is important to find new biomarkers to facilitate early detection (diagnostic biomarkers), improve prognosis (prognostic biomarkers), and for the optimization of current therapies (predictive biomarkers) [55]. According to the National Institutes of Health Biomarker Working Group, a biomarker is ''a characteristic that is objectively measured and evaluated as an indicator of normal biological process, pathogenic processes, or pharmacological responses to a therapeutic intervention'' [56].

6

The most commonly used serum marker for pancreatic cancer is carbohydrate antigen 19-9 (CA 19-9) and it remains the only Food and Drug Administration (FDA) approved blood test for pancreatic cancer [57]. CA 19-9 was first discovered in 1979 in colorectal carcinoma [58]. A study in 1988 demonstrated increased levels of the CA 19-9 antigen in the sera of pancreatic cancer patients [59]. However, the lack of adequate sensitivity and specificity is a major limitation of CA 19-9. Proteins in the pancreatic juice were investigated by liquid chromatography tandem mass spectrometry (LC-MS/MS), and observed high levels of CEA & MUC1 among more than 170 proteins unique to pancreatic cancer [60]. Since an altered metabolite profile is an important feature of pancreatic cancer, metabolomics have also been investigated as a diagnostic tool for early detection of pancreatic cancer [61]. A recent study investigated 914 patients to differentiate between pancreatic cancer and chronic pancreatitis patients. They identified a metabolic biomarker signature including metabolites like histidine, proline, sphingomyelin, pyruvate and ceramide, in combination with CA 19-9 [62].

Treatment

Surgical resection of the tumor is the only potential treatment for pancreatic cancer patients. However, only 15% to 20% of patients are eligible for surgery due to late presentation. In addition, even after surgical resection about 90% of patients die due to relapse of the disease in absence of additional therapy [63]. A study reported that patients at early stages of pancreatic adenocarcinoma were benefitted upon receiving preoperative gemcitabine based chemoradiation prior to surgery [64]. As compared to surgical resection alone, employing adjuvant chemotherapy could improve patient prognosis [65].

Gemcitabine was the first agent approved by FDA and has been the standard of care for pancreatic cancer. Two landmark phase III trials showed significant improvement in median

overall survival of patients presented with metastatic pancreatic cancer, establishing new standard of care [66,67]. A summary of the clinical trials with different combinations of drugs used to achieve the respective median overall survival is described in Table 1. Several studies which employed agents such as 5-FU, capecitabine, oxaliplatin, and cisplatin in combination with gemcitabine showed no overall improvement in survival when compared to gemcitabine alone [68-71].

In the last decade, several targeted agents have been investigated for treatment of pancreatic cancer [22]. Two new targets have been identified: The Epidermal Growth Factor Receptor (EGFR) targeted by small molecule erlotinib, and the Vascular endothelial growth factor (VEGF) targeted by the monoclonal antibody Bevacizumab [72,73]. Erlotinib is a selective epidermal growth factor receptor (EGFR) tyrosine kinase inhibitor, used in patients with advanced pancreatic cancer [74]. Bevacizumab can prevent tumor growth by inhibiting the activity of VEGF and VEGFR (Vascular endothelial growth factor receptor), thereby preventing angiogenesis in pancreatic tumor. However, there was only a modest improvement in the patients treated with these new drugs, perhaps due to the high molecular heterogeneity of pancreatic tumor [75,76]. Therefore, giving these drugs with combination chemotherapy is a better approach to kill more cancer cells.

Immunotherapy has been a breakthrough for the treatment of many cancers, but it has been relatively ineffective in pancreatic cancer. Pancreatic cancer showed delayed response to therapies targeting immune checkpoints, cytotoxic T-lymphocyte-associated antigen 4 (CTLA-4) [77] and programmed cell death 1 (PD-1) [78]. An important barrier in pancreatic cancer for the success of immunotherapy is the highly immunosuppressive tumor microenvironment [79]. Recently, the tumor microenvironment has attracted a lot of research interest. The pancreatic

tumor microenvironment (stroma) is composed of fibroblasts, immune cells, blood vessels and extracellular matrix proteins such as collagen, fibronectin and hyaluronic acid [80]. Also, the pancreatic tumor stroma is critical for several cellular processes including tumor formation, invasion, metastasis, modification of cancer cell metabolism, immune cell recruitment and drug resistance [81]. Therefore, a better understanding of the tumor microenvironment in pancreatic cancer can lead to improving the future of immunotherapy in pancreatic cancer.

Table 1: Studies that influenced current standard of care, displayed in order of publication. Taken from [82]

Median overall survival	Title	Patients
5.65 months Gem vs 4.41 months 5-fluorouracil	Improvements in survival and clinical benefit with gemcitabine as first line therapy for patients with advanced pancreas cancer: a randomized trial. [83]	126
6.24 months Gem + Erlotinib vs 5.91 months Gem	Erlotinib plus gemcitabine compared with gemcitabine alone in patients with advanced pancreatic cancer: a phase III trial of the National Cancer Institute of Canada Clinical Trials Group. [74]	569
11.1 months FOLFIRINOX, 6.8 months Gem	FOLFIRINOX versus gemcitabine for metastatic pancreatic cancer. [66]	342
8.5 months Gem + nabpaclitaxel, 6.7 months Gem	Increased survival in pancreatic cancer with nab-paclitaxel plus gemcitabine. [67]	861
6.1 months nano irinotecan + 5-fluorouracil + folinic acid, 4.2 months 5-fluorouracil + folinic acid	Nanoliposomal irinotecan with fluorouracil and folinic acid in metastatic pancreatic cancer after previous gemcitabine-based therapy (NAPOLI-1): a global, randomized, open label, phase 3 trial. [84]	417

RAGE

The receptor for advanced glycation end products (RAGE) was first described in 1992. It is a transmembrane protein and a member of the immunoglobulin superfamily [85]. RAGE

shares structural homology with other immunoglobulin like receptors [86,87]. In humans the *RAGE* gene is located close to the class III region of the major histocompatibility complex on chromosome 6 [88,89]. Full length human RAGE is a 45-55 kD protein [85]. RAGE can interact with structurally unrelated molecules because it has the ability to recognize tertiary structures of ligands rather than the specific amino acid sequences [90,91]. Hence RAGE is considered as a pattern recognition receptor (PRR) [92].

RAGE expression

RAGE is found to be constitutively expressed at high levels during early developmental stages, but its expression is highly regulated in adult tissues [93]. In contrast to embryonic cells, RAGE is expressed at relatively low levels in a wide variety of differentiated adult cells such as neutrophils, monocytes-macrophages, lymphocytes, cardiac myocytes, neurons, dendritic cells and vascular endothelial cells under normal physiological conditions [87,93,94]. However, under pathological conditions the accumulation of RAGE ligands and inflammatory mediators result in RAGE up-regulation [90,94,95]. Conversely, RAGE is found to be abundantly expressed at high levels in alveolar type I epithelial cells and alveolar type II cells of lungs in adults [96,97]. However, the exact role or function of this high expression in the physiology of these cells remains poorly defined.

RAGE structure

RAGE is comprised of three parts: an extracellular region, a transmembrane region and a short cytoplasmic tail (Figure 3) [85]. The extracellular region is made up of three Ig-like domains: one variable (V)- type domain and two constant (C)-type-domains [86]. Two N-glycosylation sites are found on the V domain which is responsible for most ligand binding to the extracellular region [98]. Following the extracellular region is a single transmembrane domain

which functions to anchor the receptor to the cell membrane [99]. The cytoplasmic tail is important for signal transduction into the cell [100], even so no phosphorylation sites, G-protein binding sites or kinase binding sites are known to be present on the cytoplasmic tail of the receptor [90,101,102].
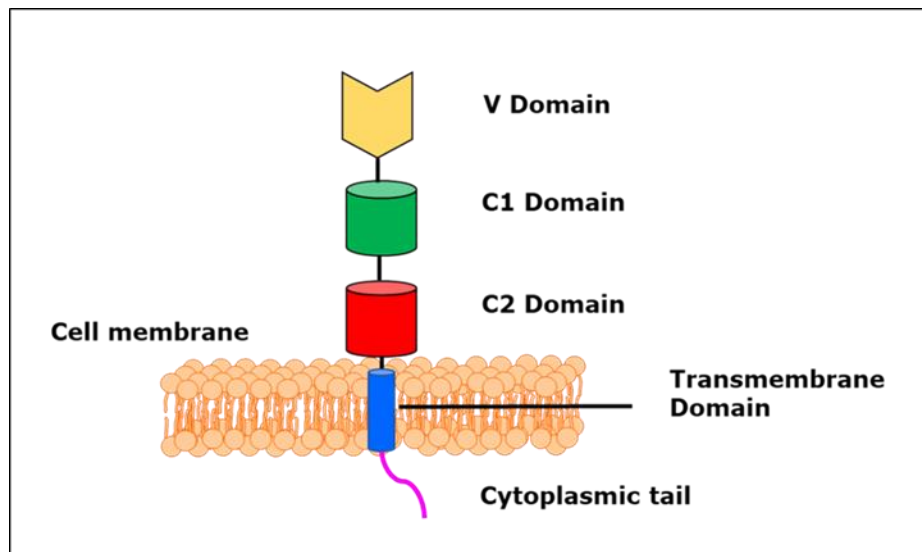
Figure 3: Schematic representation of RAGE and its domains.
RAGE is comprised of (i) an extracellular region composed of three immunoglobulin (Ig) like domains: V-domain, C1-domain, C2-domain;(ii) a transmembrane domain and (iii) an intracellular cytoplasmic domain.

RAGE variants

The full-length form of RAGE (FL-RAGE) is composed of 3 parts: extracellular, transmembrane, and cytosolic regions [85,103]. Besides FL-RAGE, a number of splice variants have been identified both at mRNA and protein levels for human RAGE [101]. The isoforms of RAGE are characterized by truncations at either the N-terminal or C-terminal, and the most prevalent isoforms are the N-truncated, dominant-negative and soluble RAGE forms [85]. The V-domain is absent in the N-truncated isoform, thereby preventing any interaction with most ligands [104] The dominant-negative isoform lacks the cytosolic domain, as a result there is no signal transduction even so it can interact with the ligands [105]. Soluble RAGE (sRAGE) is

11

formed when RAGE lacks the transmembrane domain and the cytoplasmic tail (Figure 4) [106]. This isoform of RAGE is formed by either alternative mRNA splicing or proteolytic cleavage of FL-RAGE [88,107,108]. sRAGE can be secreted out of the cell, where it interacts with the ligands and prevent their binding to FL-RAGE thereby serving as a decoy receptor [106,109]. Hence, soluble RAGE can be utilized to inhibit the effects of RAGE ligands and thereby prevent RAGE signaling in human diseases [109,110]. It has also been proposed that sRAGE does not act as a simple competitor but reduces activation of FL-RAGE by disturbing the preassembly of the receptor on the cell surface. The interaction of sRAGE with membrane bound FL-RAGE could result in formation of heteromultimers which would not be competent for signaling, as sRAGE is devoid of the cytoplasmic domain [111].

Apart from the three predominant isoforms of RAGE, so far about 20 different splice variants for human RAGE have been described [112]. However, human RAGE splicing is highly tissue specific and a lot of these variants are subjected to degradation by the nonsense-mediated mRNA decay (NMD) pathway, before they can be expressed as proteins [106,113]. Some of these variants might be expressed as proteins, but eventually undergo degradation as they lack the signal sequence on exon 1 [112,114]. Hudson *et al* summarized all the isoforms of human RAGE according to the Human Gene Nomenclature Committee [106]. Similarly, Murine fl-RAGE mRNA undergoes alternative splicing as well and so far about 17 mRNA splice variants have been identified [115]. Splice variants of murine RAGE are also expressed in a tissue specific manner and many of them undergo degradation by NMD pathway [115,116].
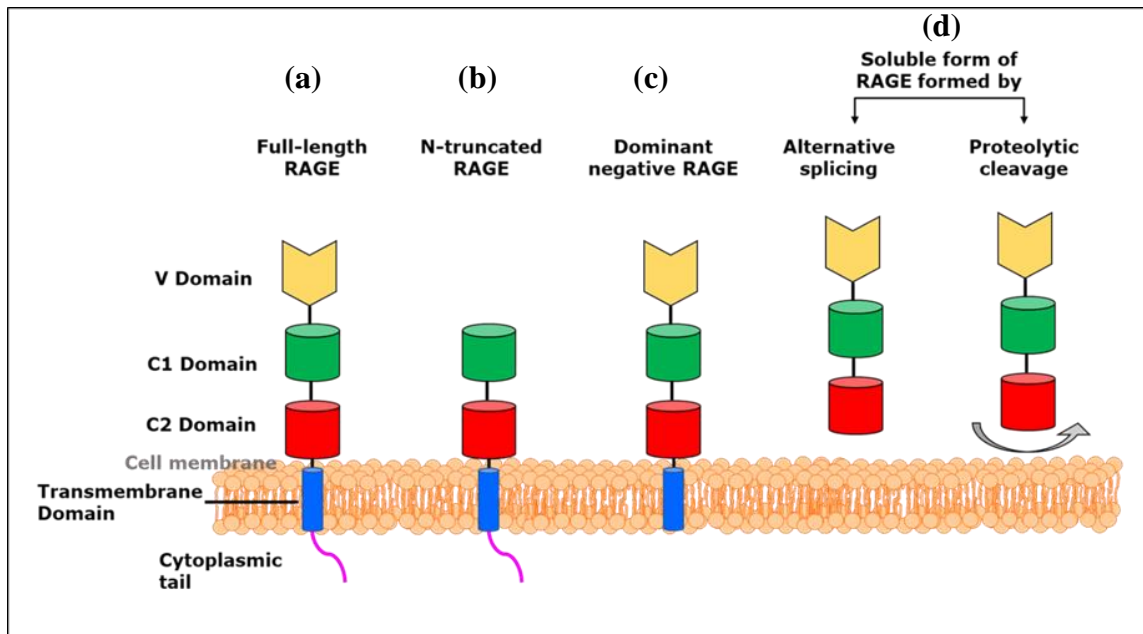
Figure 4: Structures of RAGE and its isoforms.
(a) full-length RAGE, (b) N-truncated RAGE, (c) Dominant-negative RAGE, (d) Soluble form of RAGE. The N-truncated isoform lacks the V-domain. The dominant-negative form has no cytosolic domain. Soluble isoform of RAGE is formed either by alternative splicing or cleavage by proteases and is secreted and thereby prevents binding of ligands to RAGE. Adapted from [117]

Ligands of RAGE

RAGE ligands belong to different families. RAGE was originally discovered as the cell surface receptor for advanced glycation end-products (AGEs) [117]. AGE molecules tend to accumulate in pathological conditions such as oxidative stress, vascular complications and diabetes and bind to RAGE to alter cellular properties [118,119]. Amyloid-β peptide (which accumulates in Alzheimer's disease) and amyloid A (which accumulates in systemic amyloidosis) are also known ligands of RAGE [120,121]. Some other ligands of RAGE belong to the S100 family of calcium-binding proteins which are found extracellularly at sites of inflammation [122]. RAGE is also known to interact with damage associated molecular patterns (DAMPs) such as HMGB1 (amphoterin), which is a DNA binding protein and is released by

13

necrotic cells under conditions of stress [123]. Besides these ligands, RAGE also recognizes specific pathogen associated molecular patterns (PAMPs) such as lipopolysaccharides (LPS) on the surface of bacteria [124], prions [125], and Mac-1 in leukocytes [126]. Since RAGE is able to recognize a common pattern within its different ligands, it is considered a pattern recognition receptor (PRR) [126]. The various ligands of RAGE are listed in Table 2.

Table 2: Various ligands of RAGE.
Taken from [127]

Ligand	Description	Potential role
Advanced glycation endproducts (AGEs)	Heterogeneous group of molecules derived from glycation of proteins	Diabetic complications, atherosclerosis and cardiovascular disorders, chronic inflammatory diseases, cancer
S100 proteins: S100B, S100P, S100A1, S100A2, S100A4. S100A6, S100A8/A9, S100A12, S100A13	Large group of small calcium-binding proteins	Inflammation, neurodegeneration, differentiation and cell growth, including cancer
High-mobility group box-1 protein (HMGB1)	Nuclear DNA-binding protein, extracellular HMGB1	Inflammation, cancer
Amyloid β and amyloid fibrils	Form insoluble extracellular aggregates	Alzheimer disease
β-2 integrin Mac-1	Surface receptor (CD11b/CD18) involved in leukocyte adhesion and migration	Inflammation
Glycosaminoglycans (including chondroitin sulfate, dermatan sulfate and heparan sulfate)	Attached to proteoglycans at the surface cells	Malignant transformation, metastasis
Lysophosphatidic acid	RAGE required for lysophosphatidic acid signaling	Regulation of proliferation, survival, motility and invasion of (cancer) cells

AGEs were the first identified ligands of RAGE [117,128]. AGEs are formed as a result of non-enzymatic reaction between the aldehyde group of glucose and amino groups of amino acids in proteins, leading to formation of Amadori products [129]. The most common AGE found *in vivo* is N carboxymethylysine (CML), which is formed by the glycation of a lysine residue [128]. The early glycation product are further oxidized, dehydrated and cross-linked to yield highly heterogeneous AGEs which accumulate during stress and chronic inflammation [130]. Accumulation of AGEs also occurs in various pathological conditions such as diabetes [131], renal failure [132] as well as during the process of aging [117]. The tumor microenvironment is favorable for generation of AGEs as there is higher uptake of glucose [133]. Recent research aims at investigating the contribution of AGEs in mediating cancer progression [134]. AGEs can mediate their biological function through their receptors. The interaction of AGEs and RAGE can trigger multiple signaling pathways which are involved in inflammation and tumorigenesis [135,136]. AGE-RAGE interaction stimulates activation of NADPH-oxidase and leads to formation of ROS, which further activates NF-κB [137]. AGE-RAGE interaction in different cell types also triggers activation of ERK1/2, p38 MAPK, CDC42/RAC, SAPK/JNK [138,139]. In a study investigating the association between diabetes mellitus and renal cell carcinoma, AGEs were reported to stimulate tumor cell growth, through autocrine secretion of interleukin-6 [140]. In melanoma, AGEs were found to stimulate melanoma cells growth and migration, and anti-RAGE antibodies showed improved survival by inhibiting tumor formation in athymic mice [141]. Another study reported that AGE-RAGE interaction promoted human pancreatic cancer cell proliferation through the autocrine induction of platelet-derived growth factor-β (PDGF-β) [142]. These results suggest that AGEs stimulate cancer cell proliferation by binding to RAGE. However, several other RAGE ligands may also

15

be involved in affecting tumor growth, thus the specific contribution of AGEs is yet to be explored.

The S100 proteins are a family of more than 20 small, calcium binding proteins which are exclusively expressed in vertebrates [143]. The S100 proteins are known to regulate various intracellular functions such as calcium homeostasis, cell growth and differentiation, cytoskeleton organization and energy metabolism [144]. However, S100 proteins were also found to be released from different cell types such as astrocytes [145], neurons [146], microglia [146], neutrophils [147], monocytes-macrophages [148] or Schwann cells [149] during inflammation. Some of the S100 proteins secreted include S100B [145], S100A4 [150], S100A8 [147], S100A9 [151], S100A12 [147], S100A13 [152] and S100P [153]. Many of the S100 proteins were found to interact with RAGE [154]. For example, S100A4 [150], S100B [149] and S100P [153] have clearly been shown to mediate their functions *via* RAGE activation. However, several other S100 proteins have been found to not mediate their functions by binding to RAGE [154].

Several members of the S100 family are implicated in cancer [155]. Here, only S100P will be described in detail. S100P was identified, purified from placenta and characterized in 1992 [156]. Expression of many of the S100 family members is dysregulated in human cancers, with each type of cancer showing a unique S100 profile [157]. S100P gene has been found to be expressed in pancreatic cancer [158], breast cancer [159], colon cancer [160], prostate cancer [161], and has been associated with poor clinical outcomes. Expression of S100P is specific to pancreatic cancer cells and was not found in samples of chronic pancreatitis [158]. Increase in S100P expression has been correlated with increasing grade of PanIN lesions, being expressed at much higher levels in PanIN-2 and PanIN-3 than in PanIN-1 lesions [162]. Ectopic expression of S100P in Panc-1 pancreatic cancer cells resulted in increased cell proliferation, migration,

invasion and survival *in vitro*. Also, over-expression and silencing of S100P in pancreatic cancer cells directly correlated with increased or decreased pancreatic cancer tumor growth respectively [163]. S100P is known to mediate its effects through activation of RAGE leading to stimulation of MAP kinase and NF-κB pathway in pancreatic cancer [153]. Blocking the interaction of S100P with RAGE with cromolyn inhibited tumor growth and sensitized the tumor cells to gemcitabine in an orthotopic model of pancreatic cancer [164]. Therefore, blocking the ability of S100P to activate RAGE could be used for therapeutic intervention in pancreatic cancer.

High mobility group box-1 (HMGB1) also known as amphoterin, is a nuclear DNA-binding protein [165]. HMGB1 is composed of three distinct domains: two tandem HMG box domains (A box and B box), which are spaced by a short flexible linker, and a 30 amino acid long C-terminal tail [166]. HMGB1 binds to the minor groove of DNA by the A box and B box and the unique conformation of the A and B box domains likely plays an important role in the way HMGB1 interacts with chromatin [167]. Thus, the nuclear, chromatin-associated HMGB1 acts as a transcriptional regulator because of its ability to bend the DNA [167]. In recent studies, intracellular HMGB1 has been shown to be involved in initiation of autophagy and inflammasome activation [168,169]. In addition to these intracellular functions, the current focus is at the extracellular functions of HMGB1 which is released from cells and mediates activation of innate immune responses, including chemotaxis and cytokine release [170,171]. HMGB1 can be released in 2 ways: active secretion from inflammatory cells (e.g., monocytes and macrophages) [172] or passive release from necrotic but not apoptotic cells [173]. It is evident that HMGB1 plays different roles in different compartments of the cell. HMGB1 when released extracellularly, binds to cell surface receptors to exhibit inflammatory responses. In 1995, RAGE was the first identified receptor for HMGB1 [123]. The consequences of HMGB1-RAGE

interaction were initially known, but it was later discovered that HMGB1-RAGE signaling regulates several cellular functions like chemotaxis and migration, proliferation, and differentiation of immune and cancer cells and upregulation of cell-surface receptors and autophagy [174]. Additionally, RAGE was also involved in the cross-talk between HMGB1 and other cell surface receptors. For instance, in dendritic cells crosstalk between RAGE and TLR9 was critical for HMGB1 mediated immune response [175]. Another study showed that HMGB1 mediated inflammatory cell recruitment and activation required functional interplay between Mac-1 and RAGE [176]. Some other important receptors of HMGB1 include TLR 2 [177], TLR 4 [178], and TLR 9 [175], syndecan-4 [179], CD24-Siglec-10 [180], CXCR4 [181], T cell IgG mucin-3 [182] and certain integrin [183]. The most commonly activated downstream signaling pathways by HMGB-1-RAGE interaction are Erk-1/2 [184], JNK [185], and NF-κB [186]. Taguchi *et al* reported that when rat glioma cells, stably transfected with mutated RAGE constructs, were injected into nude mice; a significant reduction in tumor growth and metastasis was observed [187]. They also demonstrated that blocking the interaction between HMGB1 and RAGE led to a reduction in cell proliferation, migration, and invasion *in vitro* [187]. In pancreatic cancer, depletion of HMGB1 in pancreatic tumor cell made them more sensitive to induced apoptotic cell death. Furthermore, targeted knockdown of *RAGE* in pancreatic tumor cells resulted in increased apoptosis, reduced autophagy and decreased tumor cell survival [188]. Therefore, inhibition of HMGB1-RAGE interaction could be used as strategy to reduce tumor growth in pancreatic cancer.

RAGE signaling

As mentioned before, RAGE is expressed in different cell types at different levels and it interacts with numerous ligands. RAGE is activated by interaction with its ligands and can

stimulate various downstream signaling pathways (Figure 5). For instance, the ERK1/2

(p44/p42) MAP kinases are stimulated in smooth muscle cells [138], tubular epithelial

myofibroblasts [189], monocytes [190] and few other cell types [191] because of RAGE

activation. RAGE has also been linked to stimulation of the JAK/STAT pathway in NRK-49F

(rat kidney fibroblast) cells [192]. RAGE activation in monocytes and tumor cells resulted in

stimulation of p38 and SAPK/JNK MAP kinases [187,193]. Rho-GTPases, Rac-1/Cdc42 and

phosphoinositol-3-kinase have also been associated with RAGE signaling [100,194]. RAGE–

ligand interaction can also induce reactive oxygen species (ROS) generation through NADPH

oxidases and other routes [119]. Subsequently, these signaling pathways lead to the activation of

proinflammatory transcription factors such as NF-κB [195,196], AP-1 [197] and STAT-3

[198,199]. As a result, these transcription factors lead to expression of target genes that regulate

cell proliferation, migration and cell survival [200]. All these characteristics of RAGE are

responsible to initiate cellular dysfunction in several pathophysiologic situations. Hence, it is

complex to understand the consequences of RAGE signaling as different ligands stimulate

different pathways which are specific to certain cell types [111].
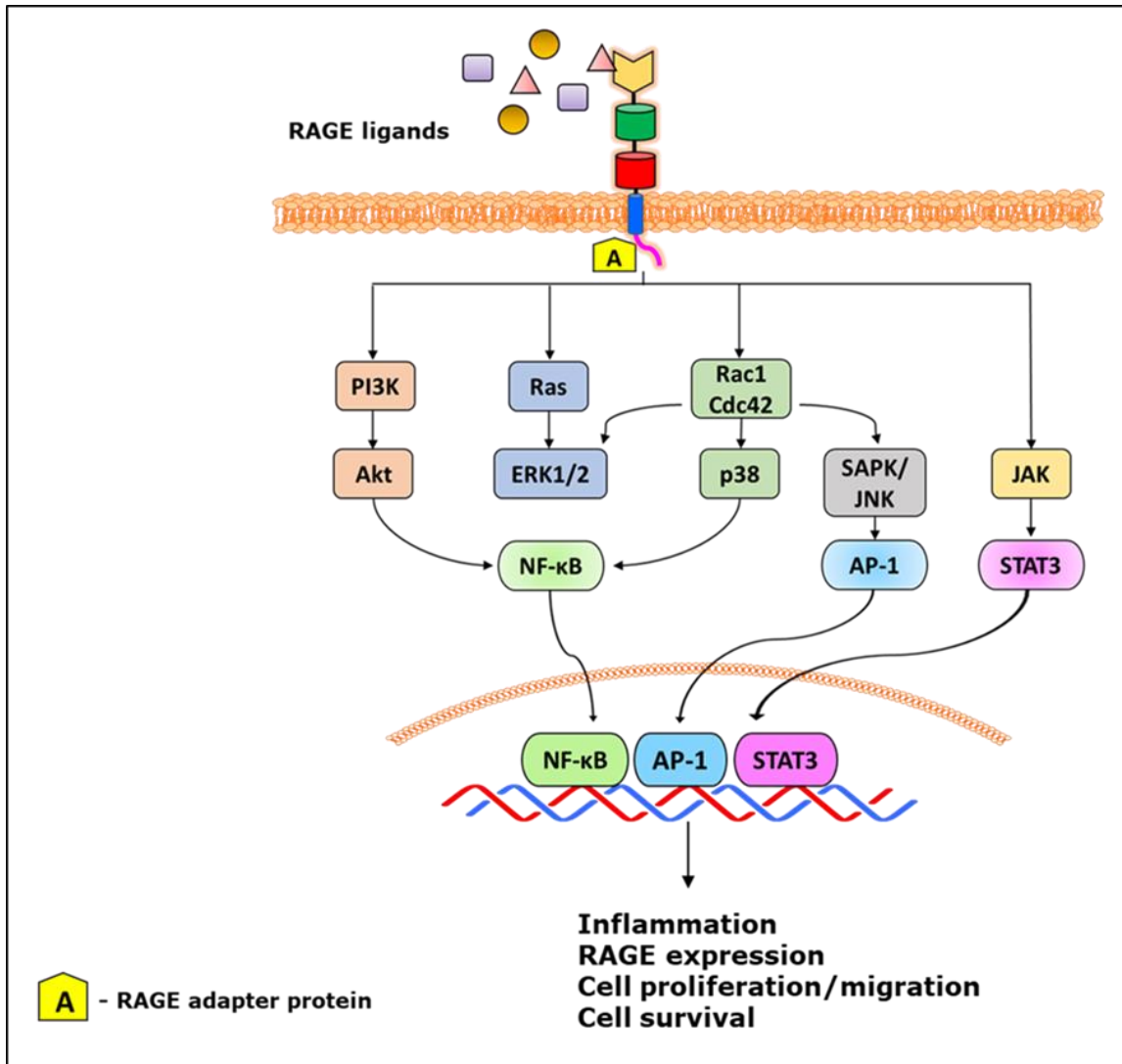
Figure 5: RAGE interacts with a variety of ligands.
The interaction of ligand and RAGE stimulate conformational changes in the intracellular domain of RAGE leading to interaction with its intracellular adapter proteins. RAGE activation of these signaling pathways leads to changes in gene expression and altered cellular function including migration, survival, inflammation, and upregulation of RAGE expression itself. Adapted from [204]

HYPOTHESIS AND APPROACH

The aim of this study was to understand the role of RAGE in pancreatic cancer.

RAGE activation has been associated with several diseases including diabetes, neurodegenerative disorders and cancer [111,201,202]. There has been growing evidence demonstrating the significance of RAGE in pancreatic cancer [188,203,204]. Engagement of RAGE with its ligands leads to activation of many intracellular signaling pathways, leading to increased pancreatic cancer cell proliferation, motility and survival [153,163,188]. The specific role of RAGE in regulating proliferation [205,206], cell migration and invasion [207,208] has previously been reported in other cancers, but has not been described in pancreatic cancer yet.

In the current study we investigated the effect of RAGE over-expression on two cellular properties of pancreatic cancer cells: proliferation and migration. We hypothesized (Hypothesis I) that RAGE over-expression could lead to the alteration of cellular properties of pancreatic cancer cells thereby contributing to the growth of pancreatic tumors.

To test our first hypothesis, we selected PANC-1 pancreatic cancer cell-line. In chapter 1 we performed a stable transfection of PANC-1 cells to generate RAGE over-expressing cells. Further we characterized those cells for the level of RAGE expression by real-time PCR, Western Blot and ELISA.

In chapter 2 we investigated the effect of RAGE over-expression on the cellular properties of PANC-1 cells. To accomplish our goal, we performed several cell-based assays. For instance, to compare the effect of RAGE over-expression on cellular proliferation, we used two independent methods: Alamar Blue assay and Trypan Blue exclusion method. To determine the effect of RAGE over-expression on the migratory properties we performed the Boyden Chamber assay and the Wound Healing assay. In addition, we also investigated the downstream

signaling pathways that could have been altered as a consequence of RAGE over-expression by Western blot.

Recent studies have reported that RAGE promotes pancreatic tumor cell survival by supporting autophagy and limiting apoptosis following oxidative injury or chemotherapy [209,210]. Another study demonstrated that RAGE played a crucial role in development of resistance to chemotherapy and radiotherapy by interacting with HMGB1 released from dying tumor cells, thereby resulting in enhanced cell survival [188]. Gemcitabine, which is used as a standard of care in pancreatic cancer, faces a major challenge of development of chemoresistance. Based on the published literature, we reasoned that RAGE could be involved in mediating resistance against gemcitabine in pancreatic cancer. Thus, we hypothesized (Hypothesis II) that the combination of RAGE inhibitors with gemcitabine could be more effective than gemcitabine alone in suppressing tumor growth in pancreatic cancer.

To test our hypothesis, we compared the combination of two RAGE inhibitors (anti-RAGE monoclonal antibody IgG2A11 and small molecule FPS-ZM1) with gemcitabine. In chapter 3, we tested these combinations in an orthotopic mouse model of pancreatic cancer. This model was generated by implanting syngeneic KPC cells in the pancreas of C57Bl/6 mice. The tumor bearing mice were then treated with either the RAGE inhibitor alone, gemcitabine alone or the combination of RAGE inhibitor and gemcitabine. Tumor growth was assessed by determining tumor weights of tumors obtained from different groups at the end of the study.

CHAPTER 1: GENERATION AND CHARACTERIZATION OF A RAGE OVER-EXPRESSING HUMAN PANCREATIC CANCER CELL LINE

Abstract

The objective of this chapter was to generate a pancreatic cancer cell model to study the effect of RAGE over-expression on important cellular properties such as proliferation, migration, wound healing in human pancreatic cancer cell-lines. In order to accomplish this, the first step was to generate RAGE over-expressing human pancreatic cancer cell lines and subsequently to characterize them for the presence of RAGE. For our study, we selected the human pancreatic cancer cell line PANC-1 because these cells express very low levels of RAGE by themselves. We stably transfected PANC-1 cells with a pcDNA3 plasmid encoding for full length RAGE (FL-RAGE) and selected the transfected cells using G418. We obtained two clones of PANC-1 cells (PANC-1 FLR2 and PANC-1 FLR3) and these cells were characterized in terms of the level of RAGE expression as well as of the cellular localization of RAGE.

The transcript levels of RAGE in the transfected cells were measured by real-time PCR. We compared the protein levels of RAGE qualitatively by western blotting and immunoprecipitation. Quantification of the protein levels of RAGE in the cells was performed by ELISA. The clones selected from the transfection exhibited about 5-fold higher levels of RAGE as compared to the wild type (WT) PANC-1 cells. Immunofluorescence staining indicated that RAGE was present not only on the cell surface but was also localized in the cytoplasm. In conclusion, we successfully generated a cellular model to understand the effect of RAGE over-expression on the cellular properties of the pancreatic cancer cells.

Introduction

Pancreatic cancer is one of the most lethal types of cancer with continuously growing rates of incidence and mortality worldwide each year. At present pancreatic cancer is the fourth leading cause of cancer mortality in the US [2]. Only about 20% of the patients with pancreatic cancer have tumors confined to the pancreas and are candidates for surgical resection [211]. Although it is not among one of the most prevalent cancers, it is one of the deadliest malignancies, with a 5 year survival of less than 10% [4]. The poor survival rate can be attributed to the delay in diagnosis and the lack of effective therapy for pancreatic cancer [4]. Over the last decade there has been no significant improvement in the clinical outcome and the impeded progress in patient outcome can be attributed to the aggressive nature of pancreatic cancer. There are several characteristics that define the aggressive biology of pancreatic cancer and which contribute to the development of resistance to therapy. Some of the distinct characteristics of pancreatic tumors are excessive and dense desmoplastic stroma [212,213], altered metabolism [214,215] poor vascularization [216] and hypoxia [217]. As described earlier, pancreatic ductal adenocarcinoma (PDAC) develops from noninvasive precursor lesions called pancreatic intraepithelial neoplasia (PanIN) and gradually progresses through severe stages of cellular atypia to aggressive PDAC commonly referred to as pancreatic cancer [46]. Examination of human pancreatic cancer cell lines and tumor specimens has revealed various signature genetic abnormalities such as mutations in *K-Ras* oncogene [22,218] and *p16/CDKN2A* [36], *TP53* [29], *SMAD4* [219] tumor suppressor genes associated with these pancreatic lesions [21]. Lately, several reports have identified RAGE as a key player in pancreatic cancer progression. An important study described the role of RAGE in the development and progression of pancreatic cancer, by utilizing mice with conditional oncogenic *KRAS* mutation in the pancreas

24

(KC mice) [220]. The authors reported that RAGE expression was found to increase with advancing stages of pancreatic PanIN lesions in KC mice [203]. Further, the authors demonstrated that targeted ablation of RAGE delayed the development and progression of PanIN lesions in KC mice lacking RAGE (Pdx1-Cre:KRAS$^{G12D/+}$ RAGE-/-) [203].

RAGE belongs to the immunoglobulin family of cell surface receptors. It is found to be substantially expressed in many cell types during embryonic stages, but the expression is significantly subjugated upon development in most tissues except a few including type I alveolar cells in the lung [90,200]. However, RAGE is remarkably upregulated in various types of cells under different pathological conditions [201,221]. Wang *et al* investigated the expression status of RAGE in gastric cancer and observed a prominent upregulation of RAGE in human gastric cancer tissues in comparison to normal gastric epithelium [222]. Another report demonstrated that RAGE was over-expressed in ovarian cancer tissue when compared to non-cancerous ovarian tissue [223]. In another study, RAGE was shown to be over-expressed in lymph node samples from chronic lymphocytic leukemia patients and was also associated with poor clinical outcome [224]. Several other studies have demonstrated that activation of RAGE by its ligands mediates cancer cell proliferation, survival and invasion *in vitro* as well as *in vivo*. As described earlier, HMGB1 and S100P are among the primary ligands of RAGE. It has been shown that HMGB1 induced increase in levels of RAGE in pancreatic tumor tissue as compared to normal tissue [188]. The authors also reported that targeting HMGB1/RAGE axis by either pharmacological inhibition of HMGB1 or by RAGE knock-down, resulted in reduced tumor growth [188]. In a study in human pancreatic cancer cell-lines PANC-1 and BxPC3, RAGE activation by S100P was shown to stimulate cell proliferation, survival, migration and invasion in *in vitro* experiments [163]. The role of RAGE in pancreatic tumor progression was also

demonstrated by deletion of RAGE, which resulted in reduced number of pancreatic lesions and longer survival of mice [204]. It has been shown that RAGE favors pancreatic tumor cell survival during chemotherapy and oxidative stress by supporting autophagy [210,225]. Logdson *et al* group demonstrated that blocking the RAGE/S100P interaction with either a S100P-derived antagonistic peptide or the small molecule S100P-binding drug cromolyn resulted in reduced growth, invasiveness and viability for the pancreatic cancer cell lines as well as reduced tumor growth and metastasis formation in orthotopic mouse models of pancreatic cancer [7]. In a different study, these authors demonstrated that RAGE contributed significantly to resistance to chemo- and radiotherapy through the release of HMGB1 by dying cells, resulting in sustained activation of RAGE and cell survival through a positive feedback loop involving NF-κB. The HMGB1/RAGE axis was also shown to control the bioenergetics of pancreatic-cancer cells [8]. RAGE signaling from stromal cells could significantly contribute to tumor development. Indeed, RAGE is expressed in many cells that form the tumor environment, such as endothelial cells, fibroblasts, myofibroblasts, T cells and myeloid-derived suppressor cells [4]. Among these cells, tumor-associated myofibroblasts have been shown to be responsible for the desmoplastic reactions that are characteristic of pancreatic tumors. Because of its expression in both cancer and stromal cells, RAGE appears to be a promising therapeutic target for pancreatic cancer.

All the above-mentioned studies have demonstrated the role of RAGE upregulation in driving tumor growth and facilitating tumor cell survival. However, the direct influence of RAGE on the proliferative and migratory properties of pancreatic cancer cell lines has not been not reported yet. To address this, we intended to generate a model cell-line to study the effect of over-expression of RAGE in pancreatic cancer cells.

The role of a protein in a cell can be studied by 2 approaches: (i) over-expressing the protein in cells which express low level of the protein (ii) knocking down the protein in cells which express elevated levels of the protein. For our study, we used the first approach. We chose PANC-1 cells which express low levels of RAGE and stably transfected them with a plasmid coding for FL-RAGE to obtain variant cell lines expressing higher levels of RAGE. In this chapter, we describe the generation of two human pancreatic cancer cell-lines derived from PANC-1 cells that moderately over-expresses RAGE. Further, we describe how these RAGE over-expressing PANC-1 cells were characterized by determining the expression of RAGE at transcript and protein levels. We further illustrate the localization of RAGE in these cells.

Materials and Methods

Cell culture

The human PANC-1 pancreatic cancer cells were purchased from American Type Culture Collection (ATCC, Manassas, VA) and were grown and maintained in DMEM (ATCC) supplemented with 10% FBS (ATCC), penicillin (100 U/ml) and streptomycin (100 µg/ml) (GE Healthcare Life Science, Pittsburg, PA) at 37 °C and 5% CO_2.

Stable cell transfection

For the transfection, 5×10^4 cells per well were seeded in each well of a 24-well plate. The cells were transfected with a pcDNA3 plasmid coding for full-length RAGE (pcDNA3-FLRAGE, kindly provided by Dr. C.W. Heizmann, Children's Hospital, Zurich, Switzerland) using Lipofectamine 2000 (Invitrogen/Thermo Fisher Scientific). After 2 days of transfection, the cells were transferred to a 6-well plate and allowed to grow. After 24 hours, selection of the transfected cells was started using 250 µg/ml G418 (Corning, Manassas, VA, USA) which went for a period of 8 weeks. The selected cells were expanded and eventually subjected to serial

dilution, to obtain single cell colonies. Two single-cell colonies were picked through this selection and named PANC-1 FLR2 and PANC-1 FLR3. These RAGE over-expressing PANC-1 clones were maintained in DMEM supplemented with 250 µg/ml G418 at 37 °C and 5% CO_2.

Real-time PCR

RAGE transcript levels were determined by real-time PCR. Total RNAs were extracted from the transfected and wild type cells using a commercial RNA extraction kit (Life Technologies, Carlsbad, CA, USA) following manufacturer's instructions. The quality of the RNA was assessed by absorbance spectroscopy and by agarose gel electrophoresis. The RNAs (50 ng/µl) were reverse transcribed into cDNA using reverse transcription reagents from Promega (Madison, WI, USA). The RT-PCR was run with 10 ng cDNA per well on a Stratagene Mx3000p thermocycler using the 5x HOT FIREPol EvaGreen qPCR Mix Plus (ROX) (Mango Biotechnology, Mountain View, CA, USA) using appropriate primers. The β-actin gene was used as the housekeeping gene. The forward (fwd) and reverse (rev) primers used to detect the transcripts of actin and RAGE were: β-actin fwd: CATGTACGTTGCTATCCAGGC, β-actin rev: CTCCTTAATGTCACGCACGAT; RAGE fwd: TGTGTGGCCACCCATTCCAG, RAGE rev: GCCCTCCAGTACTACTCTCG. The following RT-PCR program used: 15 min at 95 °C followed by 40 cycles of 15 sec at 95°C, 20 sec at 60 °C, 20 sec at 72 °C. A melting curve was recorded at the end of the cycles to evaluate the quality of the amplified products. The fold (F) of change in gene expression was calculated for each gene using the ΔΔCt method with $F = 2^{(\Delta\Delta Ct)}$ and $\Delta\Delta Ct = \Delta Ct_{RAGE} - \Delta Ct_{WT}$. $\Delta Ct = Ct_{gene} - Ct_{actin}$ for PANC-1 cells over-expressing RAGE (ΔCt_{RAGE}) and wild-type (WT) (ΔCt_{WT}). The experiments were run in triplicate using cDNAs obtained from three independent RNA preparations. The standard deviations were calculated for the fold of changes in gene expression.

Western blot

Cells (~70 % confluent) were washed with ice cold PBS and detached using trypsin or a cell scraper. Cell scraper was used to detach cells while preparing cell extracts for detection of cell surface proteins. For detection of all the other proteins, trypsin was used for detaching cells. The detached cells were collected and centrifuged at 1500 rpm to obtain a cell pellet. The cells were lysed with a cell disruption buffer provide in Paris Kit (Life Technologies, Carlsbad, CA, USA). Protein concentrations were determined using the Bicinchoninic Acid (BCA) Protein Assay Kit (Pierce, Rockford, IL, USA). 50μg proteins were then resolved on 12% SDS PAGE and transferred onto a nitro-cellulose membrane. The blot was blocked with 5% milk powder in TBS-T (Tris-buffered saline with 0.1% Tween-20) for 1 hour at room temperature. The blot was incubated with a goat polyclonal anti-RAGE antibody (sc-8230 Santa Cruz Biotechnology, Dallas, TX, USA) at 1:500 dilution, overnight at 4°C. After three washes (10 minutes each) with TBS-T, the blot was incubated with horseradish peroxidase (HRP) conjugated secondary antibody (705-035-147, Jackson Immuno Research, West Grove, PA, USA) at a dilution of 1:50,000 at room temperature for 1 hour. Proteins were detected using Clarity western ECL substrate (BIO-RAD, Hercules, CA, USA) and normalized to β-actin detected using β-actin (sc-1616, Santa Cruz Biotechnology, Dallas, TX, USA) at 1:500 dilution. The Western blots were performed at least three times.

For detection of protein by chemiluminescence, X-ray films were used. The HRP enzyme catalyzes the conversion of chemiluminescent ECL substrate to a light emitting product which is captured as a signal on the X-ray film. The signal for the protein of interest was then quantified by ImageJ software.

Immunoprecipitation

Cells (~70 % confluent) were washed with ice cold PBS, detached using a cell scraper, centrifuged at 1500 rpm to obtain a cell pellet. To lyse the cells, ice-cold RIPA (radioimmunoprecipitation) lysis buffer (Pierce, Rockford, IL, USA) was added to the pellet. To prepare the protein G sepharose, 30 µl of protein G Sepharose beads (GE Healthcare, Uppasala, Sweden) were taken in a 1.5 ml Eppendorf tube and washed with 1X PBS 3 times. The beads were then incubated with 1.5-2 µg of RAGE antibody (sc-80653, Santa Cruz Biotechnology, Dallas, TX, USA) at 4 °C for 4 h on a rocker. Subsequently, 100 µl of each cell lysate was added to the antibody-sepharose beads mixture and incubated overnight at 4 °C with gentle shaking. To test for any non-specific interaction between RAGE and protein G Sepharose beads, the beads were incubated with 100 µl of each cell lysate to serve as a control. Following incubation, the lysate-antibody-beads and lysate-beads mixture were washed 3 times (10 minutes) with 1X PBS. 15 µl of each, the lysate-antibody-beads and lysate-beads mixture were boiled with 5X SDS loading buffer to elute the proteins before SDS-PAGE electrophoresis. The proteins were resolved on a 12% SDS-PAGE gel by running at 150 V for 80 minutes. The proteins were then transferred on a PVDF membrane at 300 mA for 70 minutes. The membrane was blocked with Odyssey® blocking buffer (P/N 927-50000, LI-COR, Lincoln, NE, USA) for 1h at room temperature. The primary and secondary antibody dilutions were made in Odyssey® blocking buffer with 0.2% Tween 20, according to the manufacturer's recommendations. The membrane was incubated with the antibody for RAGE (sc-8230 Santa Cruz Biotechnology, Dallas, TX, USA) overnight at 4 °C. After washing the membrane 3 times (10 minutes each) with 1X TBS-T, the membrane was incubated with IRDye 800CW secondary antibody (P/N 926-32214, LI-COR, Lincoln, NE, USA) for 1h at room temperature. The membrane was washed 3 times (10 minutes

each) with 1X TBS-T and scanned on Odyssey® CLx Infrared Imaging System. For loading control, β-actin was detected by loading and running equal amounts of proteins on another SDS-PAGE gel. The bands obtained for RAGE were normalized to those for β-actin (sc-1616, Santa Cruz Biotechnology, Dallas, TX, USA).

Odyssey CLx imaging system works by detecting near-infrared fluorescence. LI-COR IRDye conjugated secondary antibodies are used to detect the target protein. The PVDF membranes were directly scanned on the Odyssey CLx imaging system, and densitometric analysis was performed using the LI-COR Image Studio Software.

ELISA

Protein levels of RAGE were quantified by ELISA. Cells (~70 % confluent) were washed with ice cold PBS and detached using trypsin or a cell scraper, centrifuged at 1500 rpm to obtain a cell pellet. The cells were lysed with a cell disruption buffer provided by Paris Kit (Life Technologies, Carlsbad, CA, USA). Protein concentrations were determined using the BCA Protein Assay Kit. The protein levels of RAGE in the transfected and the wild type cell lines were determined by using Quantikine ELISA Human RAGE Immunoassay kit (R & D System, Minneapolis, MN, USA), following manufacturer's instructions.

Immunofluorescence

The localization of RAGE in PANC-1 cells was examined by fluorescence microscopy. Cells (~70 % confluent) were detached using trypsin, centrifuged at 1500 rpm for 5 minutes and resuspended in growth medium. Cells were counted, and 50,000 cells were seeded in μ-dishes 35 mm (81156, ibidi, Germany) and incubate overnight at 37 °C and 5% CO_2 to allow the cells to attach. Next, the cells were washed 3 times with 1X PBS and fixed with 4% paraformaldehyde for 15 minutes at room temperature. The cells were washed 3 times (10 minutes) with 1X PBS.

For permeabilization, the cells were incubated with 0.1% Triton X-100 solution in PBS for 10 minutes at room temperature. The cells were washed 3 times (10 minutes) with 1X PBS. For blocking, the cells were incubated with 5% goat serum (Thermo Fisher Scientific, Frederick, MD, USA) for 1 hour at room temperature. The cells were washed once with 1X PBS and incubated with the primary antibody for RAGE (sc-80653, Santa Cruz Biotechnology, Dallas, TX, USA) at 1:200 dilution in 1% goat serum overnight at 4 °C. Washing was performed 3 times (10 minutes) with 1X PBS and the cells were incubated with the secondary antibody (315-545-045, Jackson Immuno Research, West Grove, PA, USA) in 1% goat serum at 1:200 dilution for 1 hour at room temperature. After washing the cells 3 times (10 minutes) with 1X PBS, the cells were incubated with Hoechst stain (Life Technologies, Eugene, OR, USA) 1:1000 dilution in PBS for 10 minutes at room temperature, for staining the nuclei. After the final washing, the cells were observed and imaged using Leica Fluorescence Microscope (Leica Microsystems Inc., Buffalo Grove, IL, USA).

Results

Generation of RAGE over-expressing human pancreatic cancer cells derived from PANC-1

After transfection of the PANC-1 cells with pcDNA3_FL_RAGE plasmid, the cells were observed every 24 hours. The cells that did not integrate the plasmid died and detached from the bottom of the wells. Very few cells survived 2 weeks after transfection. The cells that survived were allowed to expand and subsequently seeded in a 96-well plate at the low cell density of 1 cell/well. The plates were observed 24 hours after seeding and the wells containing only 1 cell were marked. The growth of these cells was then followed for 6 weeks. Five independent single cell clones were selected from this procedure. These selected clones were allowed to expand, and

initial screening was performed. After this screening, 2 clones were selected for the study and were named PANC-1 FLR2 and PANC-1 FLR3.

Levels of RAGE transcripts in PANC-1 FLR2 and PANC-1 FLR3

The new cell-lines obtained from the stable transfection were characterized for RAGE expression at transcript level. The Ct (cycle threshold) value is defined as the number of cycles required for the fluorescence signal to exceed background signal. The Ct values obtained after performing the real-time PCR were used to calculate ΔCt values. We obtained $\Delta\Delta$Ct = 3.8 +/- 0.2 for PANC-1 FLR2 and $\Delta\Delta$Ct = 3.7 +/- 0.4 for PANC-1 FLR3. Our results show 13.4 +/- 1.3-fold higher expression of RAGE transcript levels in PANC-1 FLR2 and 14.2 +/-1.1-fold higher levels of RAGE transcripts in PANC-1 FLR3, as compared to PANC-1 WT cells (Table 3).

Table 3: Transcript levels of RAGE

Cell type	Fold change in RAGE expression
PANC-1 FLR2	13.4 +/- 1.3
PANC-1 FLR3	14.2 +/-1.1

Protein levels of RAGE in PANC-1 FLR2 and PANC-1 FLR3

We next compared RAGE expression at protein level in the PANC-1 WT, PANC-1 FLR2 and PANC-1 FLR3 cells by western blot. We used 6 different anti-RAGE antibodies for western blotting (sc-80653, sc-74473, sc-8230, PA1-075, CST-6996, IgG2A11), but only one anti-RAGE antibody, sc-8230, was successful in detecting a band for RAGE. Our western blot results showed a 50 kD band for cell extracts from PANC-1 FLR2 and PANC-1 FLR3, which corresponds to the expected molecular weight of FL-RAGE. However, no band at 50 kD was detected in the PANC-1 WT cell extract. In contrast, we observed a band at 35 kD in PANC-1

WT cell extract, and this band was not observed in PANC-1 FLR2 and PANC-1 FLR3 cell

extracts (Figure 6).
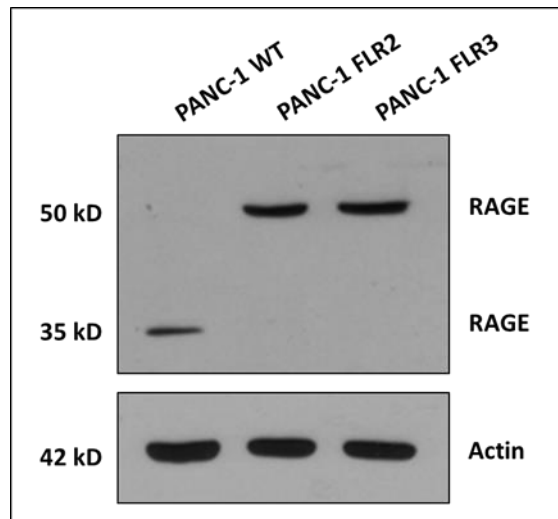
Figure 6: Western blot analysis of PANC-1 WT, PANC-1 FLR2 and PANC-1 FLR3 cell extracts.
A representative blot is shown.

In our experimental conditions, it was difficult to detect a band for RAGE at 50 kD in

PANC-1 WT cells by western blot, even when loading as high as 100 µg protein per lane and

using different anti-RAGE antibodies. Therefore, we chose to immunoprecipitate RAGE from

PANC-1 WT, PANC-1 FLR2 and PANC-1 FLR3 cell-lines. Our results show about 2-fold more

RAGE (50 kD) in PANC-1 FLR2 and PANC-1 FLR3 as compared to PANC-1 WT (Figure 7).
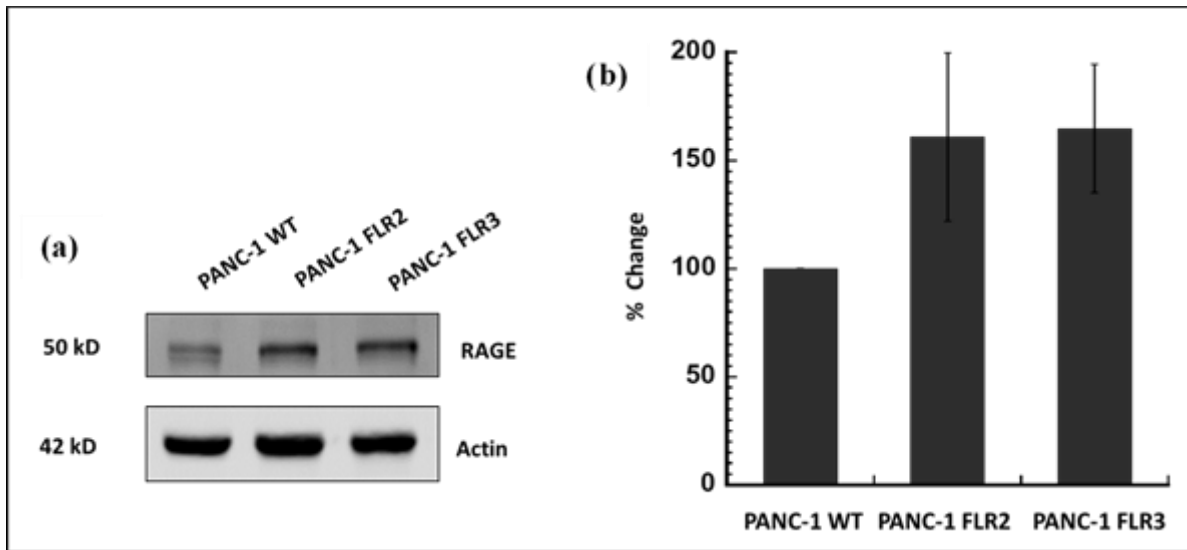
Figure 7: Western blot analysis after immunoprecipitation of RAGE from PANC-1 WT, PANC-1 FLR2 and PANC-1 FLR3 cell extracts.
(a) A representative blot is shown. (b) The relative level of RAGE in PANC-1 FLR2 and PANC-1 FLR3 cells is shown.

Next, in order to quantitatively compare the levels of RAGE between the three cell-lines, we performed a quantitative ELISA. We used a standard curve generated with known concentrations of recombinant human RAGE to determine the concentration of RAGE in the different cell extracts (Figure 8). Using this method, we determined the amount of RAGE present in the three cell-lines. The results from ELISA showed that PANC-1 cells contained 12.1 +/- 1.1 pg RAGE per mg of total protein present in the cell extracts. The levels of RAGE in the PANC-1 FLR2 and PANC-1 FLR3 cell lines were 5.4-fold (65.3 +/- 0.1 pg) and 4.4-fold (53.5 +/- 10.1 pg) higher than those in PANC-1 WT cells, respectively (Table 4).

The results from ELISA are in agreement with the results obtained from the western blot analysis and the results of real-time PCR.
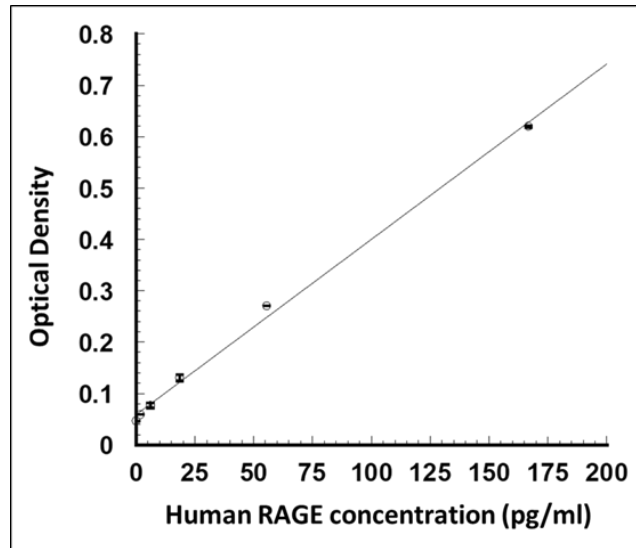
Figure 8: Standard curve for human RAGE ELISA.
A representative curve is shown.

Table 4: Quantification of RAGE in PANC-1 WT, PANC-1 FLR2 and PANC-1 FLR3 cell extracts by ELISA.

Cell type	RAGE levels in pg/mg of total protein
PANC-1 WT	12.1 +/- 1.1
PANC-1 FLR2	65.3 +/- 0.1
PANC-1 FLR3	53.5 +/- 10.1

Immunofluorescence staining in PANC-1 WT and PANC-1 FLR2 cells indicated the presence of RAGE not only at the cell surface but also in the cytoplasm (Figure 9). In our experimental conditions, RAGE expression was observed only in few PANC-1 WT cells, while the expression was observed in all PANC-1 FLR2 cells. In PANC-1 FLR2 cells we also observed puncta like structures which strongly stained for RAGE.
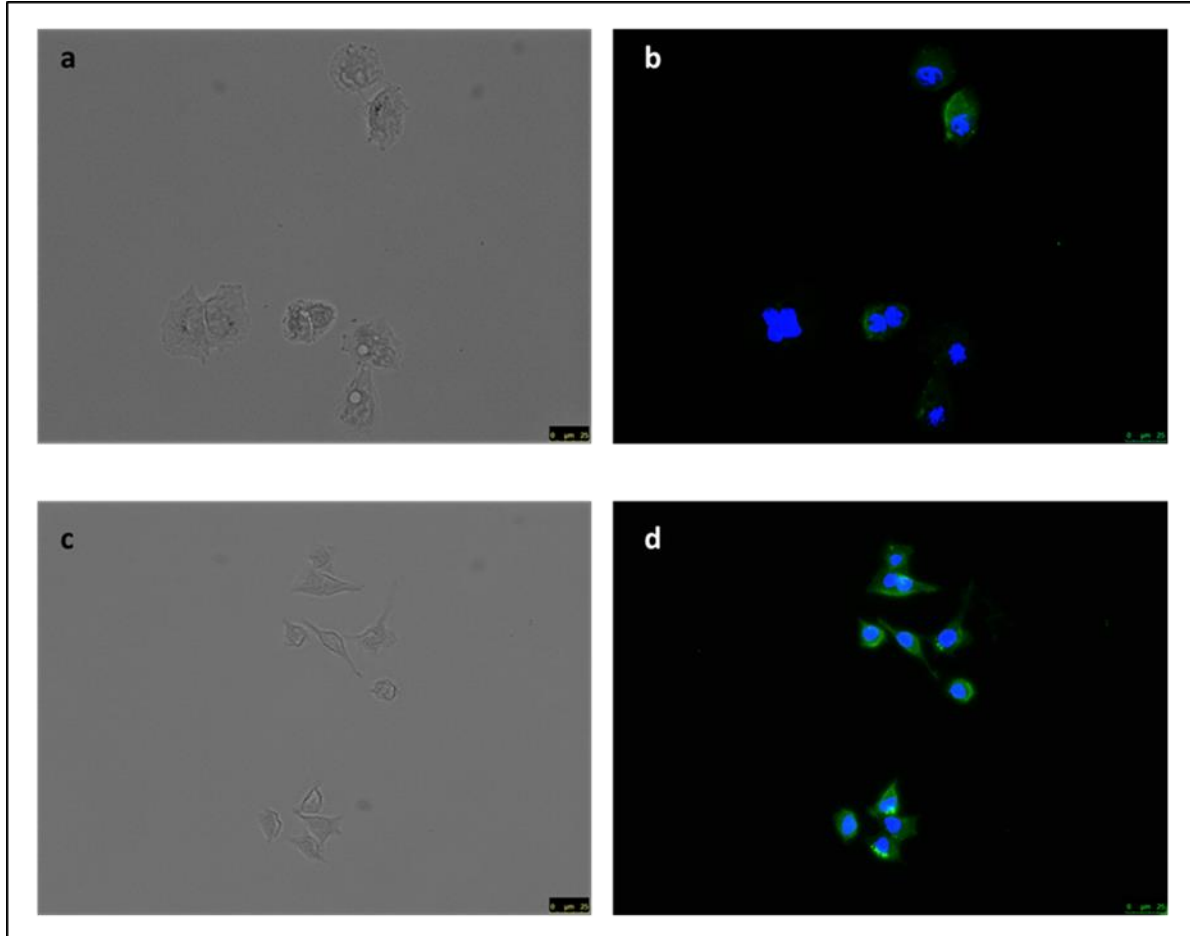
Figure 9: RAGE detection in PANC-1 cells by the immunofluorescence.
(a) Bright field image of PANC-1 WT (b) Merged images of PANC-1 WT (c) Bright field image of PANC-1 FLR2 (d) Merged images of PANC-1 FLR2. Cells stained with anti-RAGE antibody (sc-80653) and Alexa Fluor 488 conjugated secondary antibody (green) and Hoechst dye (blue). Magnification 20X.

In summary, we generated two daughter cell lines from the parent PANC-1 WT cell-line

that moderately (5.4 and 4.4-fold) over-express RAGE.

Discussion

We successfully generated two PANC-1 daughter cell-lines that moderately over-express

RAGE compared to the parental wild-type PANC-1 control cells. We also observed that PANC-1

cells were difficult to transfect. We determined the protein levels of RAGE in these cells by

different methods. Our western blot results showed a strong band at 50 kD for PANC-1 FLR2

and PANC-1 FLR3 cells but no band in PANC-1 WT cells (Figure 6). However, we detected a

35 kD band in PANC-1 WT cells which was not present in PANC-1 FLR2 and PANC-1 FLR3

cells. The 35 kD band could possibly correspond to one of the isoforms of RAGE [85]. Results

from immunoprecipitation of RAGE displayed about 1.6 times higher RAGE in PANC-1 FLR2

and PANC-1 FLR3 cells as compared to PANC-1 WT cells (Figure 7). However, we anticipated

to detect much higher levels of RAGE in PANC-1 FLR2 and PANC-1 FLR3 by

immunoprecipitation as we already detected a strong band for RAGE in western blot. Protein

quantification results from ELISA showed about 5.4- and 4.4-fold higher RAGE in PANC-1

RAGE transfected cells (Table 5). Although the fold change of RAGE expression observed is

different in immunoprecipitation and ELISA, the values fall in the same range and are not

enormously far from each other. The difference in fold change of RAGE expression observed

could be attributed to the differences in two methods and also to the different antibodies used for

the detection of RAGE.

Immunofluorescence staining (Figure 9) show higher RAGE expression in PANC-1

FLR2 as compared to PANC-1 WT. Our results indicate that not all PANC-1 WT cells expressed

RAGE, while in all the PANC-1 FLR2 cells RAGE expression could be observed. Also, RAGE

was not only expressed on the cell surface but was also distributed in the cytoplasm. Our results

are consistent with previous findings which demonstrated intracellular location of RAGE. RAGE

has been shown to be located on the cell surface and in the cytoplasm of G361 and A375 human

melanoma cells [141]. Intracellular localization of RAGE could be the result of transient ligand

induced endocytosis. Indeed, a study in Schwan cells showed that S100B stimulation induces

internalization of RAGE, which was recycled back to the cell surface by Src mediated signaling

[149]. In a different study, stimulation by AGE was shown to induce internalization of RAGE in CHO cells, which in turn led to increased phosphorylation of ERK1/2 [226]. It has also been reported that interaction of RAGE with its ligands such as AGE and S100B or with anti-RAGE antibody leads to internalization of RAGE from the cell membrane to the cytoplasm [227].

CHAPTER 2: EFFECT OF RAGE OVER-EXPRESSION ON PROLIFERATION, MIGRATION AND DOWNSTREAM SIGNALING OF PANC-1 CELLS

Abstract

In this chapter, we used the stably transfected RAGE over-expressing cells generated in chapter 1 and investigated the consequences of RAGE over-expression upon cellular properties of PANC-1 cells. To accomplish our study, we compared cellular proliferation, migration and wound healing between PANC-1 WT, PANC-1 FLR2 and PANC-1 FLR3 cells. Cell proliferation, in 2D conditions, was assessed by two methods: Alamar Blue and cell counting using Trypan Blue. Cell migration was assessed using the Boyden Chamber method and the Wound Healing assay. The effect of the RAGE ligands AGE and S100P on cell proliferation was determined by using Alamar Blue. We observed an increase in cell proliferation, but a reduced migration ability in RAGE transfected cells. This observation directed us to evaluate any alteration in the epithelial-to-mesenchymal transition (EMT) markers as a result of RAGE over-expression. Hence, we determined the expression levels of selected EMT markers and integrins by western blot. Consistent with our migration results we observed a strong downregulation of mesenchymal marker vimentin in RAGE over-expressing cells. However, the epithelial marker as well as various integrins were also found to be downregulated in RAGE over-expressing cells. To further understand this, we investigated downstream signaling pathways that could be involved. Our results indicated significantly reduced FAK, ERK1/2, Akt and NF-κB activity in RAGE over-expressing PANC-1 cells. In summary, our data indicates a phenotypic switch in PANC-1 cells because of RAGE over-expression, resulting in enhanced proliferation abilities but reduced migration and wound healing abilities in RAGE transfected cells. Our observations were

supported by reduction in expression of E-cadherin, vimentin, integrins, accompanied by a decrease in the activity of FAK, ERK1/2, Akt and NF-κB.

Introduction

The poor survival rate in pancreatic cancer can be attributed to an aggressive phenotype that is characterized by early invasion and metastasis [228,229]. In order to migrate, cancer cells must activate genes required for differentiation, slow down proliferation, downregulate the receptors involved in cell-cell attachment, upregulate the cell adhesion molecules that facilitate cell movement and alter cellular characteristics from epithelial to mesenchymal [230,231]. This cellular process is known as epithelial-to-mesenchymal transition (EMT), and activation of EMT is considered a prerequisite for metastasis [232-234]. While undergoing EMT, the cells lose their epithelial features such as loss of polarity and downregulation of E-cadherin. The cells also acquire a mesenchymal phenotype and become motile, as well as start expressing mesenchymal markers like N-cadherin, fibronectin, vimentin. Numerous studies have demonstrated that the invasiveness of pancreatic cancer correlates with EMT activation [232,235,236]

Cell migration also requires a dynamic interaction between the cell and the surface on which it is attached and over which it migrates [237]. Another group of cell-membrane receptors that mediate cell-cell interactions and cell attachment to extracellular matrix (ECM) are the integrins [238,239]. Integrins bind to the components of ECM and regulate cell motility and invasion. In addition to their role as cell adhesion molecules, integrins contribute to tumor progression and metastasis by activating signaling pathways necessary for tumor cell migration and invasion [240,241]. There are 18 different α chains and 8 β subunits in humans, which associate in different combinations to give rise to at least 24 distinct α/β integrin heterodimers[242]

Engagement of RAGE with its ligands has been shown to activate downstream signaling pathways which subsequently result in stimulation of cellular properties that can promote cancer progression [127,202,243]. There have been a considerable number of studies in different cancers, showing the effect of interaction of RAGE with its ligands on cellular properties. In breast cancer, for example, methylglyoxal derived bovine serum albumin AGEs (MG-BSA-AGEs) were shown to increase proliferation, migration and invasion in estrogen receptor (ER) negative MDA-MB-231 as well as ER positive MCF-7 breast cancer cell line, in a RAGE dependent manner [244,245]. In prostate cancer, AGE-RAGE interaction has been demonstrated to promote cell proliferation [246]. An increase in gastric tumor cell proliferation was reported as a result of the interaction RAGE and HMGB1, which was released from tumor cells [184]. In a study investigating endometrial cancer, RAGE was identified as a potential regulator of cell proliferation [247]. Radia et al illustrated the importance of RAGE in malignant transformation of breast cancer cells and the counter effect of RAGE knockdown on proliferation abilities of those cells [205].

In pancreatic cancer, Logsdon's group reported that the interaction between S100P and RAGE stimulated proliferation, migration, invasiveness and survival of human pancreatic cancer cell lines [163]. Another study from this group demonstrated a reduction in S100P mediated cancer cell growth, survival and invasiveness by blocking the interaction between S100P and RAGE with cromolyn [164,248].

But to our knowledge, there is no report yet that describes the effect of RAGE over-expression on cellular properties like proliferation and migration in pancreatic cancer. Therefore, in this chapter we have investigated the effect of RAGE over-expression on these cellular properties in PANC-1 cells. We also determined the effect of RAGE ligands on cell proliferation.

In addition, we also compared the level of EMT markers and integrins as well as RAGE mediated downstream signaling pathways in PANC-1 WT, PANC-1 FLR2 and PANC-1 FLR3 cells. Determining the influence of RAGE over-expression on the cellular properties of PANC-1 cells will help in developing a better understanding of the role of RAGE in pancreatic cancer.

Materials and Methods

Preparation of Advanced Glycation End-products

500 mM ribose BSA (bovine serum albumin) was prepared and characterized by Dr. Indurthi under the supervision of Dr. Stefan Vetter (Department of Pharmaceutical Sciences, NDSU) [249]. Briefly, 20 mg/ml BSA solubilized in sodium phosphate buffer with 1 mM EDTA and 1mM sodium azide (pH 8) was mixed with 500 mM of ribose and incubated at 37°C for 21 days. After the incubation period, the samples were dialyzed twice against 200 volumes of PBS at 4 °C.

Preparation of S100P

The expression and purification of recombinant human S100P was performed by Dr. Vetter. Briefly, a pET22b plasmid coding for human S100P was transformed into electro-competent BL21DE3 cells. After transformation, cells were grown in LB media supplemented with ampicillin. Cells were grown until $OD_{600}= 1$, then induced with IPTG for 2 h at 37 °C. The cells were then collected by centrifugation and lysed by sonication in the presence of 0.1% triton X-100, 1 mg/ml lysozyme and PMSF. The S100P containing supernatant was first run over a Q-sepharose and S100P was eluted in the presence of a gradient of NaCl (15 mM – 1.15 M) in a 50 mM Tris buffer at pH7.4. The second and last purification step on a phenyl-sepharose column yielded a protein more than 95% pure as detected on a Coomassie blue stained SDS gel.

Cell proliferation assay using Alamar Blue

In this assay, cell proliferation was measured through the reduction of the resazurin dye also known as Alamar Blue (Sigma Aldrich, St. Louis, MO, USA). 70 % confluent cells were detached using trypsin, centrifuged at 150 g for 5 minutes and resuspended in growth medium. 40,000 cells/well were seeded in a 24-well plate in media containing 2% FBS. The cells were allowed to grow for 48 hours at 37 °C and 5% CO_2. After 48 hours, 10% v/v of Alamar Blue solution (0.1 mg/ml stock) was added to each well. The fluorescence intensity in the each well was measured at 590 nm (Ex:540 nm), after 2 hours incubation.

To determine the effect of RAGE ligands on cell proliferation, 24 hours after seeding the cells 1 mg/ml AGE (Rib-BSA) or 100 nM S100P were added to the cells. The cells were allowed to proliferate in the presence of the ligand for another 24 hours. After 24 hours the cell proliferation was assessed as described above. Differences in cell proliferation were assessed by differences in fluorescence. The experiment was performed three times independently with six replicates in each experiment.

Cell proliferation assay by cell counting method

In this assay, cell proliferation was measured by counting viable cells and excluding dead cells using Trypan Blue (Corning/VWR, Chicago, IL). The Trypan Blue exclusion method is based on the principle that live cells possess intact cell membranes that exclude dyes, such as trypan blue whereas dead cells do not. When a cell suspension is mixed with Trypan Blue and then visually examined, viable cells have clear cytoplasm whereas nonviable cells have blue cytoplasm [250]. 70 % confluent cells were detached using trypsin, centrifuged at 150 g for 5 minutes and resuspended in growth medium. Cells were counted and 2×10^5 cells were seeded in each well of a 6-well plate in regular growth media and incubated at 37 °C and 5% CO_2. Cell

counting was performed at the time of seeding at 0 hour and after 24 hours, 48 hours and 72 hours. The cells were detached using trypsin, Trypan blue (0.4% solution in PBS) was added and the cells were counted using Life Technologies Countess™ II FL Automated Cell Counter. The experiment was performed three times independently with two wells per condition in each experiment.

Cell growth by spheroid formation in 3D culture conditions

For this assay, we used the Rotary Cell Culture System (RCCS) (Figure 10). RCSS is a bioreactor technology that produces 3D cultures in a dynamic system which suspends cells in a low-shear stress, microgravity-like environment allowing anchorage dependent cells to readily aggregate into 3D spheroids while simultaneously producing high mass transport of nutrients and oxygen. 70 % confluent cells were detached using trypsin, centrifuged at 150 g for 5 minutes and resuspended in growth medium. Cells were counted and 5×10^5 cells were resuspended in 10 ml DMEM supplemented with 10% FBS, penicillin and streptomycin and added to Synthecon disposable vessels. The vessels were connected to a RCCS-D (Synthecon, Houston, TX) rotary cell culture system and maintained at a speed of 5 rpm for 96 h. The cells were analyzed for their size distribution during the time of seeding at 0 hour and after 24-hour, 48-hour and 96-hour incubation. At the 24 h, 48 h and 96 h time points, the solution of each vessel was completely aspirated, transferred to a 50 ml tube and gently mixed. 1 ml from each vessel was then taken and distributed into 10 wells (100 µl/well) of a 96 well plate for image analysis. The remaining solution (9 ml) was reinjected into the vessel, in addition to 1 ml fresh media. The wells containing the spheroids were imaged using light reflection with a Laser Scanning Confocal Microscope (Olympus FV300) at 635 nm. The images were analyzed using the 'Analyze Particles' function of the ImageJ software (ImageJ NIH (40)). At each selected time point, the

cross-section area of single cell or multi-cell spheroids was calculated and normalized by the average size of a single cells at time point zero. The number of spheroids of different sizes was calculated at each time point and compared between the two cell lines. The total number of cells in the vessel was also reported at each time point.

Figure 10: Synthecon Rotary Cell Culture System that produces 3D cultures.

Cell migration assay (Boyden Chamber assay)

The migration potential of the cells was determined by using the Boyden Chamber method as shown in Figure 11. 70 % confluent cells were detached using trypsin, centrifuged at 150 g for 5 minutes and resuspended in growth medium. Cells were counted, and 5×10^4 cells were added on top of 8 µm inserts in 24-well plates (USA Scientific, Ocala, Fl, USA), in the presence of 200 µl serum free media. 500 µl of media with 10% FBS was added to each well of a 24 well plate. The inserts with cells were then placed in the media containing wells. As a control, 50,000 cells were seeded in wells without insert and these cells served as 100% migrated cells. The cells were incubated at 37 °C and 5% CO_2 and allowed to migrate for 24 hours. After 24

hours, the inserts were removed and the cells in the insert were carefully wiped using a swab.

10% v/v Alamar Blue solution (0.1 mg/ml stock) was added in each of the lower compartments

and the inserts were placed back on the corresponding wells. The cells that had migrated to the

other side of the membrane reduce Alamar Blue. The fluorescence intensity in the each well was

measured at 590 nm (Ex: 540 nm), after 2 hours incubation. For estimating the % of migrated

cells, the following formula was used:

$$\text{Percentage of migrated cells} = \frac{\text{Alamar Blue fluorescence with insert}}{\text{Alamar Blue fluorescence without insert}} \times 100$$
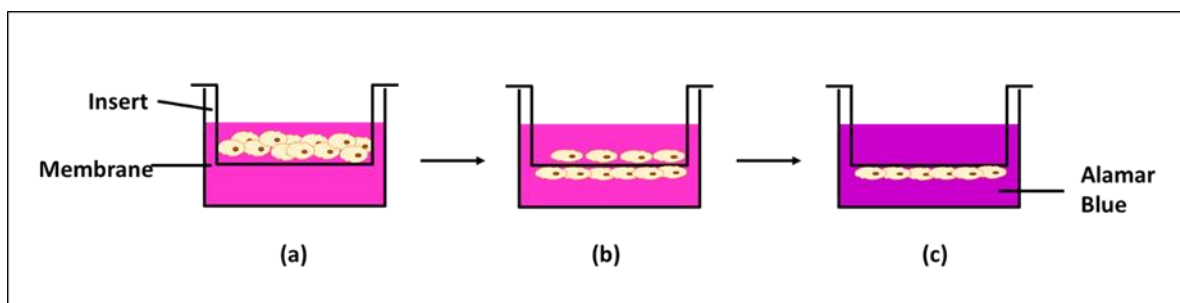
Figure 11: Schematic representation for a Boyden Chamber assay.
(a) Cells are seeded on top of a membrane containing insert (b) Cells migrate to the other side of the membrane, the cells remaining on top of membrane are removed with a swab (c) Alamar Blue is added to the media which is reduced by the cells that migrate through the membrane.

Wound healing assay

Two approaches were used for the generation of the wound: (a) Ibidi Culture-Insert with

2 well in μ-Dish 35 mm. In this method, cells are seeded on the two sides of the insert. The insert

in the dish creates a linear gap by adhering to the treated dish bottom and preventing cell growth

in a predefined region. Once the insert is removed, the wound is created (Figure 2.3). (b)

Manually generating a scratch using a pipette tip. In this method, cells are seeded at a density to

obtain a confluent monolayer. A cell-free wound is created by scratching the confluent

monolayer using a pipette tip.

Ibidi Culture-Insert with 2 well in μ-Dish 35 mm (Figure 12) were used for the following experiment. The cell suspension was prepared by detaching cells (70 % confluent) using trypsin, centrifuging the cells at 150 g for 5 minutes and resuspending in growth medium. Cells were then counted, and a cell suspension with $3x10^5$ cells/ml was prepared to obtain a confluent cell layer after 24 hours. 70 μl of this cell suspension was applied into each well of the Culture-Insert 2 Well in μ-Dish 35 mm (80206, ibidi, Germany). The cells were incubated at 37 °C and 5% CO_2 for 24-hours. Once a confluent layer of cells was observed, the insert from the culture dish was removed with sterile forceps as shown in Figure 2.3. The cell layer was washed with cell-free medium to remove cell debris and non-attached cells. 2 ml of cell free medium was added to the culture dish. The culture dish was then placed under the microscope to observe the wound at 0-hour time point. The cells were again incubated at 37 °C and 5% CO_2 for 24 hours. The culture dish was placed under the microscope to observe the wound at 24-hour time point. Similarly, the images were taken after 48-hours, to observe if the cells had migrated through the wound.
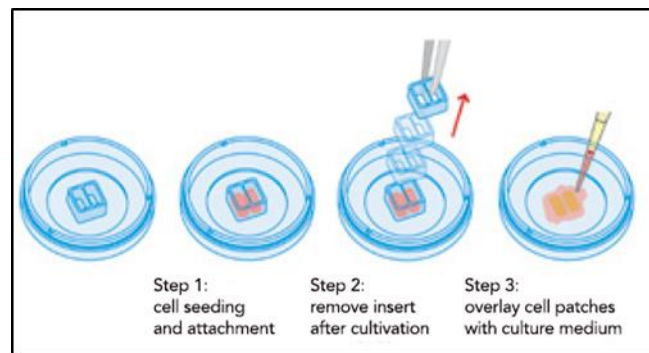
Figure 12: Schematic representation for a wound healing assay using the ibidi Culture-Insert 2 Well.

For performing the wound healing assay after RAGE silencing, we manually generated a wound using a pipette tip. 1 x 10^5 cells/well were seeded in a 24 well plate and incubated at 37

°C and 5% CO_2 for 24 hours. Once the cells were confluent, a scratch was carefully made using a 200 µl pipette tip. All the floating cells were removed, and fresh media was added. Cells were observed under the microscope and the image of the wound was taken right after making the wound at 0-hour. The cells were allowed to migrate through the wound and images were taken after 24-hours and 48-hours.

RAGE silencing

Cells were seeded at 2 x 10^5 cells/well in 2 ml antibiotic-free normal growth medium supplemented with 10% FBS, in a 6-well plate. Transfection was performed using a pool of three RAGE specific siRNAs (sc-36374) from Santa Cruz Biotechnologies. Scrambled siRNA (sc-37007) were used for the control experiment. Transfection was performed following the instructions from the manufacturer. 72 hours after transfection, the cells were detached using trypsin, counted and seeded for the cell proliferation assay and the wound healing assay, as described above. The transfection was performed two times independently.

Western blot

70 % confluent cells were detached using trypsin or a cell scraper, centrifuged at 150 g to obtain a cell pellet. The cells were lysed with a cell disruption buffer provided by the Paris Kit (Life Technologies, Carlsbad, CA, USA). Protein concentrations were determined using the Bicinchoninic Acid Protein Assay Kit (Pierce, Rockford, IL, USA). 25-50µg proteins were resolved on 10-12% SDS PAGE and transferred onto a nitro-cellulose membrane. The blot was blocked with either 5% milk or 5% BSA solution in TBS-T (Tris-buffered saline with 0.1% Tween-20) as per the recommendations from the provider of the primary antibody, for 1 hour at room temperature. The blot was then incubated with the primary antibody (sc-8230 Santa Cruz Biotechnology, Dallas, TX, USA), at a dilution recommended by the manufacturer, overnight at

49

4°C. After three washes (10 minutes each) with TBS-T, the blot was incubated with an HRP-conjugated secondary antibody (Jackson Immuno Research, West Grove, PA, USA) at a dilution recommended by the manufacturer at room temperature for 1 hour. The blot was washed 3 times (10 minutes each) with TBS-T and then the proteins were detected using Clarity western ECL substrate (BIO-RAD, Hercules, CA, USA) and normalized to β-actin detected using β-actin (sc-1616, Santa Cruz Biotechnology, Dallas, TX, USA). Each of the Western blots were performed at least three times. The antibodies used are listed in Table 5.

Table 5: Specifications of the antibodies used in the study.

Antibody	Source	Catalog No.	Concentration
E-Cadherin	Abcam	40772	1:10000
Vimentin	Santa Cruz Biotechnology	6260	1:1000
Integrin α2	Abcam	133557	1:10000
Integrin α3	Santa Cruz Biotechnology	374242	1:500
Integrin α5	Santa Cruz Biotechnology	376199	1:500
Integrin β1	Abcam	52971	1:10000
Integrin β5	Santa Cruz Biotechnology	398214	1:500
phospho-FAK	Santa Cruz Biotechnology	81493	1:500
FAK	Santa Cruz Biotechnology	271126	1:500
phospho-Akt	Cell Signaling Technology	4060	1:2000
Akt	Cell Signaling Technology	4685	1:1000
phospho-ERK1/2	Cell Signaling Technology	9101	1:1000
ERK1/2	Cell Signaling Technology	4965	1:1000
Actin	Santa Cruz Biotechnology	1616	1:1000

NF-κB luciferase reporter assay

Nuclear factor kappa B (NF-κB) activity was measured by using a luciferase reporter assay. In this assay, we transiently transfected PANC-1 cells with a construct that encoded the firefly luciferase reporter gene under the control of a NF-κB transcriptional response element. 35,000 cells/well were seeded in a 48 well plate. The cells were incubated at 37 °C and 5% CO_2 overnight to let them attach. Then the cells were transfected with the NF-κB luciferase reporter plasmid (250 ng, NF-κB cis-Reporting System, Stratagene, Santa Clara, CA, USA). The transfection was performed using lipofectamine 3000 (Life Technologies, Carlsbad, CA, USA). After 24 hours of transfection, following the manufacturer's instructions cells were lysed using the reporter lysis buffer (Promega, Madison, WI, USA). The luciferase activity in the cell lysates was quantified by mixing 100 μl Luciferin substrate (Promega, Madison, WI, USA) with 10 μl of cell lysates and the generated luminescence was measured immediately on a Quick Pak luminometer. The experiment was performed twice using three replicates.

Statistical analysis

Data are presented as mean ± standard deviations. Statistical analysis was performed by using the student's t-test. The p value of less than 0.05 was considered as statistically significant. * $p < 0.05$; ** $p < 0.01$; *** $p < 0.001$.

Results

RAGE over-expression results in increased cell proliferation

Cell proliferation in 2D culture conditions was determined by two methods: Alamar blue assay and Trypan blue exclusion method. The results obtained from both methods were complementary to each other. We observed statistically significant ($p < 0.05$) increase in proliferation of PANC-1 FLR2 and PANC-1 FLR3 cells as compared to PANC-1 WT cells from

Alamar blue assay. Our result shows about 2.5 times higher proliferation in PANC-1 FLR2 cells

(2517.4 ± 61.4 vs 1006.5 ± 138.5) and 2.4 times higher proliferation in PANC-1 FLR3 cells

(2418.7 ± 99.7 vs 1006.5 ± 138.5) when compared to PANC-1 WT cells (Figure 13).
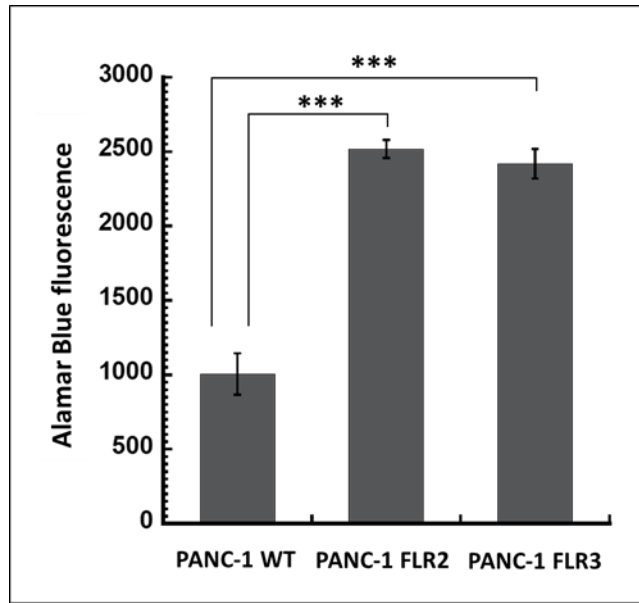
Figure 13: Comparison of the cellular proliferation of PANC-1 WT to PANC-1 FLR2 and
PANC-1 FLR3 cells using Alamar Blue after 48 hours.
Excitation was performed at 540 nm and the fluorescence emission was recorded at 590 nm.
*$p<0.05$, **$p<0.01$, ***$p<0.001$

The results from the Trypan blue exclusion method showed about 2 times increase in

both PANC-1 FLR2 cells and PANC-1 FLR3 cells as compared to PANC-1 WT cells (Figure

14).
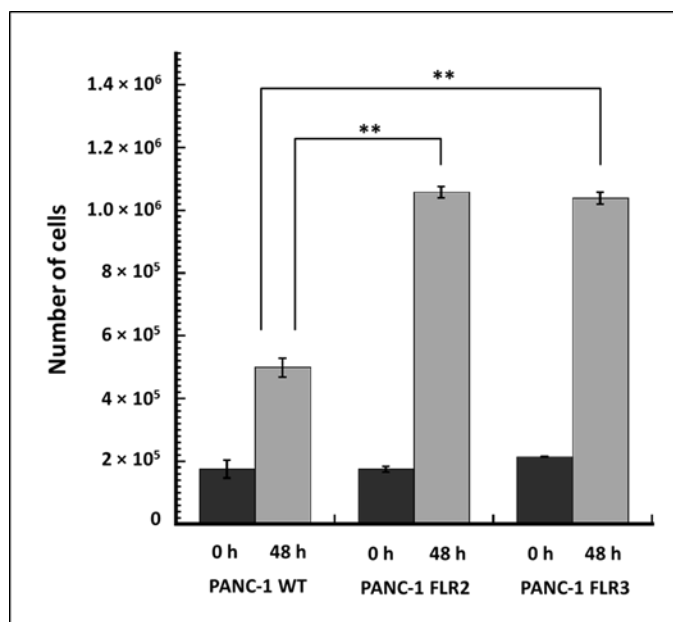
Figure 14: Comparison of cell proliferation by increase in number of cells by Trypan blue exclusion method in PANC-1 WT to PANC-1 FLR2 and PANC-1 FLR3 cells.
 *$p<0.05$, **$p<0.01$, ***$p<0.001$

RAGE ligands, AGE and S100P stimulate cell proliferation in RAGE over-expressing PANC-1 cells

To study the effect of RAGE ligands on cell proliferation we stimulated the cells by two different ligands of RAGE, namely ribose-BSA (AGE) and S100P. The change in proliferation was measured by using Alamar Blue. We observed a significant ($p < 0.05$) increase in proliferation of control as well as RAGE transfected PANC-1 cells upon stimulation with both ligands (Figure 15). AGE resulted in 12% increase in proliferation of PANC-1 WT cells ($p<0.001$), 9.5% increase in proliferation of PANC-1 FLR2 cells ($p<0.01$) and 9.7% increase in proliferation of PANC-1 FLR3 cells. Similarly, with S100P we observed in a 30% increase in proliferation of PANC-1 WT cells ($p<0.001$), 8.7% increase in proliferation of PANC-1 FLR2 cells ($p<0.01$) and 3.2% increase in proliferation of PANC-1 FLR3 cells. Although, the increase observed in proliferation of PANC-1 WT and FLR cells following stimulation with RAGE

53

ligands was small, it is in agreement with the findings from other studies. A previous study in human pancreatic cancer cells has demonstrated that stimulation of MIAPaCa-2 cells by AGE resulted in a modest but consistent increase in the growth of pancreatic cancer cells [142].
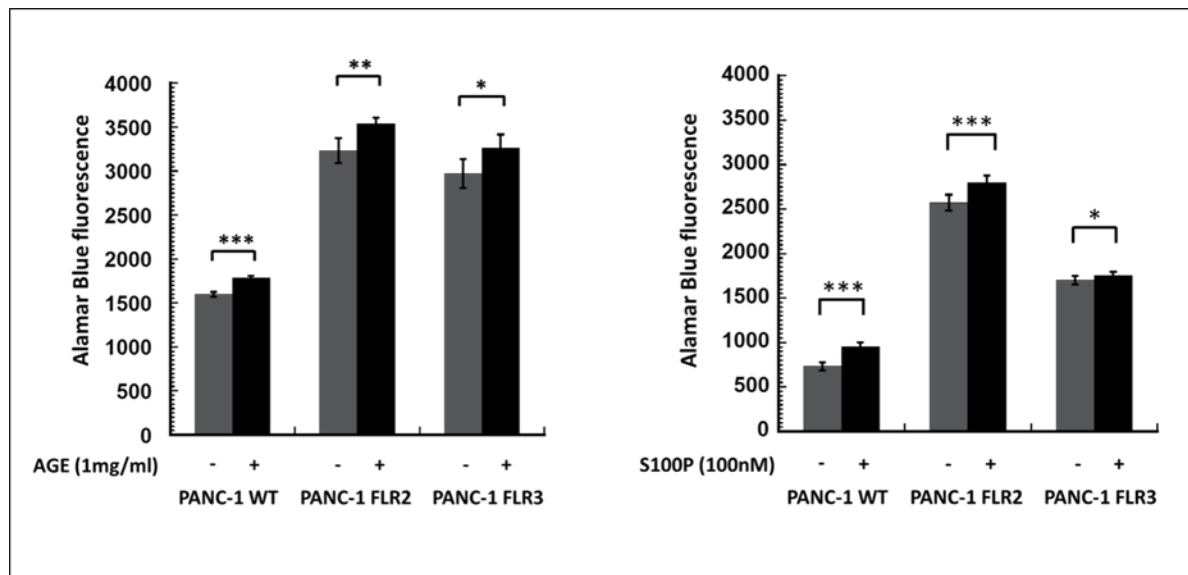
Figure 15: Comparison of the cellular proliferation of PANC-1 WT to PANC-1 FLR2 and PANC-1 FLR3 cells upon stimulation with AGE and S100P, using Alamar Blue.
Cells were incubated with the ligands for 24 hours. Excitation was performed at 540 nm and the fluorescence emission was recorded at 590 nm. *p<0.05, **p<0.01, ***p<0.001

RAGE over-expression results in increased cell growth in 3D cell culture conditions

We next compared the growth of PANC-1 WT and PANC-1 FLR2 cells in 3D cell culture conditions using a Synthecon rotary system. At the time of seeding, the cells were observed by laser scanning confocal microscopy and showed to be present mainly as monomers. The cells were then evaluated by image analysis using ImageJ at 24-hour, 48-hour, 72-hour and 96-hour time points; the number of spheroids of different sizes and the total number of cells was calculated at each time point. We observed that over time, both PANC-1 WT and PANC-1 FLR2 cells formed spheroids of increasing size. At 96-hour time point, larger spheroids were observed with PANC-1 FLR2 cells than with PANC-1 WT cells (Table 6). For each cell-line, we

calculated the percentage of spheroids containing less than 500 cells, between 500 and 1000 cells, between 1000 and 1500 cells and containing more than 1500 cells. The size distribution of the spheroids from one representative experiment is shown in Table 1. We estimated that 63% of the PANC-1 FLR2 spheroids contained more than 1500 cells, whereas no such large spheroids were observed with PANC-1 WT cells. The majority of the PANC-1 WT spheroids (46.3%) consisted of less than 500 cells. The results obtained from the 3D culture are in agreement with those obtained from the 2D cell culture conditions and suggest that PANC-1 FLR2 cells have a faster proliferation rate than the PANC-1 WT cells. The observation that the PANC-1 FLR2 cells formed larger spheroids also suggests stronger cell-cell adhesion properties of the RAGE over-expressing PANC-1 cells.

Table 6: Spheroid size distribution in terms of number of cells per spheroid

0 Hour		
	Percentage of total cells	
Number of cells in a spheroid	PANC-1 WT	PANC-1 FLR2
0-50	100	100
96 Hour		
	Percentage of total cells	
Number of cells in a spheroid	PANC-1 WT	PANC-1 FLR2
0-500	46.3	22.9
500-1000	28.5	4.6
1000-1500	25.2	9.2
1500-11500	-	63.3

RAGE over-expression in PANC-1 cells leads to a decrease in cell motility

The migration potential of the cells was examined by two methods: the Boyden Chamber assay and the Wound Healing assay. The results from the Boyden Chamber assay showed that a lower percentage of PANC-1 FLR2 and PANC-1 FLR3 cells migrated through the membrane of the insert as compared to PANC-1 WT cells. We observed about 2-fold reduction in migration of RAGE over-expressing cells as compared to the wild type cells (Figure 16a).

Also, a delay in wound healing of PANC-1 FLR2 cells was observed when compared to the PANC-1 WT. After 48 hours of creating the wound, PANC-1 WT cells had completely covered the wound whereas PANC-1 FLR2 cells display significant delay in covering the wound (Figure 16b).
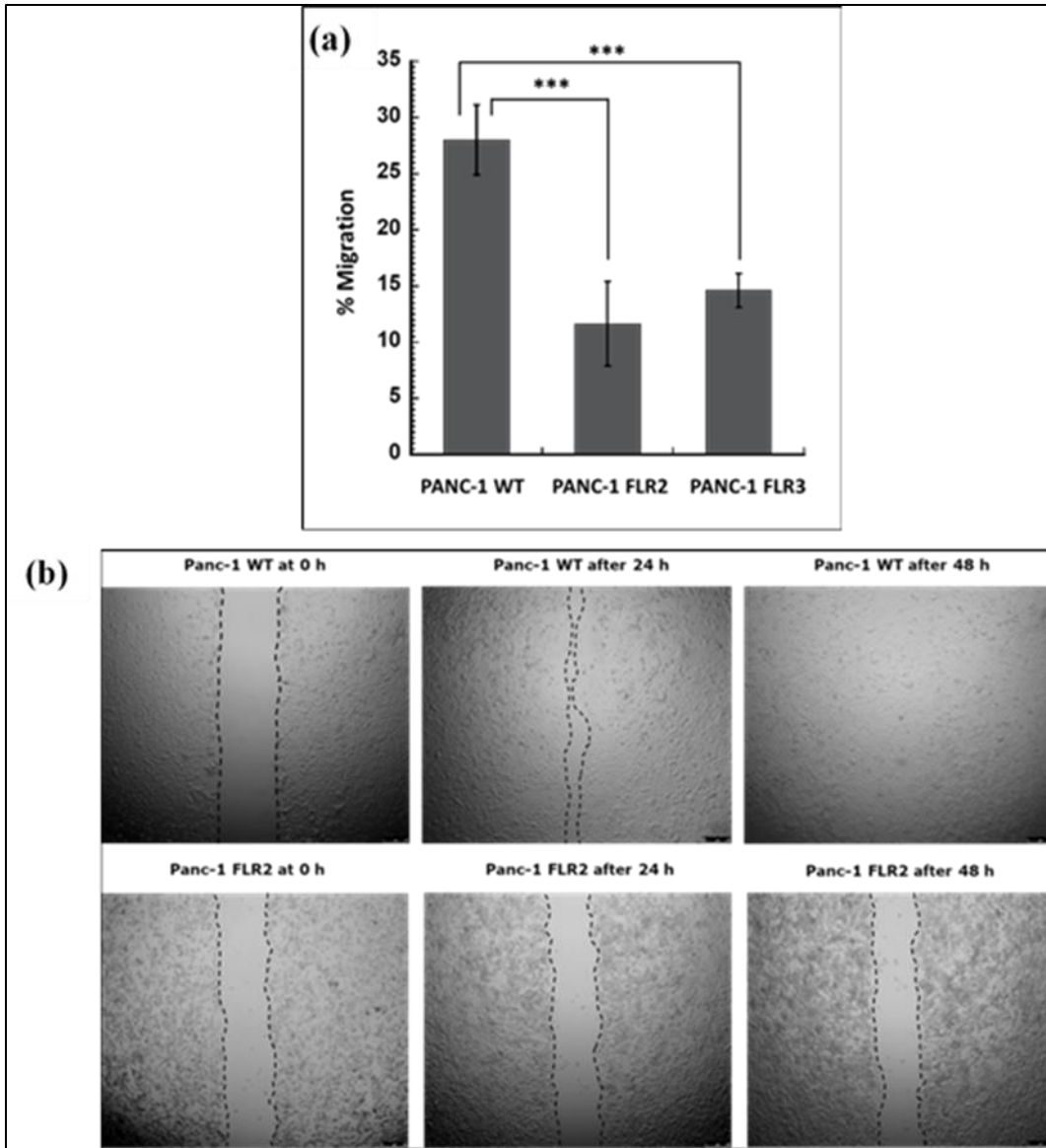
Figure 16: Comparison of the cell migration in PANC-1 WT, PANC-1 FLR2 and PANC-1 FLR3 cells.
(a) Migration of the PANC-1 WT, PANC-1 FLR2 and PANC-1 FLR3 cells by Boyden chamber assay. Alamar Blue was used to determine the percentage of migrated cells. *p<0.05, **p<0.01, ***p<0.001. (b) Migration potential of the PANC-1 WT and PANC-1 FLR2 cells by wound healing assay. The cells were imaged right after formation of the wound at 0 hour and after 24 and 48 hours.

RAGE knockdown reverses the increased proliferation and decreased migration in PANC-1 FLR2 cells

To ascertain that the changes observed in proliferation and migration properties of PANC-1 FLR2 and FLR3 cells were caused by RAGE over-expression, we silenced RAGE in PANC-1 FLR2 cells. We then investigated whether RAGE suppression by siRNA in the PANC-1 FLR2 cells could revert the increased in cell proliferation and delayed wound healing. Our western blot results showed a 25% reduction in levels of RAGE in PANC-1 FLR2 cells silenced with RAGE siRNA as compared to the ones silenced with scrambled siRNA (Figure 17a). RAGE silencing in PANC-1 FLR2 cells also resulted in a 58% decrease in proliferation as compared to PANC-1 FLR2 silenced with scrambled siRNA (Figure 17b). We also observed that when RAGE was silenced in PANC-1 FLR2 cells, the cells regained their abilities to migrate through the wound as compared to PANC-1 FLR2 cells silenced with scramble RNA (Figure 17c).
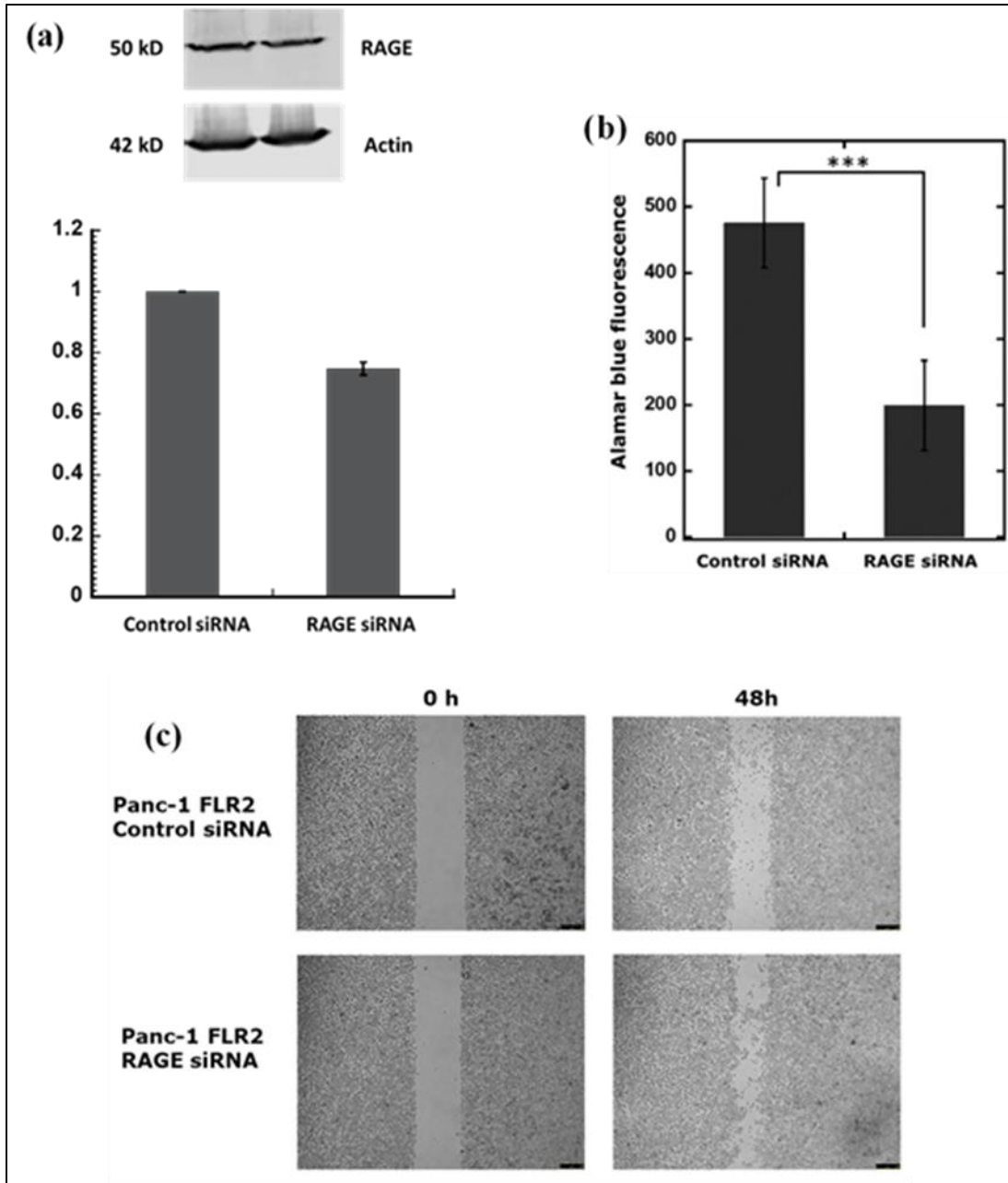
Figure 17: RAGE knockdown in PANC-1 FLR2.
(a) Western blot showing RAGE knockdown in PANC-1 FLR2, (b) Reduction in cell proliferation in PANC-1 FLR2 silenced with RAGE specific siRNAs, shown by Alamar Blue assay, (c) Wound healing assay with PANC-1 FLR2 cells silenced with RAGE specific siRNAs or scrambled siRNA. Images were taken at t = 0 h and t = 48 h. Representative images are shown.

RAGE over-expression leads to reduction in expression levels of EMT markers E-cadherin and vimentin

The increase in proliferation but reduction in migration and delayed wound healing in RAGE transfected cells reflected a phenotypic switch in the cells. This directed us to investigate the expression levels of markers of EMT by western blot analysis. We observed significant reduction in the levels of E-cadherin, which is an epithelial marker, in PANC-1 FLR2 and PANC-1 FLR3 cells as compared to WT PANC-1 cells (Figure 18). Our results also showed a significant reduction in levels of the mesenchymal marker vimentin in PANC-1 FLR2 and PANC-1 FLR3 cells as compared to WT PANC-1 cells, since no bands were detected for PANC-1 FLR2 and PANC-1 FLR3 cell extracts (Figure 18).
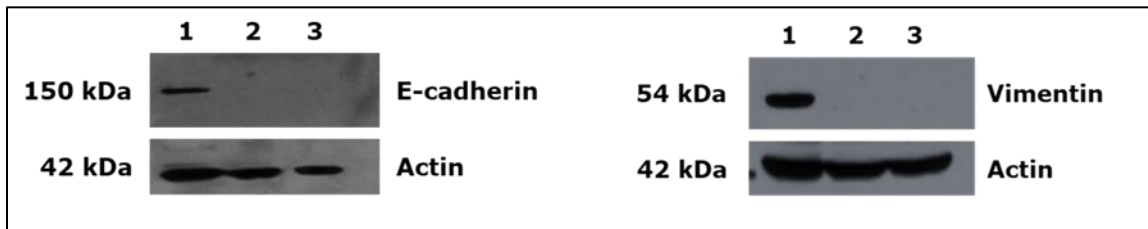
Figure 18: Western blot analysis for E-cadherin and vimentin in PANC-1 WT, FLR2 and FLR3 cell extracts.
The blots were stained with antibodies against E-cadherin and vimentin. A representative blot is shown. 1: PANC-1 WT, 2: PANC-1 FLR2, 3: PANC-1 FLR3

RAGE over-expression resulted in downregulation of α and β integrin expression levels in PANC-1 cells

As integrins play a role in cancer associated processes like proliferation, migration and invasion, we compared the levels of integrin expression between PANC-1 WT, PANC-1 FLR2 and PANC-1 FLR3 cells. The results from western blot analysis revealed strong downregulation of integrins α2, α3, α5 and integrins β1, β5 in cell extracts from PANC-1 FLR2 and PANC-1

FLR3 (Figure 19). No bands corresponding to these integrin subunits were detected in the cell extracts from PANC-1 FLR2 and PANC-1 FLR3. Our data strongly suggest that in PANC-1 cells, RAGE over-expression resulted in the down-regulation of integrin expression.
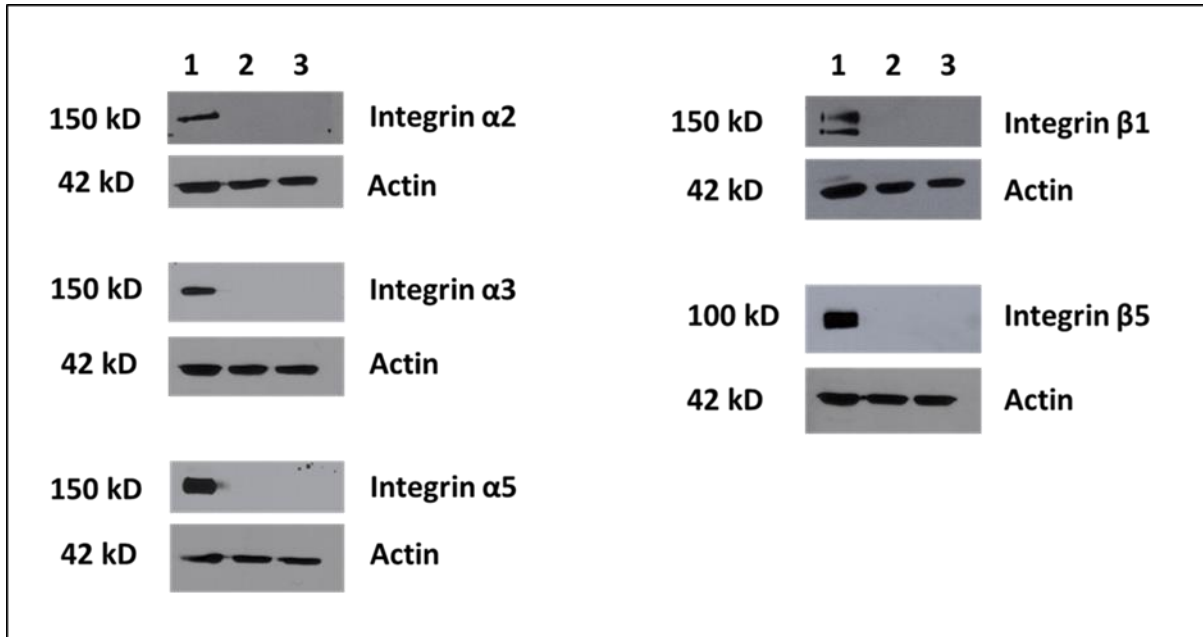
Figure 19: Western blot analysis for integrins in PANC-1 WT, FLR2 and FLR3 cell extracts. The blots were stained with antibodies against integrin α2, α3, α5, β1 and β5. A representative blot is shown. 1: PANC-1 WT, 2: PANC-1 FLR2, 3: PANC-1 FLR3

RAGE over-expression resulted in down-regulation of FAK, ERK1/2, Akt

We next investigated if the downstream signaling pathways were affected by RAGE over-expression by comparing the expression and activation levels of focal adhesion kinase (FAK) in PANC-1 WT, PANC-1 FLR2 and PANC-1 FLR3 cells. We found significantly lower levels of both phosphorylated and non-phosphorylated forms of FAK in PANC-1 FLR2 and PANC-1 FLR3 cells compared to PANC-1 WT cells (Figure 20). Because FAK signals through ERK and Akt, we also measured the levels of phosphorylated and total Akt and ERK1/2 in PANC-1 WT, PANC-1 FLR2 and PANC-1 FLR3 cells. We found lower phosphorylation levels

of Akt and ERK1/2 in PANC-1 FLR2 and FLR3 compared to wild type PANC-1 cells (Figure 20).
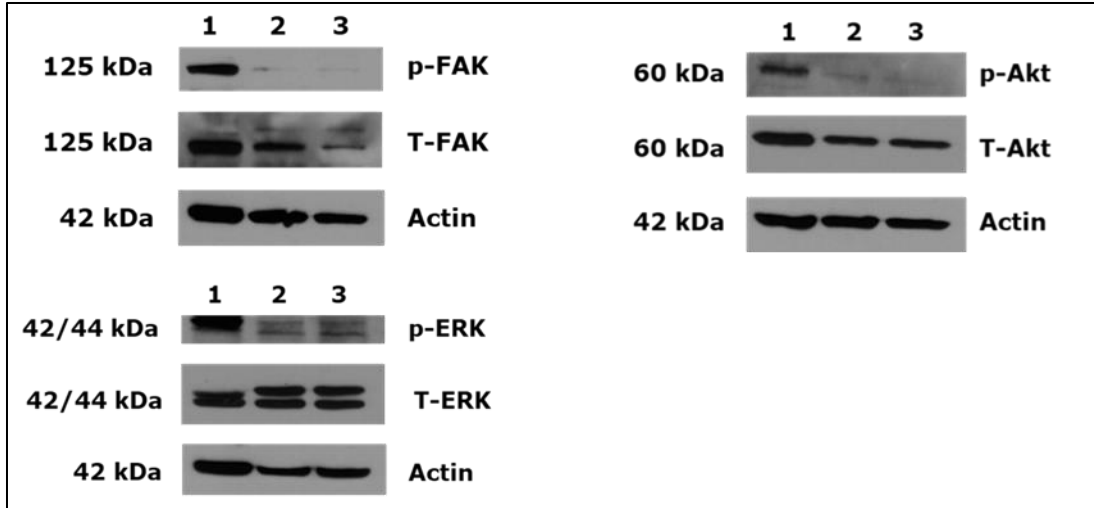
Figure 20: Western blot analysis of PANC-1 WT, FLR2 and FLR3 cell extracts.
The blots were stained with antibodies against ERK1/2, pERK1/2, Akt and P-Akt, FAK and P-FAK. A representative blot is shown. 1: PANC-1 WT, 2: PANC-1 FLR2, 3: PANC-1 FLR3

RAGE over-expression in PANC-1 cells leads to a decrease in NF-κB activity

The activation of NF-κB has frequently been associated with stimulating pancreatic cancer progression by accelerating cancer cell proliferation, invasion, metastasis, angiogenesis, inflammation and chemotherapeutic resistance [251-254]. This prompted us to determine the effect of RAGE over-expression on NF-κB activity in PANC-1 cells. We transfected PANC-1 WT and PANC-1 FLR2 cells with a luciferase NF-κB cis-reporting system. Our results showed a significant reduction in the basal activity of NF-κB in the RAGE-transfected cells. We observed a 6-fold reduction in NF-κB activity in PANC-1 FLR2 cells compared to PANC-1 WT cells (Figure 21).
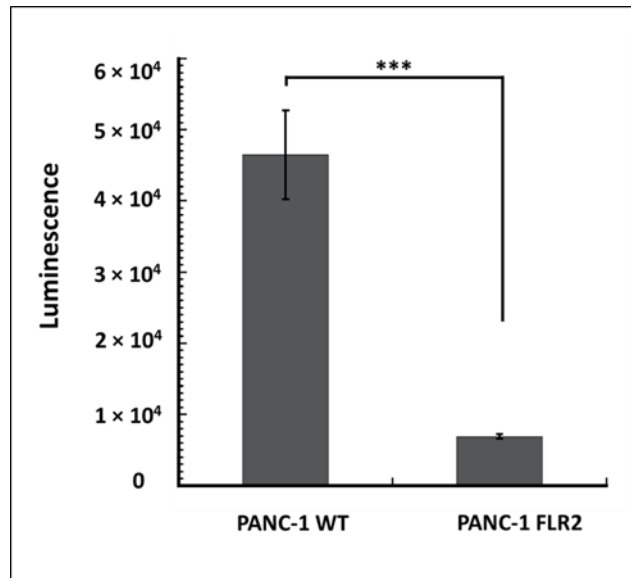
Figure 21: NF-κB activity in PANC-1 WT and PANC-1 FLR2 cells.
A NF-κB luciferase reporter plasmid was used. NF-κB activity is reported as luminescence intensity. The experiment was performed twice with three replicates in each experiment.
***p<0.001

Discussion

In this chapter we investigated the effects of RAGE over-expression on cellular properties like proliferation, migration and wound healing in PANC-1 cells. Our results indicate that RAGE over-expression induced a phenotypic change in the PANC-1 cells. We observed a strong increase in proliferation in RAGE over-expressing PANC-1 cells as compared to the control cells (Figure 13 and 14). Similar observations were made from our 3D spheroid formation experiment (Table 7). Our findings are consistent with other studies which demonstrate that RAGE stimulates cell proliferation in pancreatic cancer [142,153,163]. In addition, we also observed a moderate increase in proliferation in PANC-1 cells following stimulation with RAGE ligands, AGE (1 mg/ml) and S100P (Figure 15). However, it would be interesting to determine the dose dependent effect of RAGE ligands on proliferation PANC-1 cells, as has been reported in some other studies. A previous study has shown an increase in cell

proliferation of colon cancer cell line CT-26 at a low concentration of S100A8/A9 (1 μg/ml),

however no increase was observed with increasing concentrations of S100A8/A9 [255]. In

another study, a dose dependent effect of MG-BSA-AGE was determined in MCF-7 breast

cancer cells. The authors reported 35% increase in the proliferation upon stimulation with 50

μg/ml MG-BSA-AGE as compared to the untreated control cells. However, at a lower

concentration no effect on proliferation was observed and interestingly an inhibition of cell

proliferation was observed at a higher concentration of 200 μg/mL [245]. From our results, it can

also be said that RAGE has already been significantly activated in PANC-1 FLR2 and PANC-1

FLR3 resulting in a prominent increase in cell proliferation. Therefore, there is only a minute

possibility of RAGE activation upon addition of ligand which is seen in the modest increase in

proliferation followed by stimulation with RAGE ligands.

Next, we examined the change in migration properties of RAGE transfected cells by

Boyden Chamber method and wound healing method. Although we anticipated to see enhanced

migration following RAGE over-expression, we observed a significant reduction in the migration

abilities and delayed wound healing (Figure 16b) in RAGE over-expressing PANC-1 cells in

comparison to the control cells. By silencing RAGE in PANC-1 FLR2 cells, the cells regained

their ability to migrate through the wound (Figure 17c). Besides, the migration ability of PANC-

1 FLR2 and PANC-1 FLR 2 cells transfected with the scrambled siRNA was found to be similar

(Figure 16b and 17c). The data suggests that RAGE over-expression serves as a proliferative

switch in PANC-1 cells, which results in downregulation of migratory abilities of the cells. A

previous study from our lab on melanoma had shown that RAGE over-expression acted as a

metastatic switch and resulted in increased cell migration and invasion, but decreased cell

proliferation in the WM115 melanoma cell line [256]. Another study showed that silencing of

RAGE resulted in declined cell invasion and migration but did not alter cell proliferation in a gastric cancer cell line *in vitro* [257]. The results from these studies indicate that the outcome of RAGE expression on cancer cell properties can vary depending on the environment and cell type.

Our *in vitro* results with the PANC-1 cells suggest that in *in vivo* studies PANC-1 FLR2 cells might show low metastasis in comparison to PANC-1 WT cells. In that case RAGE inhibition may not be a suitable approach for treating pancreatic cancer, as it could lead to increased metastasis. However, this may provide us with a new perspective about the role of RAGE in pancreatic tumor biology.

The reduction in migration and delayed wound healing indicated a possible alteration in EMT markers which are associated with the migration abilities of cancer cells. The EMT process is characterized by interruption in cell-cell adhesion and cellular polarity, remodeling of the cytoskeleton and changes in cell-matrix adhesion to gain properties of mesenchymal cells such as increase in migration and invasion abilities [233,258]. Hence, we investigated the expression of EMT markers in PANC-1 cells. We observed a strong downregulation of vimentin in PANC-1 FLR2 and PANC-1 FLR3 cells (Figure 18) which could explain the decrease in migration and delayed wound healing observed in these cells. Vimentin is associated with invasion in numerous types of cancers [259,260] and is known to induce changes in cell shape, adhesion and motility during EMT, resulting in dissociation of cells from their original tumor site and their migration to a new tissue [261,262].

The strong decrease observed in the expression levels of integrins α2, α3, α5 and integrins β1, β5 (Figure 19) in RAGE over-expressing cells also supported the reduction in migratory abilities of PANC-1 cells. Integrins are known to play a role in tumor progression and

metastasis by activating signaling pathways necessary for tumor cell migration and invasion [240,241]. In pancreatic cancer, expression of several integrin subunits such as α1, α2, α3, α5, α6, β1, β3, β4 and β5 has been described [263-265]. Higher expression of integrins α6β1 [266] and αvβ3 [267] have been shown to be promote invasion in pancreatic cancer cells. A study in sub-populations of the MiaPaCa-2 cells also suggested that changes in integrin expression can alter aggressive invasive phenotype of pancreatic cancer cells [268].

In summary, our results from this chapter suggest that RAGE over-expression serves as a phenotypic switch in the PANC-1 pancreatic cancer cell line leading to a strong increase in proliferation but a decrease in migratory abilities of the cells. Furthermore, the decrease in migratory abilities of the cells are in agreement with the downregulation of mesenchymal marker vimentin and integrins α2, α3, α5 and integrins β1, β5 as well as reduced FAK, ERK1/2, Akt and NF-κB activity.

CHAPTER 3: EFFECT OF RAGE INHIBITION IN COMBINATION WITH GEMCITABINE TO REDUCE TUMOR GROWTH IN PANCREATIC CANCER[1]

Abstract

The objective of this chapter was to investigate the effect of RAGE inhibitors in combination with gemcitabine to reduce tumor growth in pancreatic cancer. RAGE has been shown to facilitate pancreatic tumor cell survival by enhancing autophagy and inhibiting apoptosis. For this purpose, we tested two different RAGE inhibitors and their combination with gemcitabine and examined the levels of autophagy and apoptosis in pancreatic tumors in mice. We employed an orthotopic tumor implantation model in male C57Bl/6 mice using syngeneic tumor cell-lines derived from pancreatic tumors in KPC mice (described in materials and methods). The first RAGE inhibitor used was an anti-RAGE monoclonal antibody (IgG2A11). For investigating the effect of IgG2A11 in combination with gemcitabine, we implanted KPC 5508 pancreatic cancer cells, which expressed relatively high levels of RAGE (as compared to other KPC cell-lines we had), in the pancreas of C57BL/6 mice. The mice were then enrolled in different groups and received the following treatments: vehicle, IgG2A11, gemcitabine or IgG2A11 + gemcitabine. The results from our study showed smaller tumors in mice treated with

---

the combination of IgG2A11 and gemcitabine as compared to gemcitabine alone treated group. Further, we compared the markers of autophagy and apoptosis in the different treatment groups. We observed that the smaller tumors in the group treated with combination were associated with higher levels of p62, indicating a reduction in autophagy. We also observed higher but statistically non-different levels of cleaved PARP in the combination treated group as compared to gemcitabine alone treated group. A reduction in phosphorylation of ERK was also observed in the combination treated group, implying a reduction in proliferation of the tumor cells.

In our second study, we used a small molecule RAGE inhibitor (FPS-ZM1) in combination with gemcitabine. Our results showed significantly smaller tumors in the combination group as compared to the gemcitabine alone treatment group. This is an ongoing study, and the effects of the combination on the markers of autophagy and apoptosis is under progress. In conclusion, our data strongly suggests that inhibiting RAGE in combination with gemcitabine could be a valid therapeutic approach for the treatment of pancreatic cancer.

Introduction

Gemcitabine, a cytotoxic nucleoside analog of deoxycytidine FDA-approved in 1996, has been widely used for the treatment of various malignancies including breast cancer, ovarian cancer and pancreatic cancer [269]. Gemcitabine became the standard of care for locally advanced and metastatic pancreatic cancer since it showed improved median survival of 5.6 months in comparison to 4.4 months for 5-fluorouracil (5-FU) treated patients [83]. Since no alternative therapeutic approach has shown better survival benefits in patients, gemcitabine remains the cornerstone of neoadjuvant and adjuvant chemotherapy in pancreatic cancer [270,271]. However, pancreatic cancer is characterized by rapid development of resistance against gemcitabine after showing initial response to the therapy [272,273]. Therefore,

understanding the molecular basis of development of gemcitabine resistance is critical for the development of more potent combination therapies. Growing evidence have established that HMGB1 is important in the development of resistance against chemotherapy [274-276]. It has been shown that HMGB1 is passively released from dying tumor cells upon treatment with chemotherapy [165,277]. Other studies have also shown that HMGB1 mediates autophagy rendering tumors resistant to chemotherapy [168,278,279]. Autophagy is a conserved cellular pathway that controls protein and organelle degradation, to sustain cellular metabolism and homeostasis [280-282]. Constitutive, basal autophagy is crucial for maintaining homeostatic function as well as preventing accumulation of damaged proteins and organelles in cells and tissues which could be deteriorating over time [283,284]. In cancer cells however, autophagy serves to ensure tumor cell survival in conditions of metabolic stresses such as nutrient deprivation, hypoxia, absence of growth factors and the presence of anti-cancer drugs resulting in resistance to chemotherapy [285-287]. A study in lung adenocarcinoma illustrated a positive correlation between HMGB1 and docetaxel induced autophagy in SPC-A1 and H1299 cells. The study also demonstrated that HMGB1 regulated autophagy significantly contributed to docetaxel resistance in these cells [288]. Another study demonstrated a significant increase in HMGB1 mediated autophagy in colorectal cancer cells upon treatment with oxaliplatin, which in turn protected HT29 and HCT116 cells from the toxicity of oxaliplatin via the MEK/ERK signaling pathway [289]. In a different study investigating the role of autophagy in bladder cancer, the authors observed that knocking-down HMGB1 suppressed gemcitabine induced autophagy as well as resulted in increased apoptosis [290].

RAGE is identified as the primary receptor for HMGB1, and their interaction is known to promote tumor cell survival by promoting autophagy and inhibiting apoptosis [291,292]. Kang et

al showed that forced expression of RAGE supported tumor cell survival by reducing apoptosis (decreased levels of cleaved caspase 3) and enhancing autophagy (increased LC3-II levels) following exposure to cytotoxic chemotherapy in mouse Panc02 and human Panc2.03 pancreatic cancer cells [209]. The authors also demonstrated that RAGE knockdown resulted in higher levels of cleaved caspase-3 and reduction in levels of LC3-II, in murine tumor cell-lines following treatment with chemotherapeutic agents [209]. All the studies suggest that RAGE is one of the critical mediators of chemoresistance in pancreatic cancer, thereby making the tumor unresponsive to treatment with chemotherapeutic drugs.

This led us to the following question: Could the combination of a RAGE inhibitor with a chemotherapeutic agent prevent tumor cell survival by inhibiting autophagy and promoting apoptosis, thereby making the tumor more sensitive towards chemotherapy in pancreatic tumor? To answer this question, we tested the combination of RAGE inhibitors and gemcitabine (the standard of care in pancreatic cancer) in an *in vivo* model of pancreatic cancer.

A distinct characteristic of pancreatic cancer is a profound desmoplastic stroma which is composed of fibroblasts, myofibroblasts (pancreatic stellate cells), extracellular matrix proteins, leukocytes, endothelial cells and other types of inflammatory cells [81,293,294]. It is well established that these components play a crucial role in facilitating tumor progression, metastasis and resistance to chemotherapy [295-298]. Many mouse models of pancreatic cancer employ immunodeficient mice implanted with human cells. However, these models have a major weakness in the fact that the tumor microenvironment is defective. To solve this issue, we chose to use a mouse model where murine pancreatic cancer cells were implanted into immunocompetent syngeneic mice.

For our study, we used a murine cell-line derived from pancreatic tumors of KPC mice. The KPC mouse model of pancreatic ductal adenocarcinoma (PDAC) was first described in 2005 by Hingorani's group [299]. The KPC mouse is a genetically engineered mouse which incorporates conditional activation of mutant endogenous alleles of the *KRAS* and *Trp53* genes through Cre-Lox technology [299].

Materials and Methods

Cell culture

The murine KPC pancreatic cancer cell-lines were provided by Dr. Hollingsworth from the University of Nebraska, in Omaha (NE). The KPC cells were grown and maintained in DMEM (ATCC) supplemented with 10% FBS (ATCC), penicillin (100 U/ml) and streptomycin (100 µg/ml) (GE Healthcare Life Science, Pittsburg, PA) at 37 °C and 5% CO_2.

ELISA

For determining the level of RAGE expression in the KPC cell-lines, we performed ELISA on cell extracts established from five KPC cell-lines. For preparing the cell lysates, the cells were detached using a cell scraper (to keep the RAGE present on cell surface intact) and lysed with the cell lysis buffer. Protein concentrations were determined using the BCA Protein Assay Kit. The protein levels of RAGE in KPC cell-lines was determined by using Quantikine ELISA Mouse RAGE Immunoassay kit (R & D System, Minneapolis, MN, USA), following manufacturer's instructions.

Cell viability

70 % confluent cells were detached using trypsin, centrifuged at 150 g for 5 minutes and resuspended in growth medium. 5,000 cells were seeded in each well of a 96 well plate and were allowed to attach. The cells were treated with increasing concentrations of gemcitabine: 0.09

71

µM- 0.19 µM- 0.39 µM - 0.78 µM - 1.56 µM - 3.125 µM - 25 µM. Gemcitabine treatment was followed by addition of 50 nM FPS-ZM1 to all the wells. Cells without any treatment served as a control for the experiment. After 24 hours, 10% v/v of Alamar Blue solution (0.1 mg/ml stock) was added to each well. The fluorescence intensity in the each well was measured at 590 nm (Ex:540 nm), after 2 hours incubation. The experiment was performed at least three times with six replicates in every experiment.

Orthotopic mouse model

(a) The first animal experiment was performed in Dr. Hollingsworth's lab at the University of Nebraska, in Omaha (NE). The surgeries and treatment were performed by Dr. Hollingworth's group. At the end of the study the mice were euthanized, and the excised tumors and tissues were sent to our lab for further studies. In this study, five to six-week-old male C57Bl/6 mice were purchased from Jackson Laboratories (Bar Harbor, ME, USA) and were quarantined for 1 week to allow them to adapt to the laboratory environment. All the animal experiments were conducted according to the guidelines of the Institutional Animal Care and Use Committees (IACUC) at the University of Nebraska under an approved protocol. KPC 5508 cells were expanded and prepared in Dr. Hollingsworth's lab for implantation in the mice. The mice were sedated using a mixture of ketamine/xylazine (100-200 mg/kg + 5-16 mg/kg). The left lateral abdominal wall was depilated and prepared for surgery. An incision was made on the abdominal wall near the tip of the spleen. The pancreas was located and 10,000 cells in 25 µl sterile PBS were injected in the tails of the pancreas using a 25-gauge needle. The peritoneum was sutured using Chromic-gut and the skin was sutured using Ethilon suture. 500 µl of sterile saline was injected subcutaneously to hydrate the mice. In addition, buprenorphine (0.05-0.10

mg/kg) was injected subcutaneously. The mice were allowed to recover from the surgery for 5 days before starting the treatment.

(b) For the second animal experiment, male C57Bl/6 mice were purchased from the Jackson Laboratories (Bar Harbor, ME, USA). The animals were housed in the Animal facility in Sudro 207 at North Dakota State University (NDSU). Before starting the experiments, the animals were quarantined for 1 week to allow them to adapt to the laboratory environment. All the animal experiments were conducted according to the guidelines of the IACUC at NDSU under an approved protocol. For the experiments, five to six-week-old mice were used and KPC 5508 cells were expanded and prepared in the lab for implantation in the mice. The mice were anesthetized with 3% isoflurane in 100% O_2 and maintained with 2% isoflurane in 100% O_2. The left lateral abdominal wall was depilated and prepared for surgery. An incision was made on the abdominal wall near the tip of the spleen. The pancreas was located and 5,000 cells in 25 µl sterile PBS were injected in the tails of the pancreas using a 25-gauge needle. The peritoneum was sutured using Chromic-gut and the skin was sutured using Ethilon suture. 500 µl of sterile saline was injected subcutaneously to hydrate the mice. In addition, buprenorphine (0.05-0.10 mg/kg) was injected subcutaneously. The mice were allowed to recover from the surgery for 5 days before starting the treatment.

Treatment

(a) For the study performed at the University of Nebraska, the mice were enrolled into 4 treatment groups and received treatment every 5 days for 30 days. The mice received either (i) Control IgG (100 µg in 100 µl sterile saline) intraperitoneally (IP) (ii) IgG2A11 (100 µg in 100 µl sterile saline) intravenously (IV), (iii) gemcitabine (100 mg/kg in 100 µl sterile saline) IP, or (iv) IgG2A11 (100 µg in 100 µl sterile saline) IV + gemcitabine (100 mg/kg in 100 µl sterile

saline) IP. At the end of the treatments, the mice were euthanized as per the IACUC guidelines and necropsied for tissue collection. Pancreas/tumors were collected and divided into two parts. One half of each tumor was fixed in neutral-buffered formalin and subsequently embedded in paraffin for immunohistochemical analysis. The other half was snap frozen in liquid N_2 for further studies.

(b) For the second study that was performed at NDSU, the mice were enrolled into 5 treatment groups and received treatment every 5 days for 30 days. The mice received either (i) vehicle (100 µl sterile saline) IP, (ii) vehicle + DMSO (100 µl sterile saline + DMSO) IP, (iii) FPS-ZM1 (5 mg/kg in 100 µl vehicle) IP, (iv) gemcitabine (100 mg/kg in 100 µl sterile saline) IP, or (v) FPS-ZM1 (5 mg/kg in 100 µl vehicle) and gemcitabine (100 mg/kg in 100 µl) IP. At the end of the treatments, the mice were euthanized as per the IACUC guidelines and necropsied for tissue collection. Pancreas/tumors were collected and divided into two parts. One half of each tumor was fixed in neutral-buffered formalin and subsequently embedded in paraffin for immunohistochemical analysis. The other half was snap frozen in liquid N_2 for further studies.

Western blot

Protein extracts from pancreatic tumors were prepared with RIPA buffer (Life Technologies, Carlsbad, CA, USA) in presence of protease and phosphatase inhibitors (Thermo Scientific, USA). Protein concentrations were determined using the BCA Protein Assay Kit. 50-100 µg proteins were then resolved on 10-12 % SDS PAGE and transferred onto a PVDF membrane. The membrane was blocked with Odyssey® blocking buffer (P/N 927-50000, LI-COR, Lincoln, NE, USA) for 1h at room temperature. The primary and secondary antibody dilutions were made in Odyssey® blocking buffer with 0.2% Tween-20, according to the manufacturer's recommendations. The membrane was incubated with the primary antibody

overnight at 4 °C. After washing the membrane 3 times (10 minutes each) with 1X TBS-T, the

membrane was incubated with IRDye secondary antibody (LI-COR, Lincoln, NE, USA) for 1h at

room temperature. The membrane was washed 3 times (10 minutes each) with 1X TBS-T and

scanned on Odyssey® CLx Infrared Imaging System. For loading control, β-actin was detected

by loading and running equal amounts of proteins on another SDS-PAGE gel. The bands

obtained for RAGE were normalized to those of β-actin (4967, Cell Signaling Technologies,

Danvers, MA, USA). The antibodies used are listed in Table 7.

Table 7: Specifications of all the antibodies used in the study.

Antibody	Source	Catalog No.	Concentration
p62 (SQSTM1)	Santa Cruz Biotechnology	28359	1:1000
Caspase-3	Cell Signaling Technology	9662	1:1000
Cleaved caspase-3	Cell Signaling Technology	9661	1:1000
PARP	Cell Signaling Technology	9542	1:1000
HMGB1	Cell Signaling Technology	3935	1:1000
Phopho-ERK1/2	Cell Signaling Technology	9101	1:1000
ERK1/2	Cell Signaling Technology	4695	1:1000
β-actin	Cell Signaling Technology	4967	1:1000

Statistical analysis

Data are presented as mean ± standard deviations. Statistical analysis was performed by

using ANOVA and the student's t-test. The P value of less than 0.05 was considered as

statistically significant. * $p < 0.05$; **$p < 0.01$; ***$p < 0.001$.

<center>**Results**</center>

KPC cells express varying levels of RAGE

In order to determine the levels of RAGE in the five KPC cell-lines, we performed a quantitative ELISA. We generated a standard curve with known concentrations of recombinant RAGE, which was used to determine the concentration of RAGE in the different cell extracts (Figure 22). Using this standard curve, we determined the amount of RAGE present in the five cell-lines. The results from ELISA showed varying levels of RAGE in the KPC cell-lines. The amount of RAGE was determined in pg/mg of total protein present in the cell extracts. KPC 7107 cells contained 167.4 ± 34.5 pg of RAGE, KPC 5517 contained 657.2 ± 84.7 pg of RAGE, KPC 4184 contained 429.4 ± 170 pg of RAGE, KPC 8060 contained 176 ± 72.5 pg of RAGE and KPC 5508 contained 650.5 ± 230.3 pg of RAGE. KPC 5508 cells were found to express relatively higher levels of RAGE, therefore this cell-line was used for further experiments (Table 8).
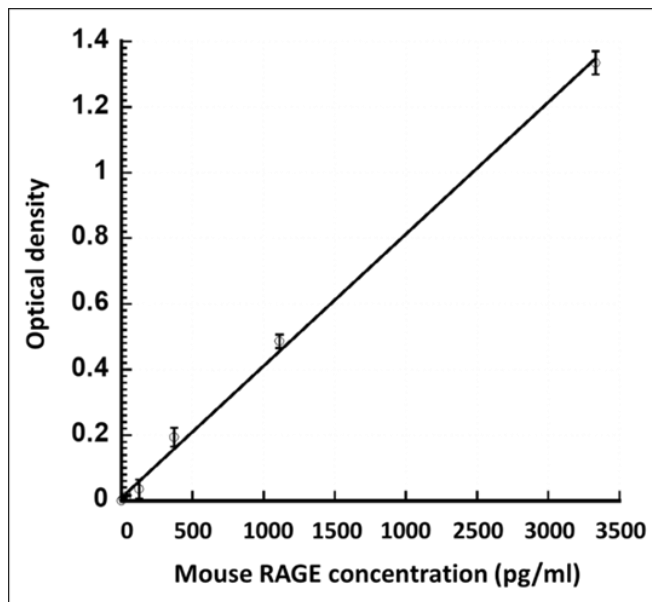
Figure 22: Standard curve for mouse RAGE ELISA.

<center>76</center>

Table 8: Quantification of RAGE in KPC cell extracts by ELISA

Cell-line	RAGE levels in pg/mg total protein
7107	167.4 +/- 34.5
5517	657.2 +/- 84.7
4184	429.4 +/- 170
8060	176 +/- 72.5
5508	650.5 +/- 230.3

KPC 5508 sensitivity to gemcitabine

Our first step was to determine the sensitivity of the KPC 5508 cells for gemcitabine. For this purpose, we determined the effect of gemcitabine on cell viability of KPC 5508 using Alamar Blue. We observed a dose dependent reduction in the cell viability upon treatment with gemcitabine. The maximum of 40% reduction in the cell viability was observed with 25 µM concentration of gemcitabine (Figure 23). The maximum reduction did not change significantly up to 100 µM gemcitabine (data not shown).
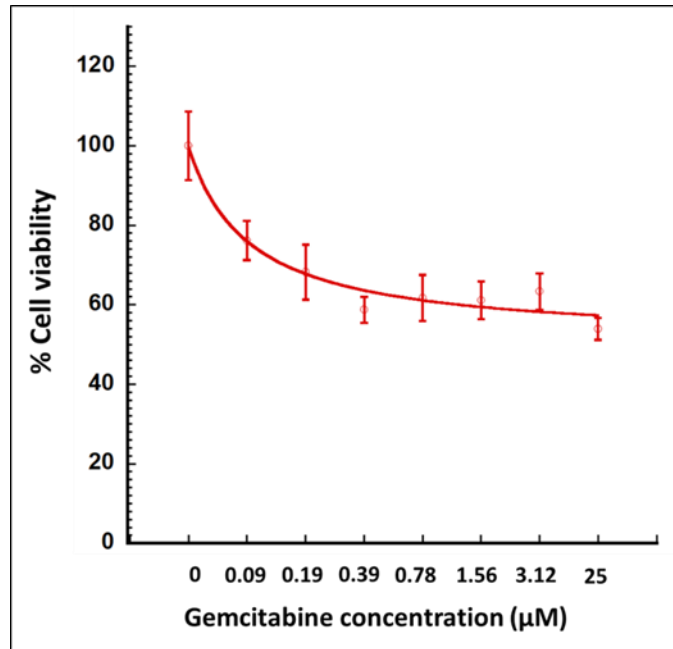
Figure 23: The effect of gemcitabine on cell viability of KPC 5508 cells.
Cells were seeded in a 96-well plate and incubated overnight. Gemcitabine, at the indicated concentrations, was added to cells and further incubated for 24 hours. Cell viability was determined using Alamar Blue.

Effect of IgG2A11 and gemcitabine on tumor growth in a mouse model of pancreatic cancer (Omaha study)

The goal of this first animal study was to determine the effect of IgG2A11 alone, gemcitabine alone and the combination of gemcitabine and IgG2A11 on pancreatic tumor growth in C57Bl/6 mice. We compared the growth of the tumors by comparing tumor weights from different treatment groups. As expected, we observed a decrease in tumor growth in mice that received gemcitabine alone as compared to the control group of mice ($p=0.06$) (Figure 24). A further reduction in tumor growth was observed in the mice that received the combination of IgG2A11 and gemcitabine as compared to the mice treated with gemcitabine alone ($p=0.03$) (Figure 24). Interestingly, no reduction in tumor growth in the mice that received IgG2A11 alone was observed, in fact there was an apparent but non-significant increase in tumor growth as

78

compared to the control group. Further investigation would be needed to better understand the effect of IgG2A11 alone on pancreatic tumor growth. It was noteworthy that the tumor weight values were largely spread out in the IgG2A11 treatment group as compared to the IgG2A11 + gemcitabine treatment group, where the spread was very small (Figure 24). Overall, our findings indicated that the response to gemcitabine was enhanced by combining it with IgG2A11.
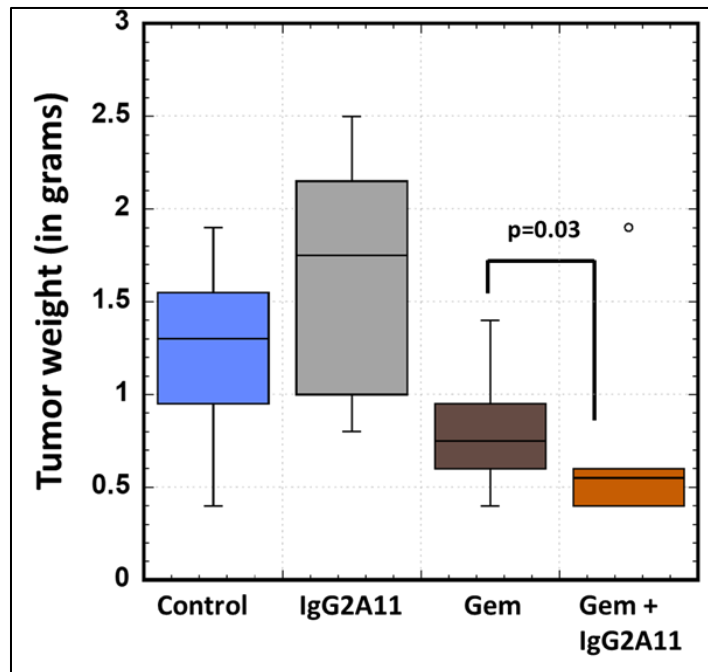
Figure 24: Comparison of tumor weights of mice from different treatment groups. Box-and-whisker plot of tumor weights harvested after treatment with Control (n=5), IgG2A11 (n=6), gemcitabine alone (n=8) or IgG2A11+ gemcitabine (n=8). P-values were calculated using ANOVA. The line in the box is the median, the box extends from the lower to the upper quartile, and the whiskers represent the lowest and highest tumor weight in each group. Control: control IgG Gem: gemcitabine, IgG2A11: anti-RAGE monoclonal antibody.

Analysis of tumor tissues by Western blot

We investigated the levels of autophagy in the tumors from the four treatment groups. The most commonly used method for measuring autophagy is the comparison of LC3 levels by immunoblotting [300]. LC3 stands for microtubule-associated protein light chain 3, which in its cytosolic form is known as LC3-I, and upon conjugation to phosphatidylethanolamine (PE)

forms LC3-II which is localized on the isolation membrane and autophagosome [301] (Figure 25). The amount of LC3-II formed is associated with the number of autophagosomes formed and conversion of LC3-I to LC3-II is used as a marker of autophagy [302]. However, LC3-II itself is degraded by autophagy, making it difficult to only conclude from the results of LC3 immunoblotting [303]. Autophagy is a dynamic process, where autophagosomes constantly form and disappear. Therefore, a reliable method of measuring autophagy is to measure the autophagic flux [303]. One of the methods for detecting autophagic flux is to measure p62 (SQSTM1/sequestosome 1) degradation. p62 serves as an adaptor protein that links ubiquitinated proteins to the autophagic machinery and enables their clearance in the lysosome [304]. p62 possesses a C-terminal ubiquitin-binding domain and a short LC3 interacting region [305,306]. p62 can bind to LC3, thereby serving as a selective substrate of autophagy. Therefore, accumulation of p62 indicates inhibition of autophagy, and decrease in p62 levels indicates activation of autophagy [304,307].
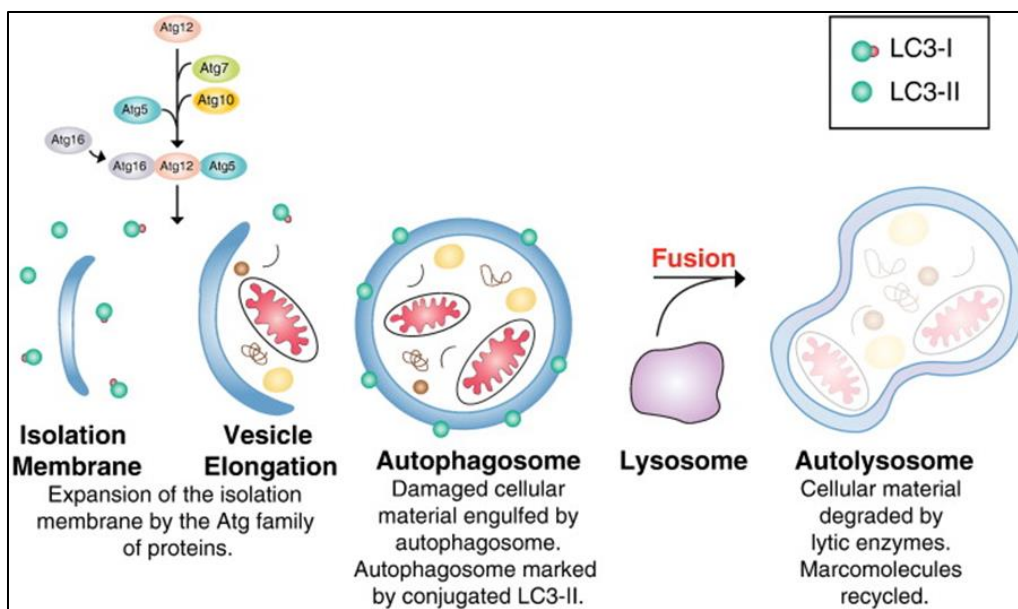
Figure 25: The autophagic pathway.
The isolation membrane is formed in the cytosol and expanded by the conjugation of the Atg family of proteins (Atg proteins 12,7,10 and conjugated Atg 5/12/16). LC3 exists as both LC3-I and LC3-II. The double membrane structure is marked by LC3-II (conjugated to phosphatidylethanolamine) on the surface. Under low pH conditions, the autophagosome fuses with the lysosome to form the autolysosome, where the organelles and proteins are degraded by lysosomal hydrolyses. Figure taken from [308]

We performed western blotting for detection of LC3-II levels. However, we did not observe any differences in the levels of LC3-II among the four treatment groups. Therefore, we determined the level of p62 in the four groups by western blotting. Our western blot results show visible differences in the levels of p62, with much stronger bands in IgG2A11 + gemcitabine treatment group as compared to gemcitabine alone treatment group (Figure 26a). Densitometric analysis also showed significantly higher levels of p62 in the tumor extracts from the group treated with the combination as compared to gemcitabine alone treatment group ($p<0.001$) (Figure 26b). This indicated more accumulation of p62, implying reduction in autophagy in the tumors.
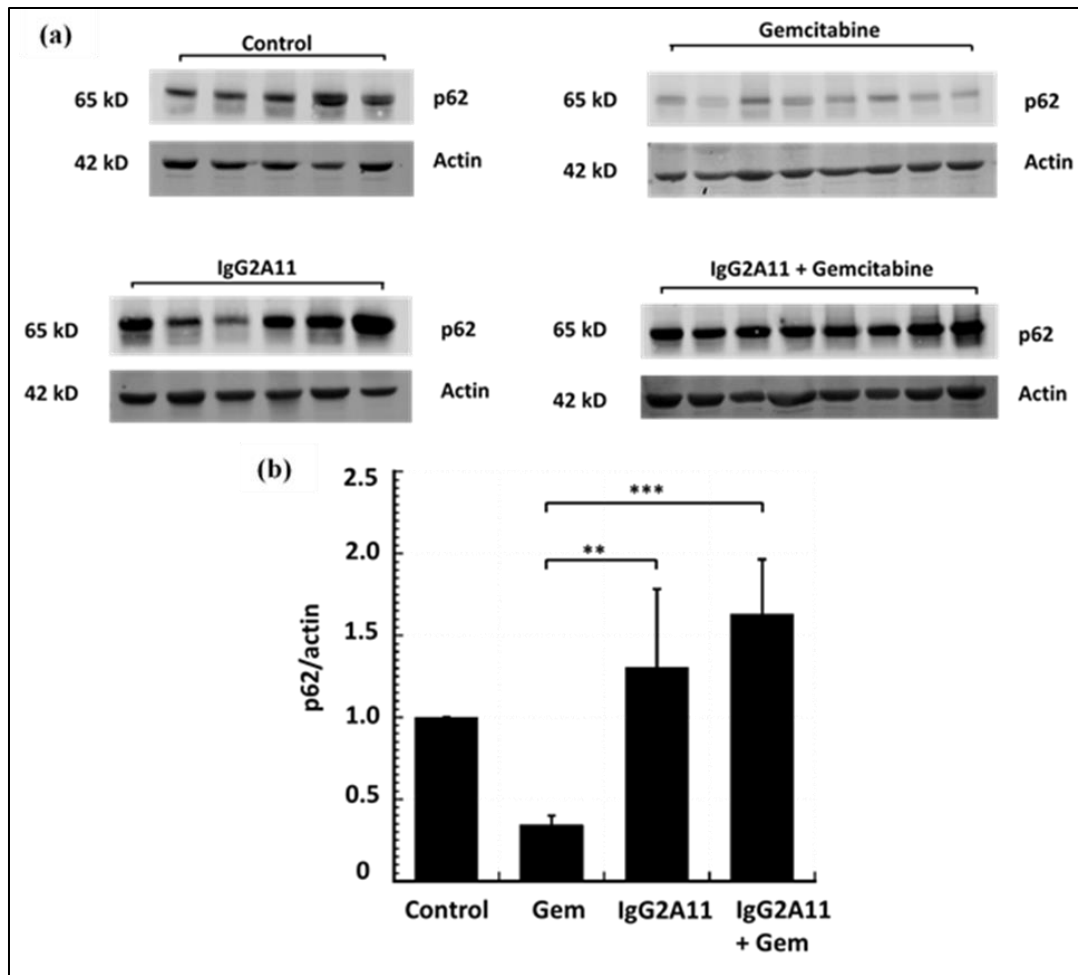
Figure 26: Expression of p62 in pancreatic tumor extracts.
(a) Western blot comparing the levels of p62 among the four groups. The western blot was performed three times. A representative blot is shown. (b) Densitometric analysis with the results normalized to actin.

Increased apoptosis in tumors treated with the combination of IgG2A11 and gemcitabine

RAGE has been shown to promote tumor cell survival by inhibiting apoptosis in pancreatic cancer [292]. Apoptosis is referred to programmed cell death which leads to elimination of unhealthy cells without damaging surrounding cells [309]. The two commonly described initiation pathways are the intrinsic (or mitochondrial) and extrinsic (or death receptor) pathways of apoptosis (Figure 27). Both pathways eventually lead to the execution phase of apoptosis [309]. Initiator caspases activate executioner caspases that subsequently coordinate

their activities to activate other enzymes [310]. A prominent event during apoptosis is the

selective cleavage of poly(ADP-ribose) polymerase (PARP), a nuclear enzyme involved in DNA

repair, DNA stability, and transcriptional regulation, by caspases, particularly by caspase-3 and

caspase-7 [311]
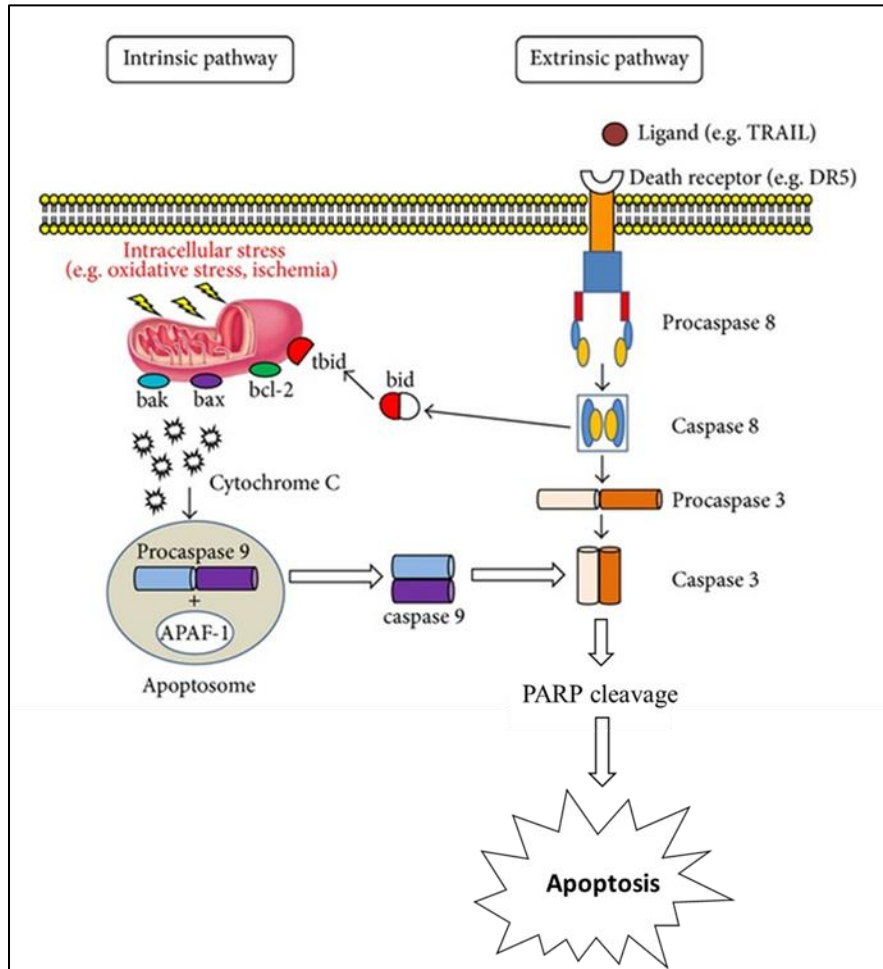
Figure 27: The apoptotic pathway.
Apoptosis works through two main pathways: extrinsic and intrinsic. Figure adapted from [312]

We initiated our study by determining the levels of cleaved caspase-3, an executioner

caspase. Our western blot results did not show any noticeable changes in the levels of cleaved

caspase 3 in the tumor extracts from the combination treatment group as compared to

gemcitabine alone treatment group (Figure 28). Therefore, we next examined another marker for

apoptosis, PARP. We investigated the levels of cleaved PARP in tumor extracts from the four

groups. Although the differences were not statistically significant, we observed higher levels of

cleaved PARP in the combination treatment group as compared to gemcitabine alone treatment
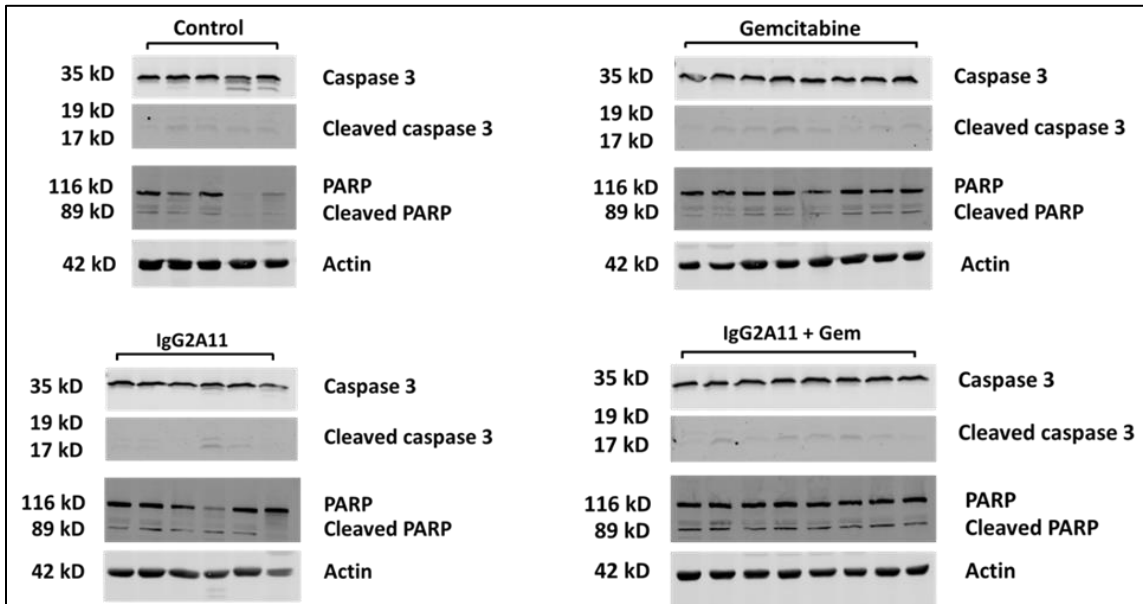
group (Figure 28).

Figure 28: Expression of caspase 3, cleaved caspase 3, PARP and cleaved PARP in pancreatic
tumor extracts.
Western blot comparing the levels of caspase 3, cleaved caspase 3, PARP and cleaved PARP
among the four groups. The western blot was performed three times. Representative blots are
shown.

Levels of HMGB1 in tumors tissues

It has been shown that treatment with chemotherapeutic agents induce passive release of

HMGB1 from dying tumor cells [313]. Moreover, the release of HMGB1 from dying tumor cells

has been demonstrated to be regulated by autophagy [314]. This is further supported by other

studies which showed that induction of autophagy resulted in increased release of HMGB1,

whereas inhibition of autophagy prevented HMGB1 release from dying tumor cells [184,279].

From our western blot results, no striking difference was observed in the HMGB1 bands among

the four groups (Figure 29a). However, densitometric analysis upon normalizing with actin

showed a significant reduction in HMGB1 levels in tumor extracts from the group that received

IgG2A11 + gemcitabine (Figure 29b). We performed the western blots on tumor extracts which

contained both intracellular HMGB1 and HMGB1 present in the tumor microenvironment.

Therefore, our data does not give information about the HMGB1 that would have been released

in the serum. Determining the levels of HMGB1 in serum by ELISA would help to correlate the

effect of the treatments on the release of HMGB1 from tumor cells.
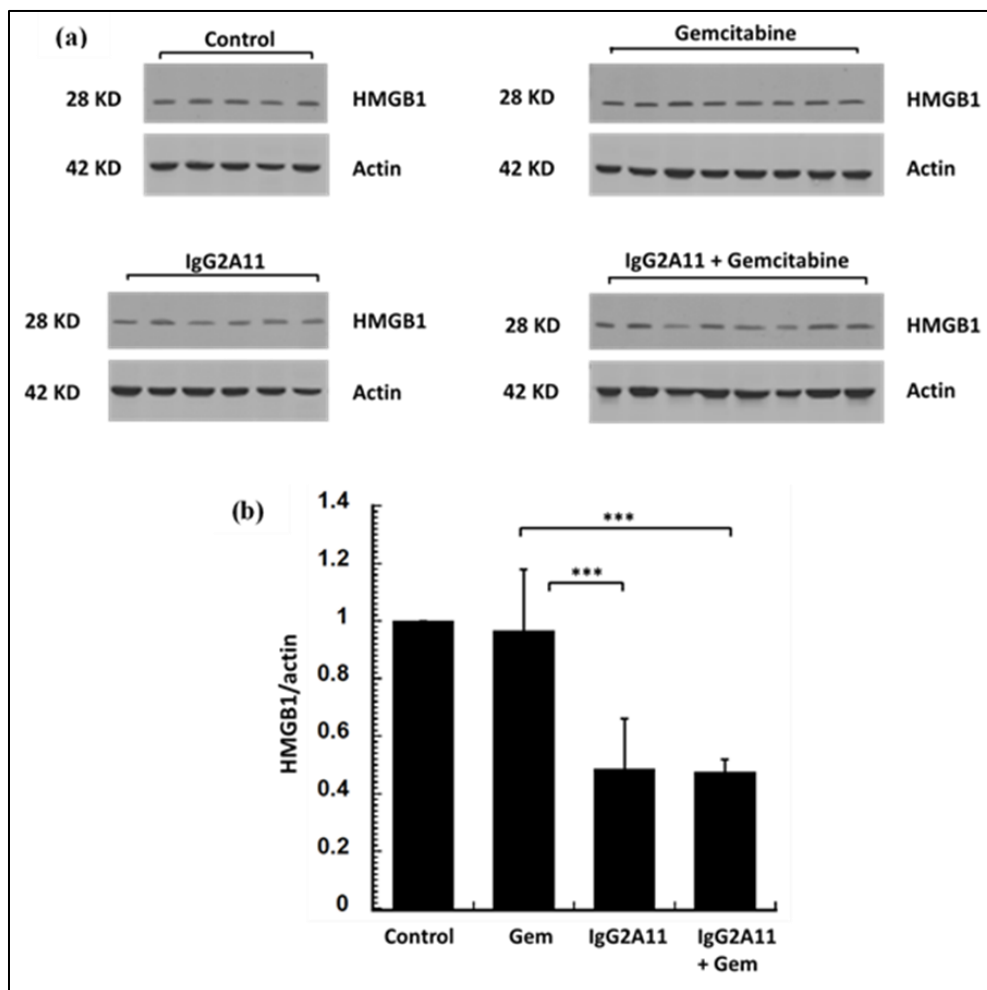
Figure 29: Expression of HMGB1 in pancreatic tumor extracts.
(a) Western blot comparing the levels of HMGB1 among the four groups. The western blot was
repeated three times. A representative blot is shown (n=3). (b) Densitometric analysis with the
results normalized to actin.

Reduction in phosphorylation of ERK in tumors treated with the combination of IgG2A11 and gemcitabine

It has been shown that the interaction between HMGB1 and RAGE stimulated phosphorylation of ERK1/2 and resulted in increased cell proliferation in gastric tumor cells [184]. Therefore, we next determined and compared the levels of phosphorylation of ERK1/2 in the tumor extracts. Our results showed a significant reduction in the phosphorylation of ERK1/2 in the tumor extracts from the group treated with IgG2A11 and gemcitabine as compared to gemcitabine alone treatment group (Figure 30). This suggests that inhibiting RAGE in combination with gemcitabine resulted in reduced cell proliferation.
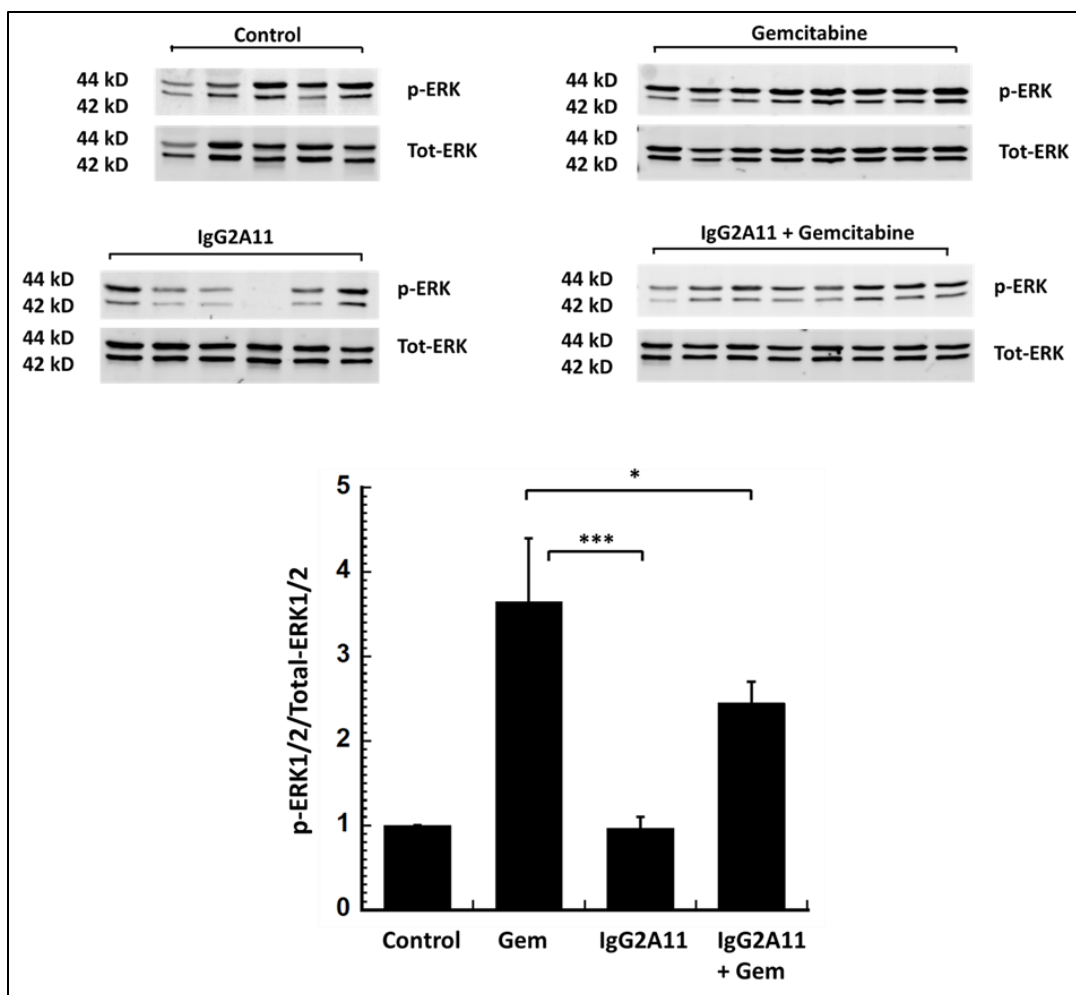
Figure 30: Expression of p-ERK1/2 in pancreatic tumor extracts.
(a) Western blot comparing the levels of p-ERK1/2 among the four groups. A representative blot is shown (b) Densitometric analysis with the results normalized to total-ERK1/2.

Effect of combination of FPS-ZM1 and gemcitabine on KPC 5508 cell viability

We previously determined the effect of gemcitabine on cell viability of KPC 5508 cells *in vitro*. We next investigated the effect of FPS-ZM1 + gemcitabine on the cell viability of KPC 5508 cells. We treated the cells with FPS-ZM1 (50 nM) + gemcitabine (concentrations indicated in Figure 31). Since we used DMSO for solubilizing FPS-ZM1, we also treated the cells with DMSO + gemcitabine to determine the effect on cell viability, if any. The final concentration of DMSO in each well (FPS-ZM1 + gemcitabine as well as DMSO + gemcitabine) was 0.03%. It has been shown that at concentration up to 10% DMSO does not produce any cytotoxicity [315].

As reported earlier in this chapter, in cells treated with gemcitabine alone, we observed a dose

dependent reduction in the cell viability upon treatment with gemcitabine. The maximum of 40%

reduction in the cell viability was observed with 25 µM concentration of gemcitabine. We also

observed a further 20% reduction in cell viability following addition of FPS-ZM1 along with

gemcitabine (Figure 31). For comparison, we also treated the cells with DMSO (0.03%) +

gemcitabine and observed almost similar reduction in cell viability as with FPS-ZM1 +

gemcitabine. Therefore, our results suggested that, in our *in vitro* experimental conditions, there

was no difference in reduction in cell viability upon treatment with FPS + gemcitabine.
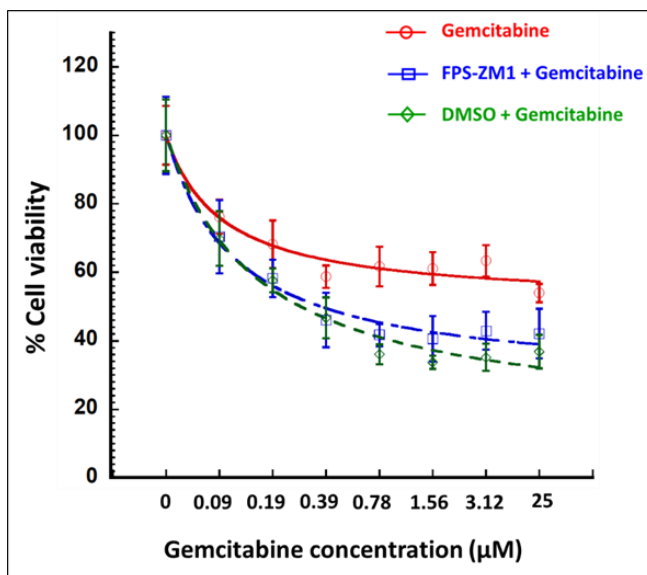
Figure 31: The effect of FPS-ZM1 and gemcitabine treatment on cell viability of KPC 5508 cells.
Cells were seeded in a 96-well plate and incubated overnight. FPS-ZM1(50nM) and gemcitabine, at the indicated concentrations, was added to cells and further incubated for 24 hours. Cell viability was determined using Alamar Blue.

Effect of FPS-ZM1 and gemcitabine on tumor growth in a mouse model of pancreatic cancer (NDSU study)

We next intended to compare the effect of the combination of FPS-ZM1 and gemcitabine on tumor growth in pancreatic cancer. Therefore, we investigated the effect of FPS-ZM1 alone, gemcitabine alone and the combination of FPS-ZM1 and gemcitabine on pancreatic tumor in C57Bl/6 mice. Mice that received sterile saline served as a control. Since FPS-ZM1 was dissolved in DMSO, another group of mice received saline + DMSO to serve as a control. We did not observe any significant difference in the tumor weights from the two control groups (Figure 32), indicating that DMSO itself did not have any cytotoxic effects on the tumor cells. As anticipated, we observed a significant reduction in tumor growth in mice that received gemcitabine alone as compared to the control group (p=0.02) (Figure 32). The difference in tumor weights between these two groups was not statistically significant (p=0.06) in the Omaha study. This can be explained by the number of cells implanted in the pancreas in this study (5,000 cells) as compared to 10,000 cells in the Omaha study. We suggest that a significant reduction in tumor weights was observed in the NDSU study because a lower number of cells was implanted. A further significant reduction in tumor growth was observed in the group that received the combination of FPS-ZM1 and gemcitabine as compared to the group that received gemcitabine alone (p=0.008). These findings are consistent with the results from our previous study (Figure 24), suggesting that RAGE inhibition increases the sensitivity of pancreatic tumor cells to gemcitabine treatment. We also observed a significant reduction in tumor growth in the FPS-ZM1 alone treatment group as compared to the control group (p=0.04) (Figure 32). FPS-ZM1 appeared to be as effective as gemcitabine. However, this result needs to be further investigated for a better understanding of the effect of FPS-ZM1 alone. Similar to the results

89

from the Omaha study (Figure 24), we observed that the tumor weight values were more spread

out in the FPS-ZM1 treatment group as compared to FPS-ZM1 + gemcitabine treatment group

(Figure 32). Overall, our findings from both studies strongly suggest that the response to

gemcitabine was enhanced by combining it with a RAGE inhibitor.
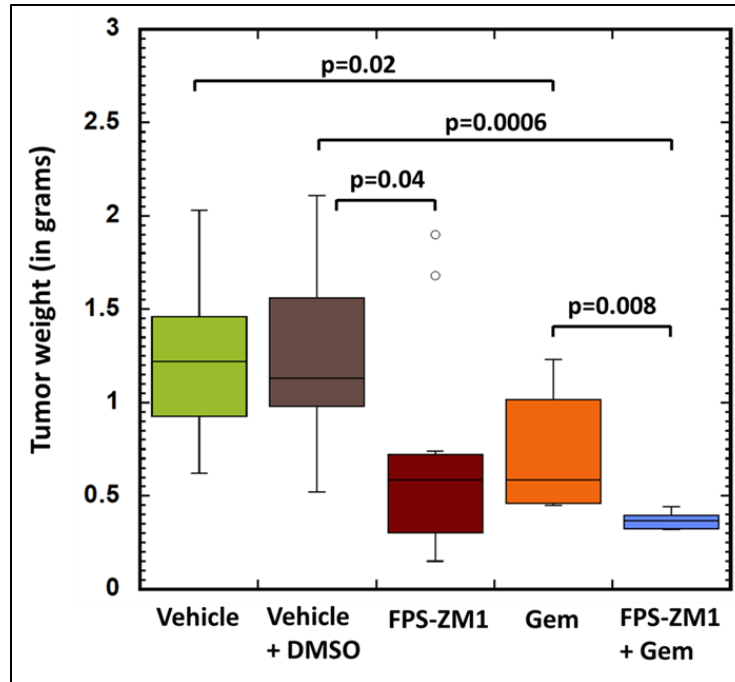
Figure 32: Comparison of tumor weights in different treatment groups.
Box-and-whisker plot of tumor weights harvested after treatment with vehicle (n=8), vehicle + DMSO (n=7), FPS-ZM1 (n=12), gemcitabine alone (n=8) or FPS-ZM1 + gemcitabine (n=8). P-values were calculated using ANOVA. Vehicle: sterile saline, FPS-ZM1: small molecule RAGE inhibitor, Gem: gemcitabine

Discussion

Our results show significant reduction in tumor growth upon treatment with both RAGE

inhibitors (IgG2A11 and FPS-ZM1) in combination with gemcitabine as compared to the

gemcitabine alone treatment group (Figure 24 and 32). Another important observation was the

low variation of the tumor weights in the groups treated with the combination of gemcitabine

with either IgG2A11 or FPS-ZM1, as seen from the very little spread of the box plots. These

findings suggest that the pancreatic tumors in mice became more responsive to gemcitabine when administered in combination with a RAGE inhibitor. We anticipated that FPS-ZM1 would be more effective than IgG2A11 when combined with gemcitabine in suppressing pancreatic tumor growth. Indeed, we anticipated that the small molecule could inhibit the activation of RAGE present at the cell surface as well as inside the cells, whereas IgG2A11 could inhibit RAGE present only on the cell surface (Figure 33). An important point to note is that the Omaha study (10,000 cells implanted) had to be terminated prematurely at 4 weeks as mice began to die, whereas in the NDSU study (5,000 cells implanted), the study reached completion as no early deaths were observed. We observed a reduction in tumor weights in mice treated with gemcitabine alone as compared to control group, with p=0.06 in the Omaha study (Figure 24) and p=0.02 in the NDSU study (Figure 32). This reduction could be explained by the difference in the number of cells implanted.
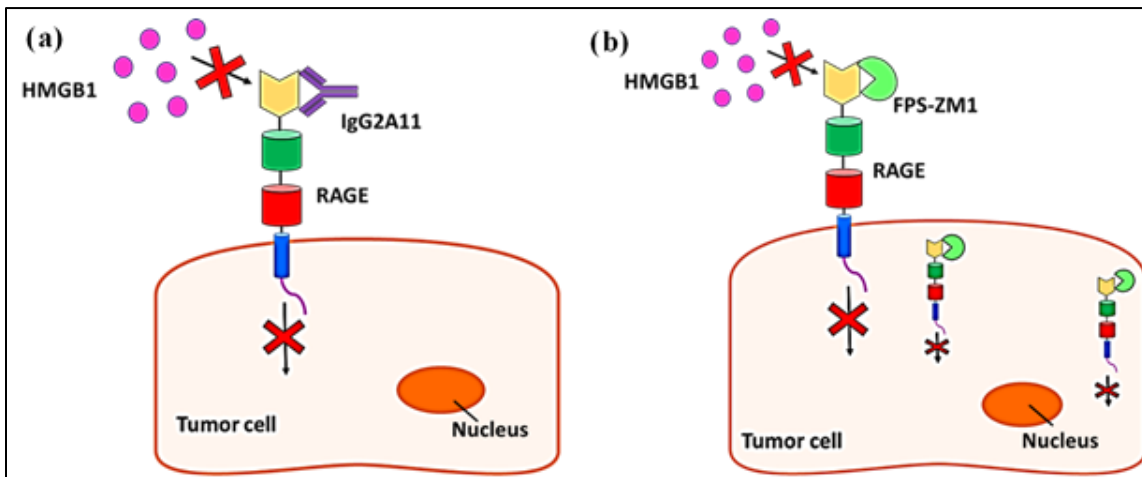
Figure 33: Inhibition of RAGE by IgG2A11 and FPS-ZM1.
(a) IgG2A11 can inhibit RAGE activation present at the cell surface. (b) FPS-ZM1 can inhibit RAGE activation present at the cell surface and inside the cells.

It has been previously demonstrated that RAGE promotes pancreatic tumor cell survival following administration of chemotherapeutic agents by enhancing autophagy in tumor cells and

preventing cancer cell death by limiting apoptosis [209]. The same study also showed that suppression of RAGE expression resulted in a decrease in chemotherapy-induced autophagy and increased apoptosis in pancreatic tumor cells [209]. Findings from another study showed that RAGE-mediated autophagy plays a critical role in facilitating pancreatic tumorigenesis [203].

We investigated the markers of autophagy in the tumor tissues from the four groups of the Omaha study. We investigated the levels of p62 in the tumor extracts. Our results showed significantly higher levels of p62 in tumor extracts from the IgG2A11 + gemcitabine treatment group as compared to the gemcitabine alone treatment group (Figure 26). These results indicated that IgG2A11 + gemcitabine inhibited autophagy in pancreatic tumor. However, when we determined LC3-II levels by western blotting, no differences were observed among the four groups. We reason that this is due to the dynamic nature of autophagy. It has been shown that there is only a transient increase in LC3-II levels upon induction of autophagy and that the levels of LC3-II decrease after longer periods of autophagy activation [303]. As we performed our experiments on tumor tissues harvested 5 days after the end of the treatment, it could be possible that the LC3-II levels would have decreased significantly, thereby showing no LC3-II bands on the western blot.

Next, we investigated the markers of apoptosis in the tumor tissues from the four groups of the Omaha study. We examined the levels of cleaved caspase-3 and cleaved PARP by western blot. Our results did not show detectable levels of cleaved caspase-3 in the tumor extracts from the different treatment groups (Figure 28). However, we observed higher, though not statistically significant, levels of cleaved PARP in the combination treatment group as compared to the gemcitabine alone treatment group (Figure 28). An explanation for this observation could be that

92

the cleavage of PARP occurred by caspases other than caspase-3. Indeed, it has been reported that PARP can also be cleaved by caspase-7 [316].

HMGB1 expression has been shown to increase following treatment with cytotoxic agents [289]. Therefore, we investigated the levels of HMGB1 in the tumor tissues (containing both intracellular HMGB1 and HMGB1 present in the tumor microenvironment). Our results showed higher levels of HMGB1 in the gemcitabine alone treatment group (Figure 29). HMGB1 has been shown to be an important mediator of autophagy and increase in HMGB1 has been correlated with increased autophagy in cancer cells following the administration of cytotoxic anti-cancer agents [279,289,317]. In the IgG2A11 + gemcitabine treatment group, we observed a significant reduction in HMGB1 levels (Figure 29), which were in alignment with the p62 western blot results that showed a reduction in autophagy in the group (Figure 26).

Inhibiting HMGB1 interaction with RAGE by silencing RAGE has been shown to abrogate phosphorylation of ERK1/2 in gastric cancer [184]. Our findings with phosphorylation of ERK1/2 were consistent with these results[184,289]. We observed a significant reduction in the phosphorylation of ERK1/2 in the IgG2A11 and gemcitabine treatment group as compared to the gemcitabine alone treatment group (Figure 30). These results suggest that the combination of IgG2A11 and gemcitabine leads to reduction in proliferation of tumor cells.

The analysis of tumor tissues by Western blot showed very large intra group variations as indicated in the differences in the band intensities within a group. The heterogenous nature of pancreatic cancer could explain these large variations. Indeed, several recent studies have reported large tumor heterogeneity in pancreatic cancer [318,319].

Based on our findings, we propose the following schematic representation of the effect of RAGE inhibition in pancreatic cancer tumors (Figure 34).
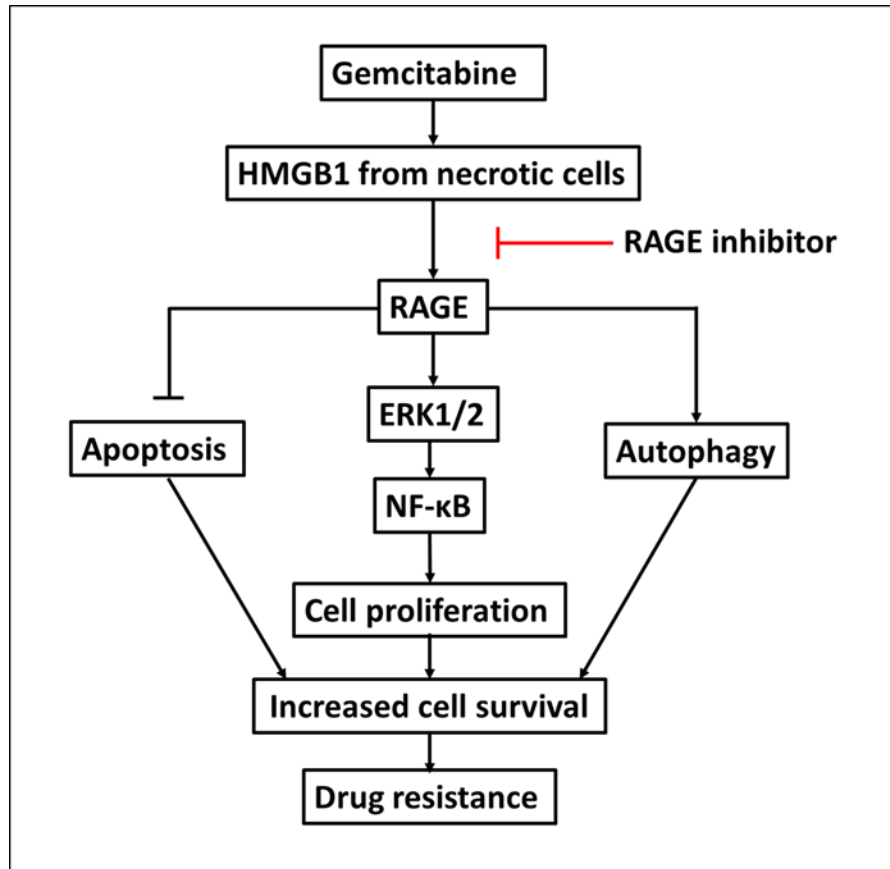
Figure 34: Schematic representation of RAGE signaling in pancreatic cancer.
Inhibition of RAGE leads to increased sensitivity of pancreatic tumor for gemcitabine. Figure
adapted from [184], [320] and [210].

The second animal study is ongoing, and it would be noteworthy to determine the effect

of FPS-ZM1 + gemcitabine treatment over the levels of autophagy and apoptosis in the

pancreatic tumors. The results would provide clearer insights about the effect of RAGE

inhibitors in pancreatic cancer and therefore support the development of novel therapies targeting

RAGE.

SUMMARY AND FUTURE DIRECTIONS

In recent years, RAGE has emerged as a therapeutic target in pancreatic cancer and has provided opportunities for intervention in pancreatic cancer. Several studies have demonstrated that RAGE is important for pancreatic tumor growth and facilitates tumor cell survival. However, not much has been described about targeting RAGE with a drug in pancreatic cancer. In our present study we investigated the role of RAGE in pancreatic cancer, which would further advance our knowledge to better utilize RAGE as a target in pancreatic cancer.

The first study was designed to investigate the effect of RAGE overexpression on cellular properties of human pancreatic cancer cell-line PANC-1 cells. Overexpression of RAGE in PANC-1 cells led to a phenotypic switch which resulted into an increase in proliferative abilities of PANC-1 cells. However, contrary to the anticipated outcome, a down-regulation of the migratory properties of PANC-1 cells was observed. The down-regulation of migratory properties was further supported by the down-regulation of the mesenchymal marker vimentin. Interestingly, we also observed a reduction in the levels of various integrins like α2, α3, α5, β1 and β5 which is in agreement with the reduced migration abilities of these cells. Furthermore, we also showed a down-regulation of FAK activity which was consistent with the reduced integrin levels. RAGE overexpression also resulted in reduction of ERK1/2, Akt and NF-κB activity in PANC-1 cells. Overall, our complementary approaches showed decreased migration abilities of the PANC-1 cells when RAGE was overexpressed.

However, it would be interesting to observe the behavior of RAGE overexpressing PANC-1 cells *in vivo*. We could compare the tumor growth after implanting PANC-1 WT, PANC-1 FLR2 and PANC-1 FLR3 cells in the pancreas of nude mice. Based on our *in vitro* data, we speculate that PANC-1 FLR2 and FLR3 cells would result in larger tumors than PANC-

95

1 WT. However, animals implanted with PANC-1 FLR2 and FLR3 may experience less metastasis than those implanted with PANC-1 WT cells. Investigating the effect of RAGE overexpression in other pancreatic cancer cell-lines would also inform if the effects observed in PANC-1 cells could be generalized to all pancreatic cancer cell-lines.

In the second study, we investigated RAGE as a therapeutic target in a mouse model of pancreatic cancer. We performed two animal studies using a murine pancreatic cancer cell-line KPC 5508 and two different RAGE inhibitors (IgG2A11 or FPS-ZM1). KPC 5508 cells were implanted in the pancreas of C57Bl/6 mice, followed by the treatment with either gemcitabine, RAGE inhibitor (IgG2A11 or FPS-ZM1) or the combination of gemcitabine and a RAGE inhibitor, thereby comparing tumor growth in different treatment groups. The results from the two animal studies showed significantly smaller tumor sizes in mice that received the combination of RAGE inhibitor (IgG2A11 or FPS-ZM1) and gemcitabine in comparison to mice that received gemcitabine alone.

Tumor tissues from the Omaha study were further examined to understand the mechanism responsible for smaller tumors in the gemcitabine + IgG2A11 treatment group. Our western blot results from the Omaha study suggested that the combination of gemcitabine and IgG2A11 resulted in reduction in autophagy in pancreatic tumors, indicated by increased levels of p62 (Figure 26). We also anticipated to observe a decrease in LC3-II levels in the IgG2A11 + gemcitabine treatment group as a consequence of reduced autophagy, however, no detectable levels of LC3-II were observed in western blots. One possible reason could be the dynamic nature of autophagy, as a result of which, after a transient increase, LC3-II disappears. Since we extracted the tumor tissues 5 days after the end of the treatment and then performed our experiments, the levels of LC3-II levels could have decreased significantly, thereby showing no

LC3-II bands on the western blot. To further support that RAGE inhibition in combination with gemcitabine leads to diminished autophagy, immunohistochemical analysis of tumor tissues could provide additional information. In comparison to western blot, immunohistochemistry could be a better tool in determining the expression of even very low levels of LC3-II and p62 along with their localization in the tumor tissue. As, when there is an overall low expression of protein in the tumor tissue, during the preparation of tumor extract the protein could be diluted to a great extent and as a result not detected by western blot. In addition, determining the levels of proteins involved in early steps of autophagy, such as ULK1 protein kinase (key regulator of autophagy initiation) and phosphorylated Beclin-1, could help determine changes in autophagy upon RAGE inhibition. For more accurate measurements, ELISA could also be performed to determine the effect of the combination of IgG2A11 + gemcitabine on p62 as well as LC3 in KPC 5508 cells *in vitro*, thereby further advancing our understanding about the contribution of RAGE in autophagy.

The western blot results from the Omaha study also indicated an increase, though not statistically significant, in levels of cleaved PARP (Figure 28) in tumors from the IgG2A11 + gemcitabine treatment group. But, no detectable levels of cleaved caspase-3 (Figure 28) were observed from western blot results. These results suggest that a mechanism different than apoptosis is responsible for the reduced tumor sizes in the combination treatment groups. We suggest that in these tumors, the observed smaller sizes are the result of growth inhibition rather than apoptosis. Reduction in growth inhibition is further supported by the reduced levels of phosphorylated ERK1/2 observed in the combination treatment group. These results further support our hypothesis that combining IgG2A11 with gemcitabine renders the pancreatic tumors more sensitive towards gemcitabine by reducing gemcitabine induced cell survival.

To further validate our hypothesis, that the combination of RAGE inhibitors with gemcitabine could be more effective than gemcitabine alone in suppressing tumor growth in pancreatic cancer, some questions still need to be answered. What is the exact mechanism involved in reducing the levels of autophagy and cell survival in tumors? Does the combination of FPS-ZM1 and gemcitabine also result in decreased autophagy and cell survival in pancreatic tumors in mice? We anticipate that higher levels of p62 would be observed in tumors treated with the combination of FPS-ZM1 and gemcitabine than in tumors treated with gemcitabine alone. Another question that arises from our study is, what is the effect of the combination of RAGE inhibitor and gemcitabine on the metastatic potential of pancreatic cancer in the mouse model? We anticipate that the combination of RAGE inhibitor and gemcitabine would prevent pancreatic cancer from metastasizing to other sites. Finally, it would also be interesting to elucidate the effect of the combination of RAGE inhibitor and gemcitabine in the tumor microenvironment in pancreatic cancer? We expect that RAGE inhibition would reduce tumor growth by preventing the interaction between RAGE, expressed on cancer cells as well as the cells like fibroblasts, leucocytes and vascular cells in the tumor microenvironment, and its ligands secreted by these tumor microenvironment cells. Indeed, studies have shown that fibroblasts, leucocytes and vascular cells express RAGE and secrete various RAGE ligands. In tumors, RAGE activation in multiple cell types, by multiple ligands could promote tumor growth by facilitating cell proliferation, cell invasion, angiogenesis and metastasis. Blocking RAGE-ligand interactions in tumors could result in multifaceted effects by reducing gemcitabine induced survival of cancer cells and reducing RAGE activation in other cell types in the tumor microenvironment.

All the aforementioned questions should be investigated in future studies. The findings would help develop a better understanding about the role of RAGE in pancreatic cancer.

REFERENCES

[1]   (2019) American Cancer Society. Cancer Facts & Figuresed.^eds). American Cancer Society, Atlanta, GA.

[2]   Patel, N., Khorolsky, C. and Benipal, B. (2018). Incidence of Pancreatic Adenocarcinoma in the United States from 2001 to 2015: A United States Cancer Statistics Analysis of 50 States. Cureus 10, e3796-e3796.

[3]   Siegel, R.L., Miller, K.D. and Jemal, A. (2019). Cancer statistics, 2019. CA Cancer J Clin 69, 7-34.

[4]   Saad, A.M., Turk, T., Al-Husseini, M.J. and Abdel-Rahman, O. (2018). Trends in pancreatic adenocarcinoma incidence and mortality in the United States in the last four decades; a SEER-based study. BMC cancer 18, 688-688.

[5]   Siegel, R.L., Miller, K.D. and Jemal, A. (2017). Cancer Statistics, 2017. CA Cancer J Clin 67, 7-30.

[6]   Röder, P.V., Wu, B., Liu, Y. and Han, W. (2016). Pancreatic regulation of glucose homeostasis. Experimental & molecular medicine 48, e219-e219.

[7]   Fesinmeyer, M.D., Austin, M.A., Li, C.I., De Roos, A.J. and Bowen, D.J. (2005). Differences in survival by histologic type of pancreatic cancer. Cancer Epidemiol Biomarkers Prev 14, 1766-73.

[8]   Kern, S.E., Hruban, R.H., Hidalgo, M. and Yeo, C.J. (2002). An introduction to pancreatic adenocarcinoma genetics, pathology and therapy. Cancer Biol Ther 1, 607-13.

[9]   Buchholz, M. and Gress, T.M. (2009). Molecular changes in pancreatic cancer. Expert Rev Anticancer Ther 9, 1487-97.

[10]   McGuigan, A., Kelly, P., Turkington, R.C., Jones, C., Coleman, H.G. and McCain, R.S. (2018). Pancreatic cancer: A review of clinical diagnosis, epidemiology, treatment and outcomes. World journal of gastroenterology 24, 4846-4861.

[11]   Midha, S., Chawla, S. and Garg, P.K. (2016). Modifiable and non-modifiable risk factors for pancreatic cancer: A review. Cancer letters 381, 269-277.

[12]   Lowenfels, A.B. and Maisonneuve, P. (2004). Epidemiology and prevention of pancreatic cancer. Jpn J Clin Oncol 34, 238-44.

[13]   (2018) International Agency for Research on Cancer, World Health   Organization. Global Cancer Observatoryed.^eds)

[14]   Becker, A.E., Hernandez, Y.G., Frucht, H. and Lucas, A.L. (2014). Pancreatic ductal adenocarcinoma: risk factors, screening, and early detection. World J Gastroenterol 20, 11182-98.

[15]   Yeo, T.P. (2015). Demographics, Epidemiology, and Inheritance of Pancreatic Ductal Adenocarcinoma. Seminars in Oncology 42, 8-18.

[16]   Borelli, I. et al. (2014). A founder MLH1 mutation in Lynch syndrome families from Piedmont, Italy, is associated with an increased risk of pancreatic tumours and diverse immunohistochemical patterns. Fam Cancer 13, 401-13.

[17]   Lynch, H.T. et al. (2002). Phenotypic variation in eight extended CDKN2A germline mutation familial atypical multiple mole melanoma-pancreatic carcinoma-prone families: the familial atypical mole melanoma-pancreatic carcinoma syndrome. Cancer 94, 84-96.

[18]   Li, D. (2001). Molecular epidemiology of pancreatic cancer. Cancer J 7, 259-65.

[19]   Huxley, R., Ansary-Moghaddam, A., Berrington de González, A., Barzi, F. and Woodward, M. (2005). Type-II diabetes and pancreatic cancer: a meta-analysis of 36 studies. British Journal Of Cancer 92, 2076.

[20]   Everhart, J. and Wright, D. (1995). Diabetes Mellitus as a Risk Factor for Pancreatic Cancer: A Meta-analysis. JAMA 273, 1605-1609.

[21]   Hezel, A.F., Kimmelman, A.C., Stanger, B.Z., Bardeesy, N. and Depinho, R.A. (2006). Genetics and biology of pancreatic ductal adenocarcinoma. Genes Dev 20, 1218-49.

[22]   Jones, S. et al. (2008). Core signaling pathways in human pancreatic cancers revealed by global genomic analyses. Science 321, 1801-6.

[23]   Almoguera, C., Shibata, D., Forrester, K., Martin, J., Arnheim, N. and Perucho, M. (1988). Most human carcinomas of the exocrine pancreas contain mutant c-K-ras genes. Cell 53, 549-54.

[24]   Jancik, S., Drabek, J., Radzioch, D. and Hajduch, M. (2010). Clinical relevance of KRAS in human cancers. J Biomed Biotechnol 2010, 150960.

[25]   Zeitouni, D., Pylayeva-Gupta, Y., Der, C.J. and Bryant, K.L. (2016). KRAS Mutant Pancreatic Cancer: No Lone Path to an Effective Treatment. Cancers (Basel) 8

[26]   Wittinghofer, A., Scheffzek, K. and Ahmadian, M.R. (1997). The interaction of Ras with GTPase-activating proteins. FEBS Lett 410, 63-7.

[27] Junttila, M.R. et al. (2015). Modeling targeted inhibition of MEK and PI3 kinase in human pancreatic cancer. Mol Cancer Ther 14, 40-7.

[28] Logsdon, C.D. and Lu, W. (2016). The Significance of Ras Activity in Pancreatic Cancer Initiation. International Journal of Biological Sciences 12, 338-346.

[29] Redston, M.S., Caldas, C., Seymour, A.B., Hruban, R.H., da Costa, L., Yeo, C.J. and Kern, S.E. (1994). p53 mutations in pancreatic carcinoma and evidence of common involvement of homocopolymer tracts in DNA microdeletions. Cancer Res 54, 3025-33.

[30] Levy, N., Yonish-Rouach, E., Oren, M. and Kimchi, A. (1993). Complementation by wild-type p53 of interleukin-6 effects on M1 cells: induction of cell cycle exit and cooperativity with c-myc suppression. Molecular and Cellular Biology 13, 7942.

[31] Bates, S., Ryan, K.M., Phillips, A.C. and Vousden, K.H. (1998). Cell cycle arrest and DNA endoreduplication following p21Waf1/Cip1 expression. Oncogene 17, 1691-703.

[32] Cicenas, J., Kveacraviciute, K., Meskinyte, I., Meskinyte-Kausiliene, E. and Skeberdyte, A. (2017). KRAS, TP53, CDKN2A, SMAD4, BRCA1, and BRCA2 Mutations in Pancreatic Cancer. Cancers 9, 42.

[33] Harada, T., Okita, K., Shiraishi, K., Kusano, N., Kondoh, S. and Sasaki, K. (2002). Interglandular cytogenetic heterogeneity detected by comparative genomic hybridization in pancreatic cancer. Cancer Res 62, 835-9.

[34] Moskaluk, C.A., Hruban, R.H. and Kern, S.E. (1997). p16 and K-ras gene mutations in the intraductal precursors of human pancreatic adenocarcinoma. Cancer Res 57, 2140-3.

[35] Grant, T.J., Hua, K. and Singh, A. (2016). Molecular Pathogenesis of Pancreatic Cancer. Progress in molecular biology and translational science 144, 241-275.

[36] Schutte, M. et al. (1997). Abrogation of the Rb/p16 tumor-suppressive pathway in virtually all pancreatic carcinomas. Cancer Res 57, 3126-30.

[37] Saif, M.W., Karapanagiotou, L. and Syrigos, K. (2007). Genetic alterations in pancreatic cancer. World journal of gastroenterology 13, 4423-4430.

[38] Hu, Y.X., Watanabe, H., Ohtsubo, K., Yamaguchi, Y., Ha, A., Okai, T. and Sawabu, N. (1997). Frequent loss of p16 expression and its correlation with clinicopathological parameters in pancreatic carcinoma. Clin Cancer Res 3, 1473-7.

[39] Nowak, N.J. et al. (2005). Genome-wide aberrations in pancreatic adenocarcinoma. Cancer Genet Cytogenet 161, 36-50.

[40] Vignali, M., Hassan, A.H., Neely, K.E. and Workman, J.L. (2000). ATP-Dependent Chromatin-Remodeling Complexes. Molecular and Cellular Biology 20, 1899.

[41] Biankin, A.V. et al. (2012). Pancreatic cancer genomes reveal aberrations in axon guidance pathway genes. Nature 491, 399-405.

[42] Goggins, M., Hruban, R.H. and Kern, S.E. (2000). BRCA2 is inactivated late in the development of pancreatic intraepithelial neoplasia: evidence and implications. Am J Pathol 156, 1767-71.

[43] Villanueva, A. et al. (1998). Disruption of the antiproliferative TGF-beta signaling pathways in human pancreatic cancer cells. Oncogene 17, 1969-78.

[44] Ghaneh, P., Costello, E. and Neoptolemos, J.P. (2007). Biology and management of pancreatic cancer. Gut 56, 1134-52.

[45] Hruban, R.H. et al. (2001). Pancreatic intraepithelial neoplasia: a new nomenclature and classification system for pancreatic duct lesions. Am J Surg Pathol 25, 579-86.

[46] Maitra, A., Fukushima, N., Takaori, K. and Hruban, R.H. (2005). Precursors to invasive pancreatic cancer. Adv Anat Pathol 12, 81-91.

[47] Hruban, R.H., Maitra, A. and Goggins, M. (2008). Update on pancreatic intraepithelial neoplasia. Int J Clin Exp Pathol 1, 306-16.

[48] Haugk, B. (2010). Pancreatic intraepithelial neoplasia-can we detect early pancreatic cancer? Histopathology 57, 503-14.

[49] van Heek, N.T. et al. (2002). Telomere shortening is nearly universal in pancreatic intraepithelial neoplasia. Am J Pathol 161, 1541-7.

[50] Hruban, R.H. et al. (2004). An illustrated consensus on the classification of pancreatic intraepithelial neoplasia and intraductal papillary mucinous neoplasms. Am J Surg Pathol 28, 977-87.

[51] Goh, B.K., Tan, Y.M., Chung, Y.F., Chow, P.K., Cheow, P.C., Wong, W.K. and Ooi, L.L. (2006). A review of mucinous cystic neoplasms of the pancreas defined by ovarian-type stroma: clinicopathological features of 344 patients. World J Surg 30, 2236-45.

[52] Perera, R.M. and Bardeesy, N. (2015). Pancreatic Cancer Metabolism: Breaking It Down to Build It Back Up. Cancer Discovery 5, 1247.

[53] Bardeesy, N. and DePinho, R.A. (2002). Pancreatic cancer biology and genetics. Nat Rev Cancer 2, 897-909.

[54]   Hidalgo, M. (2010). Pancreatic cancer. N Engl J Med 362, 1605-17.

[55]   Herreros-Villanueva, M. and Bujanda, L. (2016). Non-invasive biomarkers in pancreatic cancer diagnosis: what we need versus what we have. Annals of translational medicine 4, 134-134.

[56]   Fong, Z.V. and Winter, J.M. (2012). Biomarkers in pancreatic cancer: diagnostic, prognostic, and predictive. Cancer J 18, 530-8.

[57]   Zhang, Y., Yang, J., Li, H., Wu, Y., Zhang, H. and Chen, W. (2015). Tumor markers CA19-9, CA242 and CEA in the diagnosis of pancreatic cancer: a meta-analysis. International journal of clinical and experimental medicine 8, 11683-11691.

[58]   Koprowski, H., Steplewski, Z., Mitchell, K., Herlyn, M., Herlyn, D. and Fuhrer, P. (1979). Colorectal carcinoma antigens detected by hybridoma antibodies. Somatic Cell Genet 5, 957-71.

[59]   Glenn, J., Steinberg, W.M., Kurtzman, S.H., Steinberg, S.M. and Sindelar, W.F. (1988). Evaluation of the utility of a radioimmunoassay for serum CA 19-9 levels in patients before and after treatment of carcinoma of the pancreas. J Clin Oncol 6, 462-8.

[60]   Gronborg, M. et al. (2004). Comprehensive proteomic analysis of human pancreatic juice. J Proteome Res 3, 1042-55.

[61]   Di Gangi, I.M. et al. (2016). Metabolomic profile in pancreatic cancer patients: a consensus-based approach to identify highly discriminating metabolites. Oncotarget 7, 5815-5829.

[62]   Mayerle, J. et al. (2018). Metabolic biomarker signature to differentiate pancreatic ductal adenocarcinoma from chronic pancreatitis. Gut 67, 128.

[63]   Schnelldorfer, T. et al. (2008). Long-term survival after pancreatoduodenectomy for pancreatic adenocarcinoma: is cure possible? Ann Surg 247, 456-62.

[64]   Evans, D.B. et al. (2008). Preoperative gemcitabine-based chemoradiation for patients with resectable adenocarcinoma of the pancreatic head. J Clin Oncol 26, 3496-502.

[65]   Thomas, A., Dajani, K., Neoptolemos, J.P. and Ghaneh, P. (2010). Adjuvant therapy in pancreatic cancer. Dig Dis 28, 684-92.

[66]   Conroy, T. et al. (2011). FOLFIRINOX versus gemcitabine for metastatic pancreatic cancer. N Engl J Med 364, 1817-25.

[67]   Von Hoff, D.D. et al. (2013). Increased Survival in Pancreatic Cancer with nab-Paclitaxel plus Gemcitabine. New England Journal of Medicine 369, 1691-1703.

[68]   Oberstein, P.E. and Olive, K.P. (2013). Pancreatic cancer: why is it so hard to treat? Therap Adv Gastroenterol 6, 321-37.

[69]   Berlin, J.D., Catalano, P., Thomas, J.P., Kugler, J.W., Haller, D.G. and Benson, A.B., 3rd. (2002). Phase III study of gemcitabine in combination with fluorouracil versus gemcitabine alone in patients with advanced pancreatic carcinoma: Eastern Cooperative Oncology Group Trial E2297. J Clin Oncol 20, 3270-5.

[70]   Cunningham, D. et al. (2009). Phase III randomized comparison of gemcitabine versus gemcitabine plus capecitabine in patients with advanced pancreatic cancer. J Clin Oncol 27, 5513-8.

[71]   Herrmann, R. et al. (2007). Gemcitabine plus capecitabine compared with gemcitabine alone in advanced pancreatic cancer: a randomized, multicenter, phase III trial of the Swiss Group for Clinical Cancer Research and the Central European Cooperative Oncology Group. J Clin Oncol 25, 2212-7.

[72]   Troiani, T., Martinelli, E., Capasso, A., Morgillo, F., Orditura, M., De Vita, F. and Ciardiello, F. (2012). Targeting EGFR in pancreatic cancer treatment. Curr Drug Targets 13, 802-10.

[73]   Martin, L.K., Bekaii-Saab, T.S., Li, X., Kleiber, B., Ellison, E.C., Bloomston, M. and Zalupski, M. (2012). VEGF remains an interesting target in advanced pancreas cancer (APCA): results of a multi-institutional phase II study of bevacizumab, gemcitabine, and infusional 5-fluorouracil in patients with APCA. Annals of Oncology 23, 2812-2820.

[74]   Moore, M.J. et al. (2007). Erlotinib plus gemcitabine compared with gemcitabine alone in patients with advanced pancreatic cancer: a phase III trial of the National Cancer Institute of Canada Clinical Trials Group. J Clin Oncol 25, 1960-6.

[75]   Shepherd, F.A. and Tsao, M.S. (2006) Unraveling the mystery of prognostic and predictive factors in epidermal growth factor receptor therapy. In J Clin Oncol ed.^eds), pp. 1219-20; author reply 1220-1, United States.

[76]   Wang, J.P. et al. (2015). Erlotinib is effective in pancreatic cancer with epidermal growth factor receptor mutations: a randomized, open-label, prospective trial. Oncotarget 6, 18162-18173.

[77] Royal, R.E. et al. (2010). Phase 2 trial of single agent Ipilimumab (anti-CTLA-4) for locally advanced or metastatic pancreatic adenocarcinoma. J Immunother 33, 828-33.

[78] Brahmer, J.R. et al. (2012). Safety and activity of anti-PD-L1 antibody in patients with advanced cancer. The New England journal of medicine 366, 2455-2465.

[79] Vonderheide, R.H. and Bayne, L.J. (2013). Inflammatory networks and immune surveillance of pancreatic carcinoma. Curr Opin Immunol 25, 200-5.

[80] Neesse, A. et al. (2011). Stromal biology and therapy in pancreatic cancer. Gut 60, 861-868.

[81] Neesse, A., Algul, H., Tuveson, D.A. and Gress, T.M. (2015). Stromal biology and therapy in pancreatic cancer: a changing paradigm. Gut 64, 1476-84.

[82] Sheahan, A.V., Biankin, A.V., Parish, C.R. and Khachigian, L.M. (2018). Targeted therapies in the management of locally advanced and metastatic pancreatic cancer: a systematic review. Oncotarget 9, 21613-21627.

[83] Burris, H.A., 3rd et al. (1997). Improvements in survival and clinical benefit with gemcitabine as first-line therapy for patients with advanced pancreas cancer: a randomized trial. J Clin Oncol 15, 2403-13.

[84] Wang-Gillam, A. et al. (2016). Nanoliposomal irinotecan with fluorouracil and folinic acid in metastatic pancreatic cancer after previous gemcitabine-based therapy (NAPOLI-1): a global, randomised, open-label, phase 3 trial. Lancet 387, 545-57.

[85] Neeper, M. et al. (1992). Cloning and expression of a cell surface receptor for advanced glycosylation end products of proteins. J Biol Chem 267, 14998-5004.

[86] Schmidt, A.M. et al. (1992). Isolation and characterization of two binding proteins for advanced glycosylation end products from bovine lung which are present on the endothelial cell surface. J Biol Chem 267, 14987-97.

[87] Schmidt, A.M., Yan, S.D., Brett, J., Mora, R., Nowygrod, R. and Stern, D. (1993). Regulation of human mononuclear phagocyte migration by cell surface-binding proteins for advanced glycation end products. The Journal of Clinical Investigation 91, 2155-2168.

[88] Malherbe, P., Richards, J.G., Gaillard, H., Thompson, A., Diener, C., Schuler, A. and Huber, G. (1999). cDNA cloning of a novel secreted isoform of the human receptor for advanced glycation end products and characterization of cells co-expressing cell-surface

scavenger receptors and Swedish mutant amyloid precursor protein. Brain Res Mol Brain Res 71, 159-70.

[89] Sugaya, K., Fukagawa, T., Matsumoto, K., Mita, K., Takahashi, E., Ando, A., Inoko, H. and Ikemura, T. (1994). Three genes in the human MHC class III region near the junction with the class II: gene for receptor of advanced glycosylation end products, PBX2 homeobox gene and a notch homolog, human counterpart of mouse mammary tumor gene int-3. Genomics 23, 408-19.

[90] Schmidt, A.M., Yan, S.D., Yan, S.F. and Stern, D.M. (2001). The multiligand receptor RAGE as a progression factor amplifying immune and inflammatory responses. Journal of Clinical Investigation 108, 949-955.

[91] Bucciarelli, L.G. et al. (2002). RAGE is a multiligand receptor of the immunoglobulin superfamily: implications for homeostasis and chronic disease. Cell Mol Life Sci 59, 1117-28.

[92] Gordon, S. (2002). Pattern recognition receptors: doubling up for the innate immune response. Cell 111, 927-30.

[93] Brett, J. et al. (1993). Survey of the distribution of a newly characterized receptor for advanced glycation end products in tissues. Am J Pathol 143, 1699-712.

[94] Tanji, N. et al. (2000). Expression of advanced glycation end products and their cellular receptor RAGE in diabetic nephropathy and nondiabetic renal disease. J Am Soc Nephrol 11, 1656-66.

[95] Aleshin, A. et al. (2008). RAGE modulates myocardial injury consequent to LAD infarction via impact on JNK and STAT signaling in a murine model. Am J Physiol Heart Circ Physiol 294, H1823-32.

[96] Demling, N., Ehrhardt, C., Kasper, M., Laue, M., Knels, L. and Rieber, E.P. (2006). Promotion of cell adherence and spreading: a novel function of RAGE, the highly selective differentiation marker of human alveolar epithelial type I cells. Cell Tissue Res 323, 475-88.

[97] Fehrenbach, H., Kasper, M., Tschernig, T., Shearman, M.S., Schuh, D. and Müller, M. (1998). Receptor for advanced glycation endproducts (RAGE) exhibits highly differential cellular and subcellular localisation in rat and human lung. Cellular and molecular biology (Noisy-le-Grand, France) 44, 1147-1157.

[98]   Srikrishna, G., Huttunen, H.J., Johansson, L., Weigle, B., Yamaguchi, Y., Rauvala, H. and Freeze, H.H. (2002). N -Glycans on the receptor for advanced glycation end products influence amphoterin binding and neurite outgrowth. J Neurochem 80, 998-1008.

[99]   Schmidt, A.M. et al. (1994). The endothelial cell binding site for advanced glycation end products consists of a complex: an integral membrane protein and a lactoferrin-like polypeptide. J Biol Chem 269, 9882-8.

[100]   Hudson, B.I., Kalea, A.Z., Del Mar Arriero, M., Harja, E., Boulanger, E., D'Agati, V. and Schmidt, A.M. (2008). Interaction of the RAGE cytoplasmic domain with diaphanous-1 is required for ligand-stimulated cellular migration through activation of Rac1 and Cdc42. J Biol Chem 283, 34457-68.

[101]   Ding, Q. and Keller, J.N. (2005). Evaluation of rage isoforms, ligands, and signaling in the brain. Biochim Biophys Acta 1746, 18-27.

[102]   Thornalley, P.J. (1998). Cell activation by glycated proteins. AGE receptors, receptor recognition factors and functional classification of AGEs. Cellular and molecular biology (Noisy-le-Grand, France) 44, 1013-1023.

[103]   Gonzalez, I., Romero, J., Rodriguez, B.L., Perez-Castro, R. and Rojas, A. (2013). The immunobiology of the receptor of advanced glycation end-products: trends and challenges. Immunobiology 218, 790-7.

[104]   Yonekura, H. et al. (2003). Novel splice variants of the receptor for advanced glycation end-products expressed in human vascular endothelial cells and pericytes, and their putative roles in diabetes-induced vascular injury. Biochemical Journal 370, 1097.

[105]   Ding, Q. and Keller, J.N. (2004). Splice variants of the receptor for advanced glycosylation end products (RAGE) in human brain. Neuroscience Letters 373, 67-72.

[106]   Hudson, B.I., Carter, A.M., Harja, E., Kalea, A.Z., Arriero, M., Yang, H., Grant, P.J. and Schmidt, A.M. (2007). Identification, classification, and expression of RAGE gene splice variants. The FASEB Journal 22, 1572-1580.

[107]   Galichet, A., Weibel, M. and Heizmann, C.W. (2008). Calcium-regulated intramembrane proteolysis of the RAGE receptor. Biochem Biophys Res Commun 370, 1-5.

[108]   Raucci, A. et al. (2008). A soluble form of the receptor for advanced glycation endproducts (RAGE) is produced by proteolytic cleavage of the membrane-bound form by the sheddase a disintegrin and metalloprotease 10 (ADAM10). Faseb j 22, 3716-27.

[109] Maillard-Lefebvre, H., Boulanger, E., Daroux, M., Gaxatte, C., Hudson, B.I. and Lambert, M. (2009). Soluble receptor for advanced glycation end products: a new biomarker in diagnosis and prognosis of chronic inflammatory diseases. Rheumatology (Oxford) 48, 1190-6.

[110] Forbes, J.M. et al. (2005). Modulation of soluble receptor for advanced glycation end products by angiotensin-converting enzyme-1 inhibition in diabetic nephropathy. J Am Soc Nephrol 16, 2363-72.

[111] Kierdorf, K. and Fritz, G. (2013). RAGE regulation and signaling in inflammation and beyond. J Leukoc Biol 94, 55-68.

[112] Schlueter, C., Hauke, S., Flohr, A.M., Rogalla, P. and Bullerdiek, J. (2003). Tissue-specific expression patterns of the RAGE receptor and its soluble forms—a result of regulated alternative splicing? Biochimica et Biophysica Acta (BBA) - Gene Structure and Expression 1630, 1-6.

[113] Cheng, C. et al. (2005). Expression profiling of endogenous secretory receptor for advanced glycation end products in human organs. Mod Pathol 18, 1385-96.

[114] Kuang, C.Y., Rusliza, B., Herni, T., Hing, T.T. and Norshariza, N. Receptor for Advanced Glycation End Products and Its Involvement in Inflammatory Diseasesed.^eds). International Journal of Inflammation

[115] Harashima, A. et al. (2006). Identification of mouse orthologue of endogenous secretory receptor for advanced glycation end-products: structure, function and expression. Biochem J 396, 109-15.

[116] Kalea, A.Z., Reiniger, N., Yang, H., Arriero, M., Schmidt, A.M. and Hudson, B.I. (2009). Alternative splicing of the murine receptor for advanced glycation end-products (RAGE) gene. Faseb j 23, 1766-74.

[117] Dunn, J.A., McCance, D.R., Thorpe, S.R., Lyons, T.J. and Baynes, J.W. (1991). Age-dependent accumulation of N epsilon-(carboxymethyl)lysine and N epsilon-(carboxymethyl)hydroxylysine in human skin collagen. Biochemistry 30, 1205-10.

[118] Yamagishi, S., Nakamura, N., Suematsu, M., Kaseda, K. and Matsui, T. (2015). Advanced Glycation End Products: A Molecular Target for Vascular Complications in Diabetes. Mol Med 21 Suppl 1, S32-40.

[119] Wautier, M.-P., Chappey, O., Corda, S., Stern, D.M., Schmidt, A.M. and Wautier, J.-L. (2001). Activation of NADPH oxidase by AGE links oxidant stress to altered gene expression via RAGE. American Journal of Physiology-Endocrinology and Metabolism 280, E685-E694.

[120] Du Yan, S. et al. (1997). Amyloid-beta peptide-receptor for advanced glycation endproduct interaction elicits neuronal expression of macrophage-colony stimulating factor: a proinflammatory pathway in Alzheimer disease. Proc Natl Acad Sci U S A 94, 5296-301.

[121] Yan, S.D. et al. (2000). Receptor-dependent cell stress and amyloid accumulation in systemic amyloidosis. Nat Med 6, 643-51.

[122] Hofmann, M.A. et al. (1999). RAGE mediates a novel proinflammatory axis: a central cell surface receptor for S100/calgranulin polypeptides. Cell 97, 889-901.

[123] Hori, O. et al. (1995). The receptor for advanced glycation end products (RAGE) is a cellular binding site for amphoterin. Mediation of neurite outgrowth and co-expression of rage and amphoterin in the developing nervous system. J Biol Chem 270, 25752-61.

[124] Chapman, M.R., Robinson, L.S., Pinkner, J.S., Roth, R., Heuser, J., Hammar, M., Normark, S. and Hultgren, S.J. (2002). Role of Escherichia coli curli operons in directing amyloid fiber formation. Science 295, 851-5.

[125] Sasaki, N. et al. (2002). Advanced glycation end products (AGE) and their receptor (RAGE) in the brain of patients with Creutzfeldt-Jakob disease with prion plaques. Neurosci Lett 326, 117-20.

[126] Chavakis, T. et al. (2003). The pattern recognition receptor (RAGE) is a counterreceptor for leukocyte integrins: a novel pathway for inflammatory cell recruitment. The Journal of experimental medicine 198, 1507-1515.

[127] Tesarova, P., Cabinakova, M., Mikulova, V., Zima, T. and Kalousova, M. (2015). RAGE and its ligands in cancer - culprits, biomarkers, or therapeutic targets? Neoplasma 62, 353-64.

[128] Reddy, S., Bichler, J., Wells-Knecht, K.J., Thorpe, S.R. and Baynes, J.W. (1995). N epsilon-(carboxymethyl)lysine is a dominant advanced glycation end product (AGE) antigen in tissue proteins. Biochemistry 34, 10872-8.

[129]   Cho, S.J., Roman, G., Yeboah, F. and Konishi, Y. (2007). The road to advanced glycation end products: a mechanistic perspective. Curr Med Chem 14, 1653-71.

[130]   Akhter, F., Salman Khan, M., Shahab, U., Moinuddin and Ahmad, S. (2013). Bio-physical characterization of ribose induced glycation: A mechanistic study on DNA perturbations. International Journal of Biological Macromolecules 58, 206-210.

[131]   Goldin, A., Beckman, J.A., Schmidt, A.M. and Creager, M.A. (2006). Advanced glycation end products: sparking the development of diabetic vascular injury. Circulation 114, 597-605.

[132]   Aronson, D. (2002). Potential role of advanced glycosylation end products in promoting restenosis in diabetes and renal failure. Med Hypotheses 59, 297-301.

[133]   Bartrons, R. and Caro, J. (2007). Hypoxia, glucose metabolism and the Warburg's effect. J Bioenerg Biomembr 39, 223-9.

[134]   Vlassara, H. and Striker, G.E. (2011). AGE restriction in diabetes mellitus: a paradigm shift. Nature Reviews Endocrinology 7, 526.

[135]   Chen, H. et al. (2014). Advanced glycation end products increase carbohydrate responsive element binding protein expression and promote cancer cell proliferation. Mol Cell Endocrinol 395, 69-78.

[136]   Ramasamy, R., Vannucci, S.J., Yan, S.S., Herold, K., Yan, S.F. and Schmidt, A.M. (2005). Advanced glycation end products and RAGE: a common thread in aging, diabetes, neurodegeneration, and inflammation. Glycobiology 15, 16R-28R.

[137]   Ott, C., Jacobs, K., Haucke, E., Navarrete Santos, A., Grune, T. and Simm, A. (2014). Role of advanced glycation end products in cellular signaling. Redox Biology 2, 411-429.

[138]   Harry M. Lander, J.M.T., Jason S. Ogiste, Osamu Hori, Rebecca A. Moss, and Ann Marie Schmidt. (1997). Activation of the Receptor for Advanced Glycation End Products Triggers a p21ras-dependent Mitogen-activated Protein Kinase Pathway Regulated by Oxidant Stress*. The Journal Of Biological Chemistry 272, 17810-17814.

[139]   Bondeva, T., Wojciech, S. and Wolf, G. (2011). Advanced glycation end products inhibit adhesion ability of differentiated podocytes in a neuropilin-1-dependent manner. Am J Physiol Renal Physiol 301, F852-70.

[140]   Miki, S., Kasayama, S., Miki, Y., Nakamura, Y., Yamamoto, M., Sato, B. and Kishimoto, T. (1993). Expression of Receptors for Advanced Glycosylation End Products on Renal

Cell Carcinoma Cells in Vitro. Biochemical and Biophysical Research Communications 196, 984-989.

[141] Abe, R. et al. (2004). Regulation of human melanoma growth and metastasis by AGE-AGE receptor interactions. J Invest Dermatol 122, 461-7.

[142] Yamamoto, Y., Yamagishi, S., Hsu, C.C. and Yamamoto, H. (1996). Advanced glycation endproducts-receptor interactions stimulate the growth of human pancreatic cancer cells through the induction of platelet-derived growth factor-B. Biochem Biophys Res Commun 222, 700-5.

[143] Donato, R., Cannon, B.R., Sorci, G., Riuzzi, F., Hsu, K., Weber, D.J. and Geczy, C.L. (2013). Functions of S100 proteins. Curr Mol Med 13, 24-57.

[144] Zimmer, D.B., Wright Sadosky, P. and Weber, D.J. (2003). Molecular mechanisms of S100-target protein interactions. Microscopy Research and Technique 60, 552-559.

[145] Gerlach, R., Demel, G., König, H.G., Gross, U., Prehn, J.H.M., Raabe, A., Seifert, V. and Kögel, D. (2006). Active secretion of S100B from astrocytes during metabolic stress. Neuroscience 141, 1697-1701.

[146] Ellis, E.F., Willoughby, K.A., Sparks, S.A. and Chen, T. (2007). S100B protein is released from rat neonatal neurons, astrocytes, and microglia by in vitro trauma and anti-S100 increases trauma-induced delayed neuronal injury and negates the protective effect of exogenous S100B on neurons. Journal of Neurochemistry 101, 1463-1470.

[147] Tardif, M.R., Chapeton-Montes, J.A., Posvandzic, A., Page, N., Gilbert, C. and Tessier, P.A. (2015). Secretion of S100A8, S100A9, and S100A12 by Neutrophils Involves Reactive Oxygen Species and Potassium Efflux. J Immunol Res 2015, 296149.

[148] Rammes, A., Roth, J., Goebeler, M., Klempt, M., Hartmann, M. and Sorg, C. (1997). Myeloid-related Protein (MRP) 8 and MRP14, Calcium-binding Proteins of the S100 Family, Are Secreted by Activated Monocytes via a Novel, Tubulin-dependent Pathway. Journal of Biological Chemistry 272, 9496-9502.

[149] Perrone, L., Peluso, G. and Melone, M.A.B. (2008). RAGE recycles at the plasma membrane in S100B secretory vesicles and promotes Schwann cells morphological changes. Journal of Cellular Physiology 217, 60-71.

[150] Yammani, R.R., Carlson, C.S., Bresnick, A.R. and Loeser, R.F. (2006). Increase in production of matrix metalloproteinase 13 by human articular chondrocytes due to

stimulation with S100A4: Role of the receptor for advanced glycation end products. Arthritis Rheum 54, 2901-11.

[151] Schenten, V., Plançon, S., Jung, N., Hann, J., Bueb, J.-L., Bréchard, S., Tschirhart, E.J. and Tolle, F. (2018). Secretion of the Phosphorylated Form of S100A9 from Neutrophils Is Essential for the Proinflammatory Functions of Extracellular S100A8/A9. Frontiers in immunology 9, 447-447.

[152] Rani, S.G., Sepuru, K.M. and Yu, C. (2014). Interaction of S100A13 with C2 domain of receptor for advanced glycation end products (RAGE). Biochimica et Biophysica Acta (BBA) - Proteins and Proteomics 1844, 1718-1728.

[153] Arumugam, T., Simeone, D.M., Schmidt, A.M. and Logsdon, C.D. (2004). S100P stimulates cell proliferation and survival via receptor for activated glycation end products (RAGE). J Biol Chem 279, 5059-65.

[154] Donato, R. (2007). RAGE: a single receptor for several ligands and different cellular responses: the case of certain S100 proteins. Curr Mol Med 7, 711-24.

[155] Marenholz, I., Heizmann, C.W. and Fritz, G. (2004). S100 proteins in mouse and man: from evolution to function and pathology (including an update of the nomenclature). Biochemical and Biophysical Research Communications 322, 1111-1122.

[156] Becker, T., Gerke, V., Kube, E. and Weber, K. (1992). S100P, a novel Ca(2+)-binding protein from human placenta. cDNA cloning, recombinant protein expression and Ca2+ binding properties. Eur J Biochem 207, 541-7.

[157] Bresnick, A.R., Weber, D.J. and Zimmer, D.B. (2015). S100 proteins in cancer. Nature reviews. Cancer 15, 96-109.

[158] Logsdon, C.D. et al. (2003). Molecular profiling of pancreatic adenocarcinoma and chronic pancreatitis identifies multiple genes differentially regulated in pancreatic cancer. Cancer Res 63, 2649-57.

[159] Guerreiro Da Silva, I.D., Hu, Y.F., Russo, I.H., Ao, X., Salicioni, A.M., Yang, X. and Russo, J. (2000). S100P calcium-binding protein overexpression is associated with immortalization of human breast epithelial cells in vitro and early stages of breast cancer development in vivo. Int J Oncol 16, 231-40.

[160] Fuentes, M.K., Nigavekar, S.S., Arumugam, T., Logsdon, C.D., Schmidt, A.M., Park, J.C. and Huang, E.H. (2007). RAGE activation by S100P in colon cancer stimulates growth, migration, and cell signaling pathways. Dis Colon Rectum 50, 1230-40.

[161] Mousses, S. et al. (2002). Clinical validation of candidate genes associated with prostate cancer progression in the CWR22 model system using tissue microarrays. Cancer Res 62, 1256-60.

[162] Dowen, S.E. et al. (2005). Expression of S100P and its novel binding partner S100PBPR in early pancreatic cancer. Am J Pathol 166, 81-92.

[163] Arumugam, T., Simeone, D.M., Van Golen, K. and Logsdon, C.D. (2005). S100P Promotes Pancreatic Cancer Growth, Survival, and Invasion. Clinical Cancer Research 11, 5356-5364.

[164] Arumugam, T., Ramachandran, V. and Logsdon, C.D. (2006). Effect of cromolyn on S100P interactions with RAGE and pancreatic cancer growth and invasion in mouse models. Journal of the National Cancer Institute 98, 1806-1818.

[165] Lotze, M.T. and Tracey, K.J. (2005). High-mobility group box 1 protein (HMGB1): nuclear weapon in the immune arsenal. Nat Rev Immunol 5, 331-42.

[166] Read, C.M., Crane-Robinson, C., Cary, P.D., Norman, D.G. and Driscoll, P.C. (1993). Solution structure of a DNA-binding domain from HMG1. Nucleic Acids Research 21, 3427-3436.

[167] Thomas, J.O. and Travers, A.A. (2001). HMG1 and 2, and related 'architectural' DNA-binding proteins. Trends in Biochemical Sciences 26, 167-174.

[168] Tang, D. et al. (2010). Endogenous HMGB1 regulates autophagy. J Cell Biol 190, 881-92.

[169] Lu, B. et al. (2012). Novel role of PKR in inflammasome activation and HMGB1 release. Nature 488, 670-4.

[170] Mitola, S., Belleri, M., Urbinati, C., Coltrini, D., Sparatore, B., Pedrazzi, M., Melloni, E. and Presta, M. (2006). Cutting edge: extracellular high mobility group box-1 protein is a proangiogenic cytokine. J Immunol 176, 12-5.

[171] Yang, H., Wang, H., Czura, C.J. and Tracey, K.J. (2005). The cytokine activity of HMGB1. J Leukoc Biol 78, 1-8.

[172]   Wang, H. et al. (1999). HMG-1 as a late mediator of endotoxin lethality in mice. Science 285, 248-51.

[173]   Scaffidi, P., Misteli, T. and Bianchi, M.E. (2002). Release of chromatin protein HMGB1 by necrotic cells triggers inflammation. Nature 418, 191-5.

[174]   Sims, G.P., Rowe, D.C., Rietdijk, S.T., Herbst, R. and Coyle, A.J. (2010). HMGB1 and RAGE in inflammation and cancer. Annu Rev Immunol 28, 367-88.

[175]   Tian, J. et al. (2007). Toll-like receptor 9-dependent activation by DNA-containing immune complexes is mediated by HMGB1 and RAGE. Nat Immunol 8, 487-96.

[176]   Orlova, V.V. et al. (2007). A novel pathway of HMGB1-mediated inflammatory cell recruitment that requires Mac-1-integrin. Embo j 26, 1129-39.

[177]   Yu, M. et al. (2006). HMGB1 signals through toll-like receptor (TLR) 4 and TLR2. Shock 26, 174-9.

[178]   Harris, H.E., Andersson, U. and Pisetsky, D.S. (2012). HMGB1: a multifunctional alarmin driving autoimmune and inflammatory disease. Nat Rev Rheumatol 8, 195-202.

[179]   Simons, M. and Horowitz, A. (2001). Syndecan-4-mediated signalling. Cell Signal 13, 855-62.

[180]   Chen, G.-Y., Tang, J., Zheng, P. and Liu, Y. (2009). CD24 and Siglec-10 selectively repress tissue damage-induced immune responses. Science (New York, N.Y.) 323, 1722-1725.

[181]   Venereau, E., Schiraldi, M., Uguccioni, M. and Bianchi, M.E. (2013). HMGB1 and leukocyte migration during trauma and sterile inflammation. Molecular Immunology 55, 76-82.

[182]   Tang, D. and Lotze, M.T. (2012) Tumor immunity times out: TIM-3 and HMGB1. In Nat Immunol ed.^eds), pp. 808-10, United States.

[183]   Bianchi, M.E. (2009). HMGB1 loves company. J Leukoc Biol 86, 573-6.

[184]   Zhang, Q.Y., Wu, L.Q., Zhang, T., Han, Y.F. and Lin, X. (2015). Autophagy-mediated HMGB1 release promotes gastric cancer cell survival via RAGE activation of extracellular signal-regulated kinases 1/2. Oncol Rep 33, 1630-8.

[185]   Bangert, A. et al. (2016). Critical role of RAGE and HMGB1 in inflammatory heart disease. Proceedings of the National Academy of Sciences 113, E155.

[186] Xie, J., Mendez, J.D., Mendez-Valenzuela, V. and Aguilar-Hernandez, M.M. (2013). Cellular signalling of the receptor for advanced glycation end products (RAGE). Cell Signal 25, 2185-97.

[187] Taguchi, A. et al. (2000). Blockade of RAGE-amphoterin signalling suppresses tumour growth and metastases. Nature 405, 354-360.

[188] Kang, R. et al. (2014). The HMGB1/RAGE inflammatory pathway promotes pancreatic tumor growth by regulating mitochondrial bioenergetics. Oncogene 33, 567-77.

[189] Li, J.H., Wang, W., Huang, X.R., Oldfield, M., Schmidt, A.M., Cooper, M.E. and Lan, H.Y. (2004). Advanced Glycation End Products Induce Tubular Epithelial-Myofibroblast Transition through the RAGE-ERK1/2 MAP Kinase Signaling Pathway. The American Journal of Pathology 164, 1389-1397.

[190] Shanmugam, N., Kim, Y.S., Lanting, L. and Natarajan, R. (2003). Regulation of cyclooxygenase-2 expression in monocytes by ligation of the receptor for advanced glycation end products. J Biol Chem 278, 34834-44.

[191] Cortizo, A.M., Lettieri, M.G., Barrio, D.A., Mercer, N., Etcheverry, S.B. and McCarthy, A.D. (2003). Advanced glycation end-products (AGEs) induce concerted changes in the osteoblastic expression of their receptor RAGE and in the activation of extracellular signal-regulated kinases (ERK). Mol Cell Biochem 250, 1-10.

[192] Huang, J.-S., Guh, J.-Y., Chen, H.-C., Hung, W.-C., Lai, Y.-H. and Chuang, L.-Y. (2001). Role of receptor for advanced glycation end-product (RAGE) and the JAK/STAT-signaling pathway in AGE-induced collagen production in NRK-49F cells. Journal of Cellular Biochemistry 81, 102-113.

[193] Yeh, C.H. et al. (2001). Requirement for p38 and p44/p42 mitogen-activated protein kinases in RAGE-mediated nuclear factor-kappaB transcriptional activation and cytokine secretion. Diabetes 50, 1495-504.

[194] Sakaguchi, T. et al. (2003). Central role of RAGE-dependent neointimal expansion in arterial restenosis. J Clin Invest 111, 959-72.

[195] Johnson, D.R., Douglas, I., Jahnke, A., Ghosh, S. and Pober, J.S. (1996). A sustained reduction in IkappaB-beta may contribute to persistent NF-kappaB activation in human endothelial cells. J Biol Chem 271, 16317-22.

[196]   Bierhaus, A. et al. (2001). Diabetes-associated sustained activation of the transcription factor nuclear factor-kappaB. Diabetes 50, 2792-808.

[197]   Bianchi, R., Giambanco, I. and Donato, R. (2010). S100B/RAGE-dependent activation of microglia via NF-kappaB and AP-1 Co-regulation of COX-2 expression by S100B, IL-1beta and TNF-alpha. Neurobiol Aging 31, 665-77.

[198]   Meloche, J. et al. (2013). Critical role for the advanced glycation end-products receptor in pulmonary arterial hypertension etiology. J Am Heart Assoc 2, e005157.

[199]   Zhang, X.S. et al. (2017). Activation of the RAGE/STAT3 Pathway in the Dorsal Root Ganglion Contributes to the Persistent Pain Hypersensitivity Induced by Lumbar Disc Herniation. Pain Physician 20, 419-427.

[200]   Bierhaus, A., Humpert, P.M., Morcos, M., Wendt, T., Chavakis, T., Arnold, B., Stern, D.M. and Nawroth, P.P. (2005). Understanding RAGE, the receptor for advanced glycation end products. J Mol Med (Berl) 83, 876-86.

[201]   Sparvero, L.J. et al. (2009). RAGE (Receptor for Advanced Glycation Endproducts), RAGE ligands, and their role in cancer and inflammation. J Transl Med 7, 17.

[202]   Riehl, A., Nemeth, J., Angel, P. and Hess, J. (2009). The receptor RAGE: Bridging inflammation and cancer. Cell Commun Signal 7, 12.

[203]   Kang, R. et al. (2012). The expression of the receptor for advanced glycation endproducts (RAGE) is permissive for early pancreatic neoplasia. Proc Natl Acad Sci U S A 109, 7031-6.

[204]   DiNorcia, J. et al. (2012). RAGE gene deletion inhibits the development and progression of ductal neoplasia and prolongs survival in a murine model of pancreatic cancer. J Gastrointest Surg 16, 104-12; discussion 112.

[205]   Radia, A.M. et al. (2013). Specific siRNA targeting receptor for advanced glycation end products (RAGE) decreases proliferation in human breast cancer cell lines. Int J Mol Sci 14, 7959-78.

[206]   Yaser, A.-M. et al. (2012). The Role of receptor for Advanced Glycation End Products (RAGE) in the proliferation of hepatocellular carcinoma. International journal of molecular sciences 13, 5982-5997.

[207] Liang, H., Zhong, Y., Zhou, S. and Peng, L. (2011). Knockdown of RAGE expression inhibits colorectal cancer cell invasion and suppresses angiogenesis in vitro and in vivo. Cancer Lett 313, 91-8.

[208] Dahlmann, M. et al. (2014). RAGE mediates S100A4-induced cell motility via MAPK/ERK and hypoxia signaling and is a prognostic biomarker for human colorectal cancer metastasis. Oncotarget 5, 3220-33.

[209] Kang, R. et al. (2009). The receptor for advanced glycation end products (RAGE) sustains autophagy and limits apoptosis, promoting pancreatic tumor cell survival. Cell Death and Differentiation 17, 666-676.

[210] Kang, R., Tang, D., Lotze, M.T. and Zeh, H.J., 3rd. (2011). RAGE regulates autophagy and apoptosis following oxidative injury. Autophagy 7, 442-4.

[211] Rahib, L., Smith, B.D., Aizenberg, R., Rosenzweig, A.B., Fleshman, J.M. and Matrisian, L.M. (2014). Projecting Cancer Incidence and Deaths to 2030: The Unexpected Burden of Thyroid, Liver, and Pancreas Cancers in the United States. Cancer Research 74, 2913.

[212] Gu, J., Saiyin, H., Fu, D. and Li, J. (2018). Stroma — A Double-Edged Sword in Pancreatic Cancer: A Lesson From Targeting Stroma in Pancreatic Cancer With Hedgehog Signaling Inhibitors. Pancreas 47

[213] Vennin, C., Murphy, K.J., Morton, J.P., Cox, T.R., Pajic, M. and Timpson, P. (2018). Reshaping the Tumor Stroma for Treatment of Pancreatic Cancer. Gastroenterology 154, 820-838.

[214] Biancur, D.E. and Kimmelman, A.C. (2018). The plasticity of pancreatic cancer metabolism in tumor progression and therapeutic resistance. Biochim Biophys Acta Rev Cancer 1870, 67-75.

[215] Cameron, M.E., Yakovenko, A. and Trevino, J.G. (2018). Glucose and Lactate Transport in Pancreatic Cancer: Glycolytic Metabolism Revisited. Journal of oncology 2018, 6214838-6214838.

[216] Longo, V., Brunetti, O., Gnoni, A., Cascinu, S., Gasparini, G., Lorusso, V., Ribatti, D. and Silvestris, N. (2016). Angiogenesis in pancreatic ductal adenocarcinoma: A controversial issue. Oncotarget 7, 58649-58658.

[217] Erkan, M., Kurtoglu, M. and Kleeff, J. (2016). The role of hypoxia in pancreatic cancer: a potential therapeutic target? Expert Rev Gastroenterol Hepatol 10, 301-16.

[218] Kanda, M. et al. (2012). Presence of somatic mutations in most early-stage pancreatic intraepithelial neoplasia. Gastroenterology 142, 730-733.e9.

[219] Hahn, S.A. et al. (1996). DPC4, a candidate tumor suppressor gene at human chromosome 18q21.1. Science 271, 350-3.

[220] Hingorani, S.R. et al. (2003). Preinvasive and invasive ductal pancreatic cancer and its early detection in the mouse. Cancer Cell 4, 437-450.

[221] Soro-Paavonen, A. et al. (2008). Receptor for advanced glycation end products (RAGE) deficiency attenuates the development of atherosclerosis in diabetes. Diabetes 57, 2461-9.

[222] Wang, D. et al. (2015). Overexpression of the Receptor for Advanced Glycation Endproducts (RAGE) is associated with poor prognosis in gastric cancer. PloS one 10, e0122697-e0122697.

[223] Rahimi, F., Karimi, J., Goodarzi, M.T., Saidijam, M., Khodadadi, I., Razavi, A.N. and Nankali, M. (2017). Overexpression of receptor for advanced glycation end products (RAGE) in ovarian cancer. Cancer Biomark 18, 61-68.

[224] Norster, F., Clear, A.J., Matthews, J., Hoxha, E., Gribben, J. and Jia, L. (2015). Overexpression of HMGB1 Receptor RAGE Is Associated with Worse Clinical Outcome in Patients with Chronic Lymphocytic Leukemia. Blood 126, 617.

[225] Boone, B.A. et al. (2015). The receptor for advanced glycation end products (RAGE) enhances autophagy and neutrophil extracellular traps in pancreatic cancer. Cancer Gene Ther 22, 326-34.

[226] Sevillano, N., Giron, M.D., Salido, M., Vargas, A.M., Vilches, J. and Salto, R. (2009). Internalization of the receptor for advanced glycation end products (RAGE) is required to mediate intracellular responses. J Biochem 145, 21-30.

[227] Sbai, O., Devi, T.S., Melone, M.A., Feron, F., Khrestchatisky, M., Singh, L.P. and Perrone, L. (2010). RAGE-TXNIP axis is required for S100B-promoted Schwann cell migration, fibronectin expression and cytokine secretion. J Cell Sci 123, 4332-9.

[228] Wolfgang, C.L., Herman, J.M., Laheru, D.A., Klein, A.P., Erdek, M.A., Fishman, E.K. and Hruban, R.H. (2013). Recent progress in pancreatic cancer. CA Cancer J Clin 63, 318-48.

[229] Mayo, S.C. et al. (2012). Conditional survival in patients with pancreatic ductal adenocarcinoma resected with curative intent. Cancer 118, 2674-81.

[230] Heerboth, S., Housman, G., Leary, M., Longacre, M., Byler, S., Lapinska, K., Willbanks, A. and Sarkar, S. (2015). EMT and tumor metastasis. Clinical and translational medicine 4, 6-6.

[231] Jolly, M.K., Ware, K.E., Gilja, S., Somarelli, J.A. and Levine, H. (2017). EMT and MET: necessary or permissive for metastasis? Molecular oncology 11, 755-769.

[232] Rhim, A.D. et al. (2012). EMT and dissemination precede pancreatic tumor formation. Cell 148, 349-61.

[233] Mittal, V. (2018). Epithelial Mesenchymal Transition in Tumor Metastasis. Annual Review of Pathology: Mechanisms of Disease 13, 395-412.

[234] Thiery, J.P., Acloque, H. and Huang, R.Y. (2009). Epithelial-mesenchymal transitions in development and disease. Cell 139, 871-890.

[235] Alderton, G.K. (2013). Metastasis: Epithelial to mesenchymal and back again. Nat Rev Cancer 13, 3.

[236] Zheng, X. et al. (2015). Epithelial-to-mesenchymal transition is dispensable for metastasis but induces chemoresistance in pancreatic cancer. Nature 527, 525-530.

[237] Huttenlocher, A. and Horwitz, A.R. Integrins in cell migration. Cold Spring Harbor perspectives in biology 3, a005074-a005074.

[238] Ruoslahti, E. (1991). Integrins. J Clin Invest 87, 1-5.

[239] Desgrosellier, J.S. and Cheresh, D.A. (2010). Integrins in cancer: biological implications and therapeutic opportunities. Nature reviews. Cancer 10, 9-22.

[240] Hood, J.D. and Cheresh, D.A. (2002). Role of integrins in cell invasion and migration. Nature Reviews Cancer 2, 91.

[241] Guo, W. and Giancotti, F.G. (2004). Integrin signalling during tumour progression. Nat Rev Mol Cell Biol 5, 816-26.

[242] Hynes, R.O. (2002). Integrins: Bidirectional, Allosteric Signaling Machines. Cell 110, 673-687.

[243] Craig, D.L., Maren, K.F., Emina, H.H. and Thiruvengadam, A. (2007). RAGE and RAGE Ligands in Cancer. Current Molecular Medicine 7, 777-789.

[244] Sharaf, H., Matou-Nasri, S., Wang, Q., Rabhan, Z., Al-Eidi, H., Al Abdulrahman, A. and Ahmed, N. (2015). Advanced glycation endproducts increase proliferation, migration and

invasion of the breast cancer cell line MDA-MB-231. Biochimica et Biophysica Acta (BBA) - Molecular Basis of Disease 1852, 429-441.

[245] Matou-Nasri, S. et al. (2017). Biological impact of advanced glycation endproducts on estrogen receptor-positive MCF-7 breast cancer cells. Biochimica et Biophysica Acta (BBA) - Molecular Basis of Disease 1863, 2808-2820.

[246] Bao, J.-M. et al. (2015). AGE/RAGE/Akt pathway contributes to prostate cancer cell proliferation by promoting Rb phosphorylation and degradation. American journal of cancer research 5, 1741-1750.

[247] Zheng, L., Li, D., Zhou, Y.-M., Yang, H., Cheng, D. and Ma, X.-X. (2016). Effects of receptor for advanced glycation endproducts on microvessel formation in endometrial cancer. BMC Cancer 16, 93.

[248] Arumugam, T., Ramachandran, V., Sun, D., Peng, Z., Pal, A., Maxwell, D.S., Bornmann, W.G. and Logsdon, C.D. (2013). Designing and Developing S100P Inhibitor 5-Methyl Cromolyn for Pancreatic Cancer Therapy. Molecular Cancer Therapeutics 12, 654.

[249] Indurthi, V.S., Leclerc, E. and Vetter, S.W. (2012). Interaction between glycated serum albumin and AGE-receptors depends on structural changes and the glycation reagent. Arch Biochem Biophys 528, 185-96.

[250] Strober, W. (2001). Trypan blue exclusion test of cell viability. Curr Protoc Immunol Appendix 3, Appendix 3B.

[251] Li, Q. et al. (2018). NF-kappaB in pancreatic cancer: Its key role in chemoresistance. Cancer Lett 421, 127-134.

[252] Fujioka, S. et al. (2003). Function of nuclear factor kappaB in pancreatic cancer metastasis. Clin Cancer Res 9, 346-54.

[253] Prabhu, L., Mundade, R., Korc, M., Loehrer, P.J. and Lu, T. (2014). Critical role of NF-κB in pancreatic cancer. Oncotarget 5, 10969-10975.

[254] Pramanik, K.C., Makena, M.R., Bhowmick, K. and Pandey, M.K. (2018). Advancement of NF-kappaB Signaling Pathway: A Novel Target in Pancreatic Cancer. Int J Mol Sci 19

[255] Turovskaya, O. et al. (2008). RAGE, carboxylated glycans and S100A8/A9 play essential roles in colitis-associated carcinogenesis. Carcinogenesis 29, 2035-2043.

[256] Meghnani, V., Vetter, S.W. and Leclerc, E. (2014). RAGE overexpression confers a metastatic phenotype to the WM115 human primary melanoma cell line. Biochim Biophys Acta 1842, 1017-27.

[257] Kuniyasu, H. et al. (2002). Expression of receptors for advanced glycation end-products (RAGE) is closely associated with the invasive and metastatic activity of gastric cancer. J Pathol 196, 163-70.

[258] Moustakas, A. and de Herreros, A.G. (2017). Epithelial-mesenchymal transition in cancer. Mol Oncol 11, 715-717.

[259] Satelli, A. and Li, S. (2011). Vimentin in cancer and its potential as a molecular target for cancer therapy. Cellular and molecular life sciences : CMLS 68, 3033-3046.

[260] Yang, J. and Weinberg, R.A. (2008). Epithelial-mesenchymal transition: at the crossroads of development and tumor metastasis. Dev Cell 14, 818-29.

[261] Mendez, M.G., Kojima, S.-I. and Goldman, R.D. (2010). Vimentin induces changes in cell shape, motility, and adhesion during the epithelial to mesenchymal transition. FASEB journal : official publication of the Federation of American Societies for Experimental Biology 24, 1838-1851.

[262] Liu, C.-Y., Lin, H.-H., Tang, M.-J. and Wang, Y.-K. (2015). Vimentin contributes to epithelial-mesenchymal transition cancer cell mechanics by mediating cytoskeletal organization and focal adhesion maturation. Oncotarget 6, 15966-15983.

[263] Weinel, R.J., Rosendahl, A., Neumann, K., Chaloupka, B., Erb, D., Rothmund, M. and Santoso, S. (1992). Expression and function of VLA-alpha 2, -alpha 3, -alpha 5 and -alpha 6-integrin receptors in pancreatic carcinoma. Int J Cancer 52, 827-33.

[264] Linder, S., Castanos-Velez, E., von Rosen, A. and Biberfeld, P. (2001). Immunohistochemical expression of extracellular matrix proteins and adhesion molecules in pancreatic carcinoma. Hepatogastroenterology 48, 1321-7.

[265] Shimoyama, S., Gansauge, F., Gansauge, S., Oohara, T. and Beger, H.G. (1995). Altered expression of extracellular matrix molecules and their receptors in chronic pancreatitis and pancreatic adenocarcinoma in comparison with normal pancreas. Int J Pancreatol 18, 227-34.

[266] Sawai, H., Funahashi, H., Yamamoto, M., Okada, Y., Hayakawa, T., Tanaka, M., Takeyama, H. and Manabe, T. (2003). Interleukin-1alpha enhances integrin

alpha(6)beta(1) expression and metastatic capability of human pancreatic cancer. Oncology 65, 167-73.

[267] Hosotani, R. et al. (2002). Expression of integrin alphaVbeta3 in pancreatic carcinoma: relation to MMP-2 activation and lymph node metastasis. Pancreas 25, e30-5.

[268] Walsh, N., Clynes, M., Crown, J. and O'Donovan, N. (2009). Alterations in integrin expression modulates invasion of pancreatic cancer cells. Journal of Experimental & Clinical Cancer Research 28, 140.

[269] Wong, A., Soo, R.A., Yong, W.P. and Innocenti, F. (2009). Clinical pharmacology and pharmacogenetics of gemcitabine. Drug Metab Rev 41, 77-88.

[270] Heinemann, V. (2001). Gemcitabine: progress in the treatment of pancreatic cancer. Oncology 60, 8-18.

[271] Ellenrieder, V., Konig, A. and Seufferlein, T. (2016). Current Standard and Future Perspectives in First- and Second-Line Treatment of Metastatic Pancreatic Adenocarcinoma. Digestion 94, 44-9.

[272] de Sousa Cavalcante, L. and Monteiro, G. (2014). Gemcitabine: metabolism and molecular mechanisms of action, sensitivity and chemoresistance in pancreatic cancer. Eur J Pharmacol 741, 8-16.

[273] Kim, M.P. and Gallick, G.E. (2008) Gemcitabine resistance in pancreatic cancer: picking the key players. In Clin Cancer Res ed.^eds), pp. 1284-5, United States.

[274] Zhou, J., Chen, X., Gilvary, D.L., Tejera, M.M., Eksioglu, E.A., Wei, S. and Djeu, J.Y. (2015). HMGB1 induction of clusterin creates a chemoresistant niche in human prostate tumor cells. Scientific Reports 5, 15085.

[275] Huang, J. et al. (2012). HMGB1 Promotes Drug Resistance in Osteosarcoma. Cancer Research 72, 230.

[276] Wang, L., Zhang, H., Sun, M., Yin, Z. and Qian, J. (2015). High mobility group box 1-mediated autophagy promotes neuroblastoma cell chemoresistance. Oncol Rep 34, 2969-76.

[277] Luo, Y. et al. (2013). High mobility group box 1 released from necrotic cells enhances regrowth and metastasis of cancer cells that have survived chemotherapy. European Journal of Cancer 49, 741-751.

[278]   Livesey, K.M. et al. (2012). p53/HMGB1 complexes regulate autophagy and apoptosis. Cancer research 72, 1996-2005.

[279]   Tang, D. et al. (2010). HMGB1 release and redox regulates autophagy and apoptosis in cancer cells. Oncogene 29, 5299-310.

[280]   Yang, Z. and Klionsky, D.J. (2010). Eaten alive: a history of macroautophagy. Nat Cell Biol 12, 814-22.

[281]   Yang, Z. and Klionsky, D.J. (2009). An overview of the molecular mechanism of autophagy. Curr Top Microbiol Immunol 335, 1-32.

[282]   Baehrecke, E.H. (2005). Autophagy: dual roles in life and death? Nat Rev Mol Cell Biol 6, 505-10.

[283]   Mizushima, N. and Komatsu, M. (2011). Autophagy: renovation of cells and tissues. Cell 147, 728-41.

[284]   Rabinowitz, J.D. and White, E. (2010). Autophagy and metabolism. Science 330, 1344-8.

[285]   Kondo, Y., Kanzawa, T., Sawaya, R. and Kondo, S. (2005). The role of autophagy in cancer development and response to therapy. Nat Rev Cancer 5, 726-34.

[286]   Galluzzi, L. et al. (2015). Autophagy in malignant transformation and cancer progression. The EMBO journal 34, 856-880.

[287]   Maycotte, P. and Thorburn, A. (2011). Autophagy and cancer therapy. Cancer Biol Ther 11, 127-37.

[288]   Pan, B., Chen, D., Huang, J., Wang, R., Feng, B., Song, H. and Chen, L. (2014). HMGB1-mediated autophagy promotes docetaxel resistance in human lung adenocarcinoma. Molecular Cancer 13, 165.

[289]   Liu, W. et al. (2015). HMGB1-mediated autophagy modulates sensitivity of colorectal cancer cells to oxaliplatin via MEK/ERK signaling pathway. Cancer biology & therapy 16, 511-517.

[290]   Yin, H. et al. (2017). HMGB1-mediated autophagy attenuates gemcitabine-induced apoptosis in bladder cancer cells involving JNK and ERK activation. Oncotarget 8, 71642-71656.

[291]   Kang, R., Tang, D., Loze, M.T. and Zeh, I.I.I.H.J. (2011). Apoptosis to autophagy switch triggered by the MHC class III-encoded receptor for advanced glycation endproducts (RAGE). Autophagy 7, 91-93.

[292] Kang, R., Tang, D., Livesey, K.M., Schapiro, N.E., Lotze, M.T. and Zeh, H.J., 3rd. (2011). The Receptor for Advanced Glycation End-products (RAGE) protects pancreatic tumor cells against oxidative injury. Antioxidants & redox signaling 15, 2175-2184.

[293] Xie, D. and Xie, K. (2015). Pancreatic cancer stromal biology and therapy. Genes & Diseases 2, 133-143.

[294] Chu, G.C., Kimmelman, A.C., Hezel, A.F. and DePinho, R.A. (2007). Stromal biology of pancreatic cancer. J Cell Biochem 101, 887-907.

[295] Kalluri, R. (2016). The biology and function of fibroblasts in cancer. Nat Rev Cancer 16, 582-98.

[296] Erkan, M. et al. (2008). The activated stroma index is a novel and independent prognostic marker in pancreatic ductal adenocarcinoma. Clin Gastroenterol Hepatol 6, 1155-61.

[297] Liang, C. et al. (2017). Complex roles of the stroma in the intrinsic resistance to gemcitabine in pancreatic cancer: where we are and where we are going. Experimental &Amp; Molecular Medicine 49, e406.

[298] Sun, Q., Zhang, B., Hu, Q., Qin, Y., Xu, W., Liu, W., Yu, X. and Xu, J. (2018). The impact of cancer-associated fibroblasts on major hallmarks of pancreatic cancer. Theranostics 8, 5072-5087.

[299] Hingorani, S.R. et al. (2005). Trp53R172H and KrasG12D cooperate to promote chromosomal instability and widely metastatic pancreatic ductal adenocarcinoma in mice. Cancer Cell 7, 469-83.

[300] Yoshii, S.R. and Mizushima, N. (2017). Monitoring and Measuring Autophagy. International journal of molecular sciences 18, 1865.

[301] Xie, Z. and Klionsky, D.J. (2007). Autophagosome formation: core machinery and adaptations. Nat Cell Biol 9, 1102-9.

[302] Kabeya, Y. et al. (2000). LC3, a mammalian homologue of yeast Apg8p, is localized in autophagosome membranes after processing. Embo j 19, 5720-8.

[303] Mizushima, N. and Yoshimori, T. (2007). How to interpret LC3 immunoblotting. Autophagy 3, 542-5.

[304] Bjorkoy, G., Lamark, T., Brech, A., Outzen, H., Perander, M., Overvatn, A., Stenmark, H. and Johansen, T. (2005). p62/SQSTM1 forms protein aggregates degraded by

autophagy and has a protective effect on huntingtin-induced cell death. J Cell Biol 171, 603-14.

[305] Lippai, M. and Low, P. (2014). The role of the selective adaptor p62 and ubiquitin-like proteins in autophagy. Biomed Res Int 2014, 832704.

[306] Ciani, B., Layfield, R., Cavey, J.R., Sheppard, P.W. and Searle, M.S. (2003). Structure of the ubiquitin-associated domain of p62 (SQSTM1) and implications for mutations that cause Paget's disease of bone. J Biol Chem 278, 37409-12.

[307] Bjørkøy, G., Lamark, T., Pankiv, S., Øvervatn, A., Brech, A. and Johansen, T. (2009) Chapter 12 Monitoring Autophagic Degradation of p62/SQSTM1. In Methods in Enzymology ed.^eds), pp. 181-197. Academic Press

[308] Kotiadis, V.N., Duchen, M.R. and Osellame, L.D. (2014). Mitochondrial quality control and communications with the nucleus are important in maintaining mitochondrial function and cell health. Biochim Biophys Acta 1840, 1254-65.

[309] Wong, R.S.Y. (2011). Apoptosis in cancer: from pathogenesis to treatment. Journal of experimental & clinical cancer research : CR 30, 87-87.

[310] McIlwain, D.R., Berger, T. and Mak, T.W. (2013). Caspase functions in cell death and disease. Cold Spring Harb Perspect Biol 5, a008656.

[311] Kaufmann, S.H., Desnoyers, S., Ottaviano, Y., Davidson, N.E. and Poirier, G.G. (1993). Specific Proteolytic Cleavage of Poly(ADP-ribose) Polymerase: An Early Marker of Chemotherapy-induced Apoptosis. Cancer Research 53, 3976.

[312] Loreto, C. et al. (2014). The role of intrinsic pathway in apoptosis activation and progression in Peyronie's disease. Biomed Res Int 2014, 616149.

[313] Tang, D., Kang, R., Zeh, H.J. and Lotze, M.T. (2010). High-mobility group box 1 and cancer. Biochimica et Biophysica Acta (BBA) - Gene Regulatory Mechanisms 1799, 131-140.

[314] Thorburn, J., Horita, H., Redzic, J., Hansen, K., Frankel, A.E. and Thorburn, A. (2008). Autophagy regulates selective HMGB1 release in tumor cells that are destined to die. Cell Death And Differentiation 16, 175.

[315] Da Violante, G., Zerrouk, N., Richard, I., Provot, G., Chaumeil, J.C. and Arnaud, P. (2002). Evaluation of the cytotoxicity effect of dimethyl sulfoxide (DMSO) on Caco2/TC7 colon tumor cell cultures. Biol Pharm Bull 25, 1600-3.

[316] Chaitanya, G.V., Steven, A.J. and Babu, P.P. (2010). PARP-1 cleavage fragments: signatures of cell-death proteases in neurodegeneration. Cell communication and signaling : CCS 8, 31-31.

[317] Liu, L. et al. (2010). HMGB1-induced autophagy promotes chemotherapy resistance in leukemia cells. Leukemia 25, 23.

[318] Cros, J., Raffenne, J., Couvelard, A. and Pote, N. (2018). Tumor Heterogeneity in Pancreatic Adenocarcinoma. Pathobiology 85, 64-71.

[319] Juiz, N.A., Iovanna, J. and Dusetti, N. (2019). Pancreatic Cancer Heterogeneity Can Be Explained Beyond the Genome. Frontiers in Oncology 9, 246.

[320] Leclerc, E. and Vetter, S.W. (2015). The role of S100 proteins and their receptor RAGE in pancreatic cancer. Biochim Biophys Acta 1852, 2706-11.